

# Orthogonal Random Forest for Heterogeneous Treatment Effect Estimation

Miruna Oprescu\*

Vasilis Syrgkanis<sup>†</sup>

Zhiwei Steven Wu<sup>‡</sup>

June 9, 2022

## Abstract

We study the problem of estimating heterogeneous treatment effects from observational data, where the treatment policy on the collected data was determined by potentially many confounding observable variables. We propose *orthogonal random forest*<sup>1</sup>, an algorithm that combines orthogonalization, a technique that effectively removes the confounding effect in two-stage estimation, with generalized random forests [Athey et al., 2017], a flexible method for estimating treatment effect heterogeneity. We prove a consistency rate result of our estimator in the partially linear regression model, and en route we provide a consistency analysis for a general framework of performing generalized method of moments (GMM) estimation. We also provide a comprehensive empirical evaluation of our algorithms, and show that they consistently outperform baseline approaches.

## 1 Introduction

Treatment effect estimation is at the heart of many decision-making processes, including clinical trial assignment to patients, price adjustments of products, and ads placement by a search engine. In many situations, we would like to take the heterogeneity of the population into account and estimate the *heterogeneous treatment effect (HTE)*—the effect of a treatment  $T$  (e.g. drug treatment, price discount, and ad position), on the outcome  $Y$  of interest (e.g. clinical response, demand, and click-through-rate), as a function of heterogeneous characteristics  $x$  of the treated subject (e.g. individual patient, product, and ad). HTE estimation is a fundamental problem in causal inference from observational data [Imbens and Rubin, 2015, Wager and Athey, 2015, Athey et al., 2017], and is also intimately related to many areas in machine learning, including contextual bandits, off-policy evaluation [Swaminathan et al., 2016, Wang et al., 2017], optimization [Nie and Wager, 2017], and counterfactual prediction [Swaminathan and Joachims, 2015, Hartford et al., 2016].

The key challenge in HTE estimation is that the observations are typically collected by a policy that depends on confounders or controls variables  $W$ , which also directly influence the outcome. Performing a direct regression of the outcome  $Y$  on the treatment  $T$  and features  $x$ , without controlling for a multitude of other potential confounders, will produce biased estimation. In machine learning, similar problems are studied under the literature of off-policy evaluation and contextual bandits, where the learner observes the outcome only for the selected treatment. The standard approach in these lines of work is to impose active experimentation or to assume that the data collection or logging policy is known to the analyst. However, in many real-world settings, active experimentation may be infeasible, and there can be a vast amount of observational data for which the logging policy is unknown. Leveraging such observational data can also benefit the optimization of online learning algorithms (e.g. by identifying a suitable policy class for the contextual bandit algorithm).

---

\*Microsoft Research-New England

<sup>†</sup>Microsoft Research-New England

<sup>‡</sup>Microsoft Research-New York City

<sup>1</sup>Source code and Monte Carlo simulations available at [github.com/Microsoft/EconML/tree/master/prototypes/orthogonal\\_forests](https://github.com/Microsoft/EconML/tree/master/prototypes/orthogonal_forests)

There is a surge of recent work at the interplay of machine learning and causal inference that studies efficient estimation of treatment effects in the presence of high-dimensional controls. Most notably, [Chernozhukov et al. \[2017\]](#) propose a two-stage estimation method called *double machine learning* (double ML) that first orthogonalizes out the effect of high-dimensional confounding factors using sophisticated machine learning algorithms, including Lasso, deep neural nets and random forests, and then estimates the effect of the lower dimensional treatment variables, by running a low-dimensional linear regression between the residualized treatments and residualized outcomes. They show that under the Neyman orthogonality condition, as long as the first-stage estimation is consistent at rate as fast as  $n^{-1/4}$ , the second-stage estimate is  $n^{-1/2}$ -consistent. However, their parametric approach heavily relies on linear dependence between the treatment and the outcome, and can only handle a limited form a heterogeneity.<sup>2</sup> In particular, their approach becomes ineffective when the treatment effect heterogeneity has a non-linear variation.

Another line of work that brings machine learning to causal inference provides fully flexible non-parametric HTE estimation based on random forest techniques [[Wager and Athey, 2015](#), [Athey et al., 2017](#), [Powers et al., 2017](#)]. However, these methods heavily rely on low-dimensional assumption and tend to perform poorly in the presence of high-dimensional controls.

The goal of our work is to bridge the gap between these two lines of work. We propose *orthogonal random forests* (ORF), a method that inherits the flexibility of the random forest framework in capturing heterogeneity of the treatment on a low dimensional set of observables, and the robustness of the double ML method in orthogonalizing the confounding effects of high-dimensional controls.

At a high level, we incorporate double ML into the *generalized random forests* (GRF) algorithm of [Athey et al. \[2017\]](#), which allows us to orthogonalize the effect from the high-dimensional confounders and when performing HTE estimation. Combining the two approaches is highly non-trivial, and it requires careful modifications and new analysis techniques. On the GRF side, we perform local residualization on treatments and outcomes before choosing the splits on the features. This ensures that ORF selects effective splits that maximize the heterogeneity of treatment effects. On the double ML side, we perform a forest-based kernel estimation in the first stage. Consequently, we provide a new analysis for a local kernel Lasso algorithm, which combines techniques from Lasso theory [Hastie et al. \[2015\]](#) with  $U$ -statistics concentration inequality [Hoeffding \[1963\]](#). Focusing on the case where the nuisance functions (of how the controls influence the treatments and outcomes) are high-dimensional linear functions, we show that the nuisance estimation error has a lower order influence on the treatment estimation error, as long as the functions are sufficiently sparse. As a result, our convergence rate is in the same order as oracle convergence rate (as if the true nuisance parameters were known in advance).

Moreover, we show that the framework of ORF can be generalized to a broader class of estimators that we call kernel orthogonal GMM estimators, which allow us to combine other kernel learners (e.g. nearest neighbors) with arbitrary double ML methods. We prove a consistency result for this general class of estimators.

Finally, we provide a comprehensive empirical evaluations on ORF and performs a comparison with several benchmarks, including three variants of GRF. We show that by setting the parameters according to what our theory suggests, ORF consistently outperform all of the benchmarks.

## 2 Orthogonal Random Forest

To describe our algorithm, we consider the following variant of the *partially linear regression* (PLR) model due to [Robinson \[1988\]](#). We have  $n$  observations  $D = \{Z_i = (T_i, Y_i, W_i, x_i)\}_{i=1}^n$  drawn i.i.d. from some underlying distribution such that for each  $i$ ,  $T_i \in \mathbb{R}$  represents the treatment or policy applied,  $Y_i \in \mathbb{R}$  represents the outcome,  $W_i \in \mathbb{R}^p$  represents the control, and  $x_i \in \mathcal{X} \subseteq \mathbb{R}^d$  is the feature vector that captures the hetero-

<sup>2</sup>[Chernozhukov et al. \[2017\]](#) extends double ML to perform HTE estimation by transforming treatments into composite treatments, obtained by taking cross products of heterogeneity features and treatment variables.

geneity. The set of parameters are related via the following equations:

$$Y_i = \theta_0(x_i) T_i + f_0(W_i) + \varepsilon, \quad (1)$$

$$T_i = g_0(W_i) + \eta_i, \quad (2)$$

where  $\eta_i, \varepsilon_i$  represent the unobserved noises such that  $\mathbb{E}[\varepsilon_i | W_i, x_i, T_i] = 0$  and  $\mathbb{E}[\eta_i | x_i, W_i] = 0$ .

In the main equation (1),  $\theta_0: \mathbb{R}^d \rightarrow [-1, 1]$  represents the treatment effect function, and our goal is to estimate the treatment effect  $\theta_0(x)$  for some target feature  $x$ . Note that  $\theta_0$  is a sufficient statistics for optimizing any treatment policy that depends on the features  $x$ , since we can re-write the policy optimization objective as the difference to reference treatment of 0:

$$\operatorname{argmin}_{\pi \in \mathcal{X} \rightarrow \mathbb{R}} \mathbb{E}[\theta_0(x_i) \pi(x_i) + f_0(W_i)] = \operatorname{argmin}_{\pi \in \mathcal{X} \rightarrow \mathbb{R}} \mathbb{E}[\theta_0(x_i) \pi(x_i)]$$

Our approach also extends to the case where  $\theta_0(x_i)$  is replaced with a function that also depends on the controls, albeit in a linear manner  $\theta_0(x_i, W_i) = \alpha(x_i) + \langle \beta(x_i), W_i \rangle$ , and  $\beta(x_i)$  is a sparse vector with support that is invariant to  $x_i$ , while we are interested in estimating the average effect conditioned on  $x_i$  and averaged over  $W_i$ . We focus on the case where the treatment effect solely depends on  $x_i$  for expository purposes.

The confounding equation (2) keeps track of the dependence of the treatment variable on controls: the controls  $W$  affect the treatment  $T$  via the function  $g_0$  and also affect the outcome  $Y$  via the function  $f_0$ . We consider functions  $f_0$  and  $g_0$  that are high-dimensional linear functions:

$$f_0(W_i) = \langle W_i, \beta_0 \rangle, \quad g_0(W_i) = \langle W_i, \gamma_0 \rangle \quad (3)$$

where  $\beta_0, \gamma_0$  are both  $k$ -sparse vectors in  $\mathbb{R}^p$ . Moreover, let  $q_0(x_i) = \theta_0(x_i) \gamma_0 + \beta_0$ . Consequently, this means

$$\langle W_i, q_0(x_i) \rangle = \mathbb{E}[Y_i | x_i, W_i].$$

Our framework actually extends to other forms of  $f$  and  $g$ , as long as the expected functions  $\mathbb{E}[Y | x, W]$  and  $\mathbb{E}[T | W]$  can be estimated by at a sufficiently fast rate (e.g. via non-parametric estimation methods). We focus on sparse linear functions since we can establish a formal guarantee for the non-parametric estimator via our kernel Lasso analysis.

Following the approach of generalized random forest (GRF) by [Athey et al. \[2017\]](#), we estimate  $\theta_0(x)$  by first assigning a set of similarity weights over the observations, and then computing  $\hat{\theta}$  via a kernel regression with the set of weights. However, to overcome the confounding effects from the high-dimensional controls  $W_i$ , we rely on double ML method due to [Chernozhukov et al. \[2017\]](#) that orthogonalizes the effects from  $W_i$  when estimating  $\theta$ . We will first introduce our forest-based kernel learner, and then describe how orthogonal random forest (ORF) uses it to perform kernel estimation.

## 2.1 Random Forest as a Kernel Learner

Our random forest algorithm proceeds over  $B$  iterations. In each iteration  $b$ , we first randomly subsample without replacement a subset  $S_b$ , and then the tree learner  $\mathcal{L}_T$  randomly partitions  $S_b$  into two subsets of equal sizes  $S_b^1, S_b^2$ . The learner uses  $S_b^1$  to place splits in the tree, and uses the features  $x_i$  in  $S_b^2$  for stopping rules and balance maintenance. To ensure honesty of the tree,  $\mathcal{L}_T$  does not select the splits using the controls and outcomes in  $S_b^2$ , which will be used for the kernel estimation later.

Similar to GRE, our tree learner starts with a root node that contains the entire feature vector space  $\mathcal{X}$  and iteratively grows the tree by greedily selecting the splits that maximize a certain splitting criterion, until a certain stopping condition is met. To incorporate double ML in placing the splits, each internal node  $P$  of  $\mathcal{L}_T$  will perform the following two-stage estimation for  $\hat{\theta}_P$  over the set of observations of  $S_b^1$  that

reach  $P$  (denoted  $P \cap S_b^1$ ). First, we compute Lasso estimates  $\hat{q}_P$  and  $\hat{\gamma}_P$ :

$$\begin{aligned}\hat{\gamma}_P &= \operatorname{argmin}_{\gamma} \frac{1}{2|P \cap S_b^1|} \sum_{Z_i \in P \cap S_b^1} (T_i - \langle W_i, \gamma \rangle)^2 + \lambda_\gamma \|\gamma\|_1 \\ \hat{q}_P &= \operatorname{argmin}_q \frac{1}{2|P \cap S_b^1|} \sum_{Z_i \in P \cap S_b^1} (Y_i - \langle W_i, q \rangle)^2 + \lambda_q \|q\|_1\end{aligned}$$

for some regularization parameters  $\lambda_\gamma$  and  $\lambda_q$ . We then use  $\hat{\gamma}_P$  and  $\hat{q}_P$  to residualize the outcomes and treatments:

$$\hat{Y}_i = Y_i - \langle W_i, \hat{q}_P \rangle, \quad \hat{T}_i = T_i - \langle W_i, \hat{\gamma}_P \rangle$$

The residualization step partials out the confounding effects from  $W_i$  in each observation. Then second-stage estimation for  $\hat{\theta}_P$  is obtained by simply solving the residualized least square regression:

$$\hat{\theta}_P = \operatorname{argmin}_{\theta} \frac{1}{|P \cap S_b^1|} \sum_{Z_i \in P \cap S_b^1} \frac{1}{2} (\langle \hat{T}_i, \theta \rangle - \hat{Y}_i)^2$$

Given the estimates  $\hat{\theta}_P$ ,  $\hat{\gamma}_P$  and  $\hat{q}_P$  at each parent node  $P$ , we would like to find an axis-aligned split of some node into two children  $C_1$  and  $C_2$  such that if we perform the same two-stage estimation separately at each child, the new estimates  $\hat{\theta}_{C_1}$  and  $\hat{\theta}_{C_2}$  will maximize the following heterogeneity score:

$$\Delta(C_1, C_2) = \sum_{j=1}^2 \frac{1}{|C_j|} (\hat{\theta}_{C_j} - \hat{\theta}_P)^2.$$

However, performing the two-stage estimation of  $\hat{\theta}_{C_1}$  and  $\hat{\theta}_{C_2}$  for all possible splits is too computationally expensive. Instead, we will approximate these estimates by taking a Newton step from the parent node estimate  $\hat{\theta}_P$ . More formally, let us write  $\ell_{\text{res}}(\theta, Z_i) = \frac{1}{2} (\langle \hat{T}_i, \theta \rangle - \hat{Y}_i)^2$  to denote the residualized square loss function. Then for each observation  $Z_i$  that reaches the node  $P$ , the gradient is:

$$\nabla_{\theta} \ell_{\text{res}}(\hat{\theta}_P, Z_i) = (\hat{Y}_i - \hat{\theta}_P \hat{T}_i) \hat{T}_i \quad (4)$$

The empirical Hessian over the observations in  $P \cap S_b^1$  is:

$$A_P = \nabla_{\theta}^2 \left( \frac{\sum_{i \in P \cap S_b^1} \ell_{\text{res}}(\hat{\theta}_P, Z_i)}{|P \cap S_b^1|} \right) = - \frac{\sum_{i \in P \cap S_b^1} \hat{T}_i^2}{|P \cap S_b^1|}$$

Then for any child node  $C$  given by a candidate split, our proxy estimate is then given by taking a Newton step with observations that reach node  $C$ :

$$\tilde{\theta}_C = \hat{\theta}_P - \sum_{i \in C} A_P^{-1} (\hat{Y}_i - \hat{\theta}_P \hat{T}_i) \hat{T}_i$$

Given the estimates  $\tilde{\theta}_C$ , we will select the split that maximizes the following proxy heterogeneity score:<sup>3</sup>

$$\tilde{\Delta}(C_1, C_2) = \sum_{j=1}^2 \frac{1}{|C_j|} (\tilde{\theta}_{C_j} - \hat{\theta}_P)^2 \quad (5)$$

<sup>3</sup>Our splitting criterion can be viewed as an instantiation of the one in [Athey et al. \[2017\]](#) with a moment function defined by the gradient of the residualized square loss.

When building the tree, the learner also ensures that the leaf contains at least  $r$  observations in  $S_b^2$  (in the experiments  $r = 5$ ). For each tree indexed  $b \in [B]$ , let  $L_b(x) \subseteq \mathcal{X}$  be its leaf containing the target feature  $x$ . For each  $b$ , will then assign the following *tree weight* to each observation  $i$ :

$$K(x_i, x, (S_b^1, S_b^2)) = \frac{\mathbf{1}[(x_i \in L_b(x)) \wedge (Z_i \in S_b^2)]}{|L_b^2(x)|} \quad (6)$$

Finally, we assign the following *importance weight* by taking an average over all of the  $B$  trees:

$$K(x_i, x) = \frac{1}{B} \sum_{b=1}^B K(x_i, x, (S_b^1, S_b^2)) \quad (7)$$

The importance weights will be useful for our next kernel two-stage estimation.

## 2.2 Kernel Two-Stage Estimation

We are now ready to present the full algorithm ORF. The algorithm first partitions the input dataset  $D$  into  $D_1$  and  $D_2$ , and then runs the forest-based kernel learner on  $D_1$  and  $D_2$  to build two forests. We will write  $\{w_{ib}\}_{b=1}^B$  and  $w_i$  to denote the tree weights and importance weights over the observations in  $D_1$ , and write  $\{a_{ib'}\}_{b'=1}^B$  and  $a_i$  to denote the tree weights and importance weights over the observations in  $D_2$ . We will utilize these weights to perform a kernel two-stage estimation. First, we solve the following two weighted Lasso problem using observations in  $D_1$ :

$$\hat{\gamma} = \operatorname{argmin}_{\gamma} \frac{1}{2} \sum_{i: Z_i \in D_1} w_i (T_i - \langle W_i, \gamma \rangle)^2 + \lambda_{\gamma} \|\gamma\|_1 \quad (8)$$

$$\hat{q} = \operatorname{argmin}_q \frac{1}{2} \sum_{i: Z_i \in D_1} w_i (Y_i - \langle W_i, q \rangle)^2 + \lambda_q \|q\|_1 \quad (9)$$

Then for each observation  $Z_i = (T_i, Y_i, W_i, x_i) \in D_2$ , we compute the residuals using Lasso estimates  $\hat{\gamma}$  and  $\hat{q}$ :

$$\hat{Y}_i = Y_i - \langle X, \hat{q} \rangle, \quad \hat{T}_i = T_i - \langle W_i, \hat{\gamma} \rangle \quad (10)$$

Finally, we compute the following weighted residualized regression problem on the dataset:

$$\hat{\theta} = \operatorname{argmin}_{\theta} \sum_{i=1}^n a_i (\theta \hat{T}_i - \hat{Y}_i)^2 \quad (11)$$

The full algorithm is presented in Section 2.2.

## 2.3 Convergence Rate

To state the convergence result of ORF, we will rely on the same set of assumptions in [Wager and Athey \[2015\]](#), [Athey et al. \[2017\]](#) on the behavior of the tree learner.

**Assumption 2.1** (Tree learner assumption). *We assume the tree learner  $\mathcal{L}_T$  takes a data set  $S$  as input, randomly partition  $S$  as two random subsets  $S^1, S^2$  of equal sizes, and builds a tree that is*

- $\omega$ -regular for  $\omega \leq 0.2$ : each split leaves at least a fraction  $\omega$  of the observations in  $S^2$  on each side of the split and, moreover, the trees are fully grown to depth  $k$  for some  $k \in \mathbb{N}$ , i.e., there are between  $r$  and  $2r - 1$  observations in each leaf of the tree.
- a random-split tree: if at every step of the tree-growing procedure, marginalizing over the internal randomness of the learner, the probability that the next split occurs along the  $j$ -th feature is bounded below by  $\pi/d$  for some  $0 < \pi \leq 1$ , for all  $j = 1, \dots, d$ .

---

**Algorithm 1** Orthogonal Random Forest (ORF)
 

---

- 1: **Input:** data set  $D$  of size  $n$ , target point  $x$ , base tree learner  $\mathcal{L}_T$ , parameter  $B$  for number of trees, parameter  $s$  subsamples size
  - 2: Randomly partition  $D$  into two data sets  $D_1$  and  $D_2$  of equal size
  - 3: **Random forest for nuisance estimation:**
  - 4:   **For** each tree  $b = 1, \dots, B$ :
  - 5:     Let  $S_b$  be a set of  $s$  observations randomly subsampled without replacement from  $D_1$
  - 6:     Randomly partition  $S_b$  into two data sets of even size:  $S_b^1$  and  $S_b^2$
  - 7:     Apply learner  $\mathcal{L}_T$  to build a tree  $T_b$  using data set  $S_b^1$ , the feature vectors in  $S_b^2$
  - 8:     Assign importance weight  $w_i$  to each observation  $i$  in  $D_1$  according to Equation (7)
  - 9:     Compute  $\hat{\gamma}$  and  $\hat{q}$  by solving the kernel Lasso with weights  $w_i$  (as in Equations (8) and (9))
  - 10: **Random forest for target estimation:**
  - 11:   **For** each tree  $b' = 1, \dots, B$ :
  - 12:     Let  $S_{b'}$  be a set of  $s$  observations randomly subsampled without replacement from  $D_2$
  - 13:     Randomly partition  $S_{b'}$  into two data sets of even size:  $S_{b'}^1$  and  $S_{b'}^2$
  - 14:     Apply learner  $\mathcal{L}_T$  to build a tree  $T_{b'}$  using data set  $S_{b'}^1$ , the feature vectors in  $S_{b'}^2$
  - 15:     Assign weight  $a_i$  to each observation  $i$  in  $D_2$  according to Equation (7)
  - 16:     **For** each  $Z_i \in D_2$ : compute residuals  $\hat{Y}_i$  and  $\hat{T}_i$  (as in Equation (10))
  - 17:     Compute  $\hat{\theta}$  as a solution to the kernel residualized regression problem as in Equation (11)
  - 18: **Output:**  $\hat{\theta}$
- 

We will also rely on the following assumptions on the partial linear regression (PLR) model.

- Assumption 2.2** (PLR assumption). 1.  $\theta_0: \mathbb{R}^d \rightarrow \mathbb{R}$  is 1-Lipschitz w.r.t  $\ell_2$  norm. The sparse vectors have bounded norms  $\|\beta_0\|_1, \|\gamma_0\|_1 \leq O(k)$ , and the noise terms have bounded scales  $|\eta_i|, |\varepsilon_i| \leq 1$ .
2. The feature  $x_i$  is drawn from the uniform distribution  $U[0, 1]^d$ . The control  $W_i$  lies in the range of  $[-1, 1]^p$ , and for any feature  $x_i$ , the conditional covariance matrix has minimum eigenvalue bounded away from 0, that is, there is some  $\lambda$  with  $1/\lambda_0 \leq O(1)$  such that

$$\mathbb{E}[W_i W_i^\top | x_i] \geq \lambda_0 I_p$$

The first assumption imposes standard Lipschitzness and boundedness conditions, and the second assumption is useful for the kernel Lasso analysis.

**Theorem 2.3.** Under Assumption 2.1 and Assumption 2.2, suppose ORF is instantiated with parameters  $B \geq n/s$  and  $s = \left(\frac{n}{k^2 \ln p}\right)^{\frac{1}{2\tau+1}}$  with  $\tau = \frac{1}{2\alpha d}$  and  $\alpha = \frac{\log(\omega^{-1})}{\pi \log((1-\omega)^{-1})}$ , then the output estimate  $\hat{\theta}$  by the kernel orthogonal random forest satisfies

$$\mathbb{E}[|\hat{\theta} - \theta_0(x)|] \leq O\left(\left(\frac{\ln p}{n}\right)^{\frac{\tau}{2\tau+1}}\right)$$

as long as the support size of the linear functions  $\beta_0$  and  $\gamma_0$  satisfy  $k \leq O\left(\left(\frac{n}{\ln p}\right)^{\frac{\tau}{10\tau+4}}\right)$ .

### 3 Kernel Orthogonal GMM Estimation

In this section, we provide formal theoretical analysis to justify our approach. To demonstrate the generality of our framework, we will actually study a more general problem of generalized method of moments (GMM) estimation problem, and present general algorithmic framework that combines kernel methods and double ML for GMM estimation.

**GMM estimation problem.** Suppose we have access to a data set  $D$  of  $n$  observations  $Z_1, \dots, Z_n$  drawn independently from some underlying distribution  $\mathcal{D}$  over the observation domain  $\mathcal{Z}$ . Let  $\psi: \mathcal{Z} \times \mathbb{R}^p \times \mathbb{R}^\ell \rightarrow \mathbb{R}^p$  be a score function that maps an observation  $Z$ , parameter vector  $\theta \in \Theta \subset \mathbb{R}^p$ , and nuisance vector  $\nu$  to a vector-valued score  $\psi(Z, \theta, \nu)$ . Each observation  $Z_i$  contains a feature vector  $x_i$  in the feature domain  $\mathcal{X} \subseteq \mathbb{R}^d$ . A nuisance function  $h: \mathbb{R}^L \rightarrow \mathbb{R}^\ell$  that takes as input a subvector  $W_i$  (and sometimes the feature vector  $x_i$ ) in the input, and outputs a nuisance vector in  $\mathbb{R}^\ell$ . Throughout the section we will be assuming that the dimensions  $p, \ell, d$  are constants, while  $L$  can be growing with  $n$ .

For any feature vector  $x_i \in \mathcal{X}$  and parameter vector  $\theta \in \Theta$ , and nuisance function  $h: \mathbb{R}^L \rightarrow \mathbb{R}^\ell$ , define function

$$m(x_i; \theta, h) = \mathbb{E}[\psi(Z, \theta, h(W)) | x_i] \quad (12)$$

to denote the expected score of  $\theta$  and  $h$  conditioned on  $x'$ . Let  $x$  be the target feature vector. Our goal is to estimate the quantity  $\theta_0(x)$  via local moment condition:

$$\theta_0(x) \text{ solves: } m(x; \theta, h_0) = \mathbb{E}[\psi(Z, \theta, h_0(W)) | x] = 0$$

where  $h_0$  is the target nuisance function (given by the sparse vectors  $q_0$  and  $\gamma_0$  in the PLR model).

The key assumption for applying double ML is the following local orthogonality condition. Intuitively, the condition says that for any target feature vector  $x$ , the score function is not sensitive to tiny perturbations in the nuisance parameters.

**Definition 3.1** (Local Orthogonality). Fix any estimator  $\hat{h}$  for the nuisance function. Then the Gateaux derivative with respect to  $h$  is defined as:

$$D_\psi[\hat{h} - h_0 | x] = \mathbb{E}[\nabla_h \psi(Z, \theta(x), h_0(W)) \cdot (\hat{h}(W) - h_0(W)) | x]$$

where  $\nabla_h$  denotes the gradient of  $\psi$  with respect to the final  $\ell$  arguments. We say that the moment conditions are locally orthogonal if for all  $x$ :  $D_\psi[\hat{h} - h_0 | x] = 0$ .

An even stronger condition that implies local orthogonality is the following conditional orthogonality:

$$\mathbb{E}[\nabla_h \psi(Z, \theta_0(x), h_0(W)) | W, x] = 0 \quad (13)$$

We will now introduce the moment condition for PLR. In the appendix, we will also establish its conditional orthogonality.

**Moments condition for PLR:** We adopt the score function of the double machine learning method due to [Chernozhukov et al. \[2017\]](#): for any observation  $Z = (T, Y, W, x)$  (with  $T \in \mathbb{R}$ ,  $Y \in \mathbb{R}$ ,  $W \in \mathbb{R}^L$ ,  $x \in \mathbb{R}^d$ ), any parameter  $\theta \in \mathbb{R}$ , nuisance estimate  $h$  parameterized by vectors  $q(x), \gamma(x) \in \mathbb{R}^L$ , the score function is defined as:

$$\psi(Z; \theta(x), h(W, x)) = \{Y - \langle W, q(x) \rangle - \theta(x)(T - \langle W, \gamma(x) \rangle)\} (T - \langle W, \gamma(x) \rangle), \quad (14)$$

where  $h(W, x) = (\langle W, q(x) \rangle, \langle W, \gamma(x) \rangle)$ . Moreover, the target nuisance function is defined as

$$h_0(W, x) = (\langle W, q_0(x) \rangle, \langle W, \gamma_0(x) \rangle),$$

where  $q_0(x) = \theta_0(x)\gamma_0 + \beta_0$  as defined in the previous section.

A centerpiece of the algorithm is a base kernel learner  $\mathcal{L}_k$ . The goal of the kernel learner is to identify observations that look similar to our target point  $x$ , so that we can compute an accurate local estimation using such nearby observations.

**Base kernel learner.** The learner  $\mathcal{L}_k$  takes a dataset of observations as input, and outputs a kernel weighting function  $K: \mathcal{X} \times \mathcal{X} \times \mathcal{Z}^m \rightarrow [0, 1]$ . In particular, given any target feature  $x$  and a set of observations  $S$ , the weight of each observation  $Z_i$  in  $S$  with feature vector  $x_i$  is  $K(x_i, x, S)$ . For the convenience of our analysis, we will assume that the weights among the observations in  $S$  are non-negative and normalized such that  $\sum_{Z_i \in S} K(x_i, x, S) = 1$ .

The following kernel shrinkage assumption on the weighting function is a key ingredient in our theoretical analysis.

**Assumption 3.2** (Kernel Shrinkage). *The kernel weighting function output by the learner  $\mathcal{L}_k$  when it is given  $s$  i.i.d. observations drawn from distribution  $\mathcal{D}$  satisfies*

$$\mathbb{E}[\sup\{\|x - x_i\|_2 : K(x_i, x, S) > 0\}] = O(s^{-\tau})$$

We are now ready to present our general algorithm in Algorithm 2. The algorithm can be viewed as a generalization of orthogonal random forest. It computes  $B$  different weighting functions over  $B$  random subsets of the input data, and then uses the weighting functions to perform local two-stage estimation.

---

**Algorithm 2** Orthogonal GMM estimation

---

- 1: **Input:** data set  $D$  of size  $n$ , target point  $x$ , kernel base learner  $\mathcal{L}_k$ , parameter  $B$ : number of kernels, parameter  $s$  subsample size
- 2: Randomly split the data set  $D$  into two data sets of equal size  $D_1$  and  $D_2$
- 3: **First stage: nuisance estimation:** For each  $Z_i \in D_1$ , set weight  $w_{ib} = 0$  for all  $b \in [B]$
- 4: **For**  $b = 1, \dots, B$ :
  - 5: Let  $S_b$  be a set of  $s$  observations randomly subsampled without replacement from  $D_1$
  - 6: Randomly partition  $S_b$  into two data sets of even size:  $S_b^1$  and  $S_b^2$
  - 7: Let  $K_b$  be the kernel function computed by  $\mathcal{L}_k$  using  $S_b^1$  and the feature vectors in  $S_b^2$
  - 8: **For** each  $Z_i \in S_b^2$ , compute weight  $w_{ib} = K_b(x_i, x, S_b)$
- 9: Compute nuisance estimate  $\hat{h}$  by performing a kernel nuisance estimation with the weights  $\{w_{ib}\}$
- 10: **Second stage: moment estimation with  $\hat{h}$ :** For each  $Z_i \in D_2$ , set weight  $a_{ib} = 0$  for all  $b \in [B]$
- 11: **For**  $b' = 1, \dots, B$ :
  - 12: Let  $S_{b'}$  be a set of  $s$  observations randomly subsampled without replacement from  $D_2$
  - 13: Randomly partition  $S_{b'}$  into two data sets of even size:  $S_{b'}^1$  and  $S_{b'}^2$
  - 14: Let  $K_{b'}$  be the kernel function computed by  $\mathcal{L}_k$  using  $S_{b'}^1$  and the feature vectors in  $S_{b'}^2$
  - 15: **For** each  $Z_i \in S_{b'}^2$ : let  $a_{ib} = K_{b'}(x, x_i, S_{b'})$
- 16: Compute  $\hat{\theta}$  as a solution to:

$$\frac{1}{B} \sum_{i: Z_i \in D_2} \sum_{b=1}^B a_{ib'} \psi(Z_i; \theta, \hat{h}(W_i)) = 0$$


---

### 3.1 Convergence Rate

Now we establish the convergence rate of  $\|\hat{\theta} - \theta_0(x)\|$ . In this section, we will assume consistency of the overall estimation process, i.e. that  $\|\hat{\theta} - \theta_0(x)\| = o_p(1)$ , and prove a rate of convergence conditional on consistency. In the next section we will also argue consistency under some extra set of convexity conditions. In essence, consistency allows us to restrict the estimate  $\hat{\theta}$  in a cone around the true parameter, such that  $\|\hat{\theta} - \theta_0(x)\|^2 < \kappa_n \|\hat{\theta} - \theta_0(x)\|$ , for some  $\kappa_n = o_p(1)$ . Within this cone, we prove an explicit convergence rate of the estimation error.

To show our convergence rate, in addition to Assumption 3.2 on kernel shrinkage, we only rely on the following assumptions on the moment condition.

**Assumption 3.3.** *The moment condition and the score function satisfy the following:*

1. *The moment condition satisfies local orthogonality.*
2. *The Jacobian  $M_0 = \nabla_{\theta} m(x; \theta_0, h_0)$  has minimum eigenvalue bounded away from zero.*
3. *For every  $j \in [p]$ , the expected Hessian  $\mathbb{E} \left[ \nabla_{\theta, \hat{h}}^2 \psi_j(Z; \theta, h(W)) \mid x \right]$  has eigenvalues bounded above by a constant  $O(1)$  for all  $\theta$  and  $h$ .*
4. *For any fixed parameters  $\theta$  and  $h$ ,  $m(x; \theta, h)$  is a  $L$ -Lipschitz function in  $x$  for some constant  $L$ .*
5. *The estimate  $\hat{\theta}$  output by the algorithm lies in some bounded set  $\Theta$  with constant diameter.*
6. *There exists a bound  $\psi_{\max}$  such that for any observation  $Z$ , the nuisance estimate  $\hat{h}$  computed by the algorithm satisfies  $\|\psi(Z; \theta, \hat{h})\|_{\infty} \leq \psi_{\max}$  for any  $\theta \in \Theta$ .*
7. *The moment  $\psi(Z; \theta, \hat{h})$  is  $L$ -Lipschitz in  $\theta$  for any  $Z, \hat{h}$ .*

**Theorem 3.4.** *Under Assumption 3.3 and Assumption 3.2, if the first stage estimates are consistent at a sufficiently fast rate:*

$$\mathbb{E} \left[ \|\hat{h}(W) - h_0(W)\|^2 \mid x \right] = o_p \left( \sqrt{p} \left( s^{-\tau} + \psi_{\max} \sqrt{\frac{sp \ln(pn/s)}{n}} \right) \right)$$

*and the second stage estimate is consistent, i.e.  $\mathbb{E} \left[ \|\hat{\theta} - \theta_0(x)\| \right] = o_p(1)$ , then the first stage estimation error can asymptotically be ignored and the final stage estimate  $\hat{\theta}$  converges at an oracle rate of:*

$$\mathbb{E} \left[ \|\hat{\theta} - \theta_0(x)\| \right] \leq O \left( \sqrt{p} \left( s^{-\tau} + \psi_{\max} \sqrt{\frac{sp \ln(pn/s)}{n}} \right) \right) \quad (15)$$

The following functions will be useful for our analysis:

$$\begin{aligned} \Psi(\theta, \hat{h}) &= \frac{1}{B} \sum_{b=1}^B \sum_{i: Z_i \in D_2} a_{ib} \psi(z_i; \theta, \hat{h}(W_i)), \\ \Lambda_n(\theta) &= m(x; \theta, \hat{h}) - \Psi(\theta, \hat{h}) \end{aligned}$$

Moreover, let  $\mu(\theta) = \mathbb{E} \left[ \Psi(\theta, \hat{h}) \right]$ , where the expectation is taken over both the random draws of the observations and the internal randomness of the algorithm.

**Lemma 3.5.** *For any  $\theta$ ,*

$$\mu(\theta) = \frac{1}{B} \mathbb{E} \left[ \sum_{b=1}^B \sum_{i: Z_i \in D_2} a_{ib} m(x_i; \theta, \hat{h}) \right].$$

*Proof of Lemma 3.5.* Consider any example  $Z_i \in D_2$  and iteration  $b \in [B]$ . We will write  $\xi$  to denote the internal randomness of the algorithm, and write  $Z_{-i}$  to denote the random draws of all of the examples in  $D$  other than  $Z_i$ . For any realized feature vector  $x_i$ , we know the weight  $a_{ib}$  is a deterministic function of  $Z_{-i}, x_i$  and  $\xi$ . At the same time, we have for any estimate  $\hat{h}$ ,

$$\mathbb{E} \left[ \psi(Z_i; \theta, \hat{h}(W_i)) \mid Z_{-i}, x_i, \xi \right] = \mathbb{E} \left[ \psi(Z_i; \theta, \hat{h}(W_i)) \mid x_i \right] = m(x_i; \theta, \hat{h})$$

Thus, we can write:

$$\begin{aligned}
\mathbb{E}\left[a_{ib} \psi(Z_i; \theta, \hat{h}(W_i)) \mid x_i, \hat{h}\right] &= \mathbb{E}_{Z_{-i}, \xi \mid x_i, \hat{h}} \left[ \mathbb{E}\left[a_{ib} \psi(Z_i; \theta, \hat{h}(W_i)) \mid Z_{-i}, x_i, \hat{h}, \xi\right] \right] \\
&= \mathbb{E}_{Z_{-i}, \xi \mid x_i, \hat{h}} \left[ \mathbb{E}\left[a_{ib} \mid Z_{-i}, x_i, \hat{h}, \xi\right] \mathbb{E}\left[\psi(Z_i; \theta, \hat{h}(W_i)) \mid Z_{-i}, x_i, \hat{h}, \xi\right] \right] \\
&= \mathbb{E}_{Z_{-i}, \xi \mid x_i, \hat{h}} \left[ \mathbb{E}\left[a_{ib} \mid Z_{-i}, x_i, \hat{h}, \xi\right] m(x_i; \theta, \hat{h}) \right] \\
&= \mathbb{E}_{Z_{-i}, \xi \mid x_i, \hat{h}} \left[ \mathbb{E}\left[a_{ib} m(x_i; \theta, \hat{h}) \mid Z_{-i}, x_i, \hat{h}, \xi\right] \right] = \mathbb{E}\left[a_{ib} m(Z_i; \theta, \hat{h}) \mid x_i, \hat{h}\right]
\end{aligned}$$

By the law of iterated expectation, we also get

$$\mathbb{E}\left[a_{ib} \cdot \psi(Z_i; \theta, \hat{h}(W_i))\right] = \mathbb{E}_{x_i, \hat{h}} \left[ \mathbb{E}\left[a_{ib} \psi(Z_i; \theta, \hat{h}(W_i)) \mid x_i, \hat{h}\right] \right] = \mathbb{E}_{x_i, \hat{h}} \left[ \mathbb{E}\left[a_{ib} m(Z_i; \theta, \hat{h}) \mid x_i, \hat{h}\right] \right] = \mathbb{E}\left[a_{ib} m(Z_i; \theta, \hat{h})\right]$$

By linearity of expectation, we can then rewrite  $\mu(\theta)$  as follows:

$$\mu(\theta) = \frac{1}{B} \sum_{b=1}^B \sum_{i: Z_i \in D_2} \mathbb{E}\left[a_{ib} m(x_i; \theta, \hat{h})\right]$$

This completes the proof.  $\square$

The following Lemma allows us to bound the difference  $(\theta - \theta_0)$  as of a sum of  $m(x; \theta, \hat{h})$  and second order terms.

**Lemma 3.6.** *Under Assumption 3.3, for any nuisance estimate  $\hat{h}$  and parameter  $\theta$ ,*

$$\|\theta - \theta_0\| \leq O(\|m(x; \theta, \hat{h})\|) + \sqrt{p} O\left(\mathbb{E}\left[\|\hat{h}(W) - h_0(W)\|^2 \mid x\right] + \|\theta - \theta_0\|^2\right).$$

*Proof of Lemma 3.6.* Fix a conditioning vector  $x$ . By performing a second order Taylor expansion of each coordinate  $j \in [p]$  of the expected score function around the true parameters  $\theta_0 = \theta_0(x)$  and  $h_0$  and applying the multi-dimensional mean-value theorem, we can write

$$\begin{aligned}
m_j(x; \theta, \hat{h}) &= m_j(x; \theta_0, h_0) + \nabla_{\theta} m_j(x; \theta_0, h_0)' (\theta - \theta_0) + D_{\psi_j}[\hat{h} - h_0 \mid x] \\
&\quad + \underbrace{\mathbb{E}\left[\left((\theta, \hat{h}(W)) - (\theta_0, h_0(W))\right)^\top \nabla_{\theta, h}^2 \psi_j(Z; \tilde{\theta}_j, \tilde{h}_j(W)) \left((\theta, \hat{h}(W)) - (\theta_0, h_0(W))\right) \mid x\right]}_{\rho_j}
\end{aligned}$$

where each  $\tilde{\theta}_j$  is some convex combination of  $\theta$  and  $\theta_0$  and each  $\tilde{h}_j(W)$  is some convex combination of  $\hat{h}(W)$  and  $h_0(W)$ . Note that  $m(x; \theta_0, h_0) = 0$  by definition and  $D_{\psi_j}[\hat{h} - h_0 \mid x] = 0$  by local orthogonality. Let  $\rho$  denote the vector of second order terms. We can thus write the above set of equations in matrix form as:

$$M(\theta - \theta_0) = m(x; \theta, \hat{h}) - \rho$$

where we remind that  $M = \nabla_{\theta} m(x; \theta_0, h_0)$  is the Jacobian of the moment vector. Since by our assumptions  $M$  is invertible and has eigenvalues bounded away from zero by a constant, we can write:

$$(\theta - \theta_0) = M^{-1} m(x; \theta, \hat{h}) + M^{-1} \rho$$

By the boundedness of the eigenvalues of  $M^{-1}$ , we thus have:

$$\|\theta - \theta_0\| = O(\|m(x; \theta, \hat{h})\|) + O\left(\sqrt{p} \|\rho\|_{\infty}\right)$$

By our bounded eigenvalue Hessian assumption, we know that:

$$\|\rho\|_\infty = O\left(\mathbb{E}\left[\|\hat{h}(W) - h_0(W)\|^2 \mid x\right] + \|\theta - \theta_0\|^2\right)$$

Combining the above two equations recovers our claim.  $\square$

Recall that our estimate  $\hat{\theta}$  at the target point  $x$  is the solution to the equation:  $\Psi(\hat{\theta}, \hat{h}) = 0$ . Equivalently, we can also view  $\hat{\theta}$  as the solution for

$$m(x; \hat{\theta}, \hat{h}) = \Lambda_n(\hat{\theta}).$$

This means we can write  $(\hat{\theta} - \theta_0)$  in terms of  $\Lambda_n(\hat{\theta})$ .

**Corollary 3.7.** *Let  $\hat{\theta}$  be the output estimate. Then*

$$\|\hat{\theta} - \theta_0\| = O\left(\|\Lambda_n(\hat{\theta})\| + \sqrt{p} \left(\mathbb{E}\left[\|\hat{h}(W) - h_0(W)\|^2 \mid x\right] + \|\theta - \theta_0\|^2\right)\right)$$

Next, we focus on bounding the scale of  $\Lambda_n(\theta)$  for any  $\theta \in \Theta$ .

**Lemma 3.8** (Uniformly Bounding  $\Lambda_n(\theta)$ ). *For any  $x$ :*

$$\mathbb{E}\left[\sup_{\theta \in \Theta} \|\Lambda_n(\theta)\|_\infty\right] = O\left(s^{-\tau} + \psi_{\max} \sqrt{\frac{s \ln(n)}{n}}\right) \quad (16)$$

*Proof.* The first step is to rewrite the expression of  $\Lambda_n(\theta)$  by adding and subtracting the term  $\mu(\theta)$ . This allows us to decompose  $\Lambda_n(\theta)$  as a sum of two error terms such that the first one is due to the kernel averaging around a neighborhood of  $x$ , and the second one is due to the sampling error of the moment at every data point. Formally, for any  $\theta$ ,

$$\begin{aligned} \Lambda_n(\theta) &= m(x; \theta, \hat{h}) - \mu(\theta) + \mu(\theta) - \frac{1}{B} \sum_{b=1}^B \sum_{i: Z_i \in D_2} a_{ib} \cdot \psi(Z_i; \theta, \hat{h}) \\ &= \underbrace{\frac{1}{B} \mathbb{E}\left[\sum_{b=1}^B \sum_{i: Z_i \in D_2} a_{ib} \cdot (m(x; \theta, \hat{h}) - m(x_i; \theta, \hat{h}))\right]}_{\Gamma(\theta)=\text{kernel error}} + \underbrace{\mu(\theta) - \frac{1}{B} \sum_{b=1}^B \sum_{i: Z_i \in D_2} a_{ib} \cdot \psi(Z_i; \theta, \hat{h})}_{\Delta(\theta)=\text{sampling error}} \end{aligned}$$

**Bounding kernel error via shrinkage.** The Kernel error  $\Gamma$  is bounded by the Lipschitzness of the conditional moment function and the kernel shrinkage assumption:

$$\begin{aligned} \mathbb{E}\left[\sup_{\theta \in \Theta} \|\Gamma(\theta)\|_\infty\right] &\leq \mathbb{E}\left[\sup_{\theta \in \Theta} \frac{1}{B} \sum_{b=1}^B \sum_{i: Z_i \in D_2} a_{ib} \cdot \|m(x; \theta, \hat{h}) - m(x_i; \theta, \hat{h})\|_\infty\right] \\ &\leq L \cdot \mathbb{E}\left[\frac{1}{B} \sum_{b=1}^B \sum_{i: Z_i \in D_2} a_{ib} \cdot \|x - x_i\|_2\right] \\ &\leq L \frac{1}{B} \sum_{b=1}^B \mathbb{E}[\sup\{\|x - x_i\|_2 : a_{ib} > 0\}] \leq \mathcal{O}(s^{-\tau}) \end{aligned}$$

where the first inequality follows from triangle inequality, second follows from Lipschitzness of  $m$ , third follows from the form of the normalization of kernel weighting function, and the last follows from the kernel shrinkage assumption.

**Bounding sampling error via  $U$ -statistics.** Fix any nuisance estimate  $\hat{h}$ , then each term  $\sum_{i:Z_i \in D_2} a_{ib} \cdot \psi_j(Z_i; \theta, \hat{h})$  is computed based on a random sub-sample of  $D_2$  (without replacement) in the input data set  $S$ . In particular, it can be viewed as a Monte Carlo approximation to a  $U$ -statistics. By the concentration of  $U$ -statistic and standard Chernoff bound [Hoeffding \[1963\]](#), we can obtain the following tail bound on  $\Psi(\theta, \hat{h})$ . (See the appendix for proofs.)

**Lemma 3.9.** Fix any estimate  $\theta$ , moment coordinate  $j \in [p]$  and  $\delta \in (0, 1)$ . Then with probability at least  $1 - \delta$  over the randomness of the random draws of  $D$  and the internal randomness of the algorithm,

$$|\Delta_j(\theta)| = |\Psi_j(\theta, \hat{h}) - \mu_j(\theta)| \leq \mathcal{O}\left(\psi_{\max} \sqrt{\ln(1/\delta)} \left(\frac{s}{n}\right)\right)$$

as long as  $B \geq n/s$  and  $|\psi_j(Z; \theta, \hat{h})| \leq \psi_{\max}$  for any  $\theta \in \Theta$  and observation  $Z$ .

Next, we will use a covering number argument to bound

$$\mathbb{E}\left[\sup_{\theta \in \Theta} \|\Psi(\theta, \hat{h}) - \mu(\theta)\|_{\infty}\right]$$

Let  $\mathcal{C} = \mathcal{C}(\Theta, \varepsilon)$  be  $\varepsilon$ -cover over the set  $\Theta$ , that is, for any  $\theta \in \Theta$ , there exists some  $\theta' \in \mathcal{C}$  such that  $\|\theta - \theta'\|_2 \leq \varepsilon$ . Observe, that when  $\Theta$  is a bounded set in  $\mathbb{R}^p$  with constant diameter, then by standard arguments, there exists a cover of size  $1/\varepsilon^p$ .

**Lemma 3.10.** Fix any nuisance estimate  $\hat{h}$  from the first stage such that  $\|\psi(Z; \theta, \hat{h})\|_{\infty} \leq \psi_{\max}$  for any  $\theta \in \Theta$  and observation  $Z$ . Then

$$\mathbb{E}\left[\sup_{\theta \in \Theta} \|\Delta(\theta)\|_{\infty}\right] = \mathbb{E}\left[\sup_{\theta \in \Theta} \|\Psi(\theta, \hat{h}) - \mu(\theta)\|_{\infty}\right] \leq \mathcal{O}\left(\psi_{\max} \sqrt{\frac{sp \ln(pn/s)}{n}}\right)$$

*Proof.* Let  $\mathcal{C}(\Theta, \varepsilon)$  be a cover of  $\Theta$ , of size  $O(1/\varepsilon^p)$ , which is guaranteed to exist by the boundedness of  $\Theta$ . By applying the concentration bound in [Lemma 3.9](#) and a union bound over all  $\theta \in \mathcal{C}(\Theta, \varepsilon)$  and  $j \in [p]$ , we have with probability at least  $1 - \delta$  that

$$\sup_{\theta \in \mathcal{C}} \|\Psi(\theta, \hat{h}) - \mu(\theta)\|_{\infty} = \mathcal{O}\left(\psi_{\max} \sqrt{\frac{s \ln(|\mathcal{C}|p/\delta)}{n}}\right) = \mathcal{O}\left(\psi_{\max} \sqrt{\frac{sp \ln(p/(\varepsilon\delta))}{n}}\right)$$

Then by the Lipschitzness of  $\psi$  in  $\theta$  for any  $\hat{h}$  and  $Z_i$  and also the boundedness of  $\psi$ , we also have

$$\mathbb{E}\left[\sup_{\theta \in \Theta} \|\Psi(\theta, \hat{h}) - \mu(\theta)\|_{\infty}\right] = \mathcal{O}\left(\psi_{\max} \sqrt{\frac{sp \ln(p/(\varepsilon\delta))}{n}} + \varepsilon + \delta\psi_{\max}\right)$$

Setting the parameters  $\varepsilon \leq O(\sqrt{s/n})$  and  $\delta \leq O(\sqrt{s/n})$ , we can obtain the stated bound. □

Combining our bounds on  $\Gamma(\theta)$  and  $\Delta(\theta)$  yields the proof of [Lemma 3.8](#). □

**Wrapping up: proof of [Theorem 3.4](#)** Combining the bound on  $\Lambda_n(\hat{\theta})$ , and the result in [Corollary 3.7](#), together with our assumption on the first stage rate, we get that:

$$\|\hat{\theta} - \theta_0(x)\| = \sqrt{p} \mathcal{O}\left(s^{-\tau} + \psi_{\max} \sqrt{\frac{sp \ln(pn/s)}{n}} + \|\hat{\theta} - \theta_0(x)\|^2\right)$$

Since  $\hat{\theta}$  is consistent, we have that for sufficiently large  $n$ , the second term on the right hand side is at most  $\frac{1}{2}\|\hat{\theta} - \theta_0(x)\|$ . Hence, we can conclude that:

$$\|\hat{\theta} - \theta_0(x)\| = \sqrt{p}O\left(s^{-\tau} + \psi_{\max}\sqrt{\frac{sp \ln(pn/s)}{n}}\right)$$

as desired.  $\square$

## 3.2 Consistency

The latter proof assumes consistency of  $\hat{\theta}$  so as to argue that the quadratic term  $\|\hat{\theta} - \theta_0\|_2^2$  is negligible for  $n$  large enough. It remains to show that  $\hat{\theta}$  is also consistent to conclude the proof. We first provide a simple proof of consistency that simply adds the extra assumptions of a strictly unique solution to the moment equation and also Lipschitzness of the expected moment equation with respect to both parameters. This proof does not yield an explicit preliminary rate, but is asymptotic. In the next section we provide a setting under which we can argue consistency at an explicit preliminary rate, which is more desirable for finite sample performance.

**Lemma 3.11.** *Suppose that:*

1.  $\theta_0(x)$  is the unique solution to  $m(x; \theta, h_0) = 0$ , i.e.  $\forall \epsilon > 0 : \inf\{\|m(x; \theta, h_0)\| : \|\theta - \theta_0(x)\| \geq \epsilon\} > 0$
2. The moment  $m(x; \theta, h)$  is  $L$ -Lipschitz continuous in  $\theta$  w.r.t.  $\|\cdot\|$  and also continuous in  $h$  w.r.t. the  $L^1$  norm  $\|f\| = \mathbb{E}[\|f(W)\| \mid x]$  for every  $\theta, h$  and  $x$ .
3. The first stage estimate is consistent w.r.t. the  $L^2$  norm:  $\sqrt{\mathbb{E}[\|\hat{h}(W) - h_0(W)\|^2 \mid x]} = O_p(h_n) = o_p(1)$
4. The subsampling level  $s$  is chosen such that  $\epsilon_n = O\left(s^{-\tau} + \psi_{\max}\sqrt{\frac{s \ln(n)}{n}}\right) = o(1)$

Then the estimate  $\hat{\theta}$  is consistent for  $\theta_0(x)$ , i.e.  $\|\hat{\theta} - \theta_0(x)\| = o_p(1)$ .

*Proof.* By Lemma 3.8 and our assumption on the setting of  $s$ , we have that  $\|m(x; \hat{\theta}, \hat{h})\| = \|\Lambda_n(\theta)\| = o_p(1)$ . Since  $m(x; \theta, h)$  is Lipschitz in  $h$  and  $\hat{h}$  is consistent at a rate  $h_n$  w.r.t to the  $L^2$  and hence also  $L^1$  norm, we have:  $\|m(x; \hat{\theta}, h_0)\| = \|m(x; \hat{\theta}, \hat{h})\| + O_p(h_n) = o_p(1)$ . By our first assumption, for any  $\epsilon$ , there exists a  $\delta$ , such that:  $\Pr[\|\hat{\theta} - \theta_0(x)\| \geq \epsilon] \leq \Pr[\|m(x; \hat{\theta}, h_0)\| \geq \delta]$ . Since  $\|m(x; \hat{\theta}, h_0)\| = o_p(1)$ , the probability on the right-hand-side converges to 0 and hence also the left hand side. Hence,  $\|\hat{\theta} - \theta_0(x)\| = o_p(1)$ .  $\square$

### 3.2.1 Consistency for Gradients of Convex Losses

We show that the latter is true if the moment  $\psi$  is the sub-gradient of a convex loss function  $\ell$ , i.e.  $\psi(Z; \theta, h(W)) = \partial_\theta \ell(Z; \theta, h(W))$ , moreover, we require that gradient of  $m(x; \theta, h)$  with respect to  $\theta$  is Lipschitz in  $h$ .

**Lemma 3.12** (Consistency under Convexity). *Suppose that:*

1. The moment  $\psi$  is the gradient of a convex loss  $\ell$ , i.e.  $\psi(Z; \theta, h(W)) = \nabla_\theta \ell(Z; \theta, h(W))$ .
2. The eigenvalues of the Jacobian  $\nabla_\theta m(x; \theta, h_0)$  are lower bounded by  $\sigma > 0$  for every  $\theta$  and  $x$ . Every entry of the Jacobian  $\nabla_\theta m(x; \theta, h)$  is  $L$ -Lipschitz in  $h$  w.r.t. the  $L^1$  norm  $\|f\| = \mathbb{E}[\|f(W)\| \mid x]$  for every  $\theta$  and  $x$ .
3. The first stage estimate is consistent w.r.t. the  $L^2$  norm:  $\sqrt{\mathbb{E}[\|\hat{h}(W) - h_0(W)\|^2 \mid x]} = O_p(h_n) = o_p(1)$

4. The subsampling level  $s$  is chosen such that  $\epsilon_n = O\left(s^{-\tau} + \psi_{\max} \sqrt{\frac{s \ln(n)}{n}}\right) = o(1)$

Then the estimate  $\hat{\theta}$  is consistent for  $\theta_0(x)$  at a rate  $O_p\left(\frac{2}{\sigma - O_p(Lh_n p)} \sqrt{p}(\epsilon_n + h_n^2)\right)$ .

*Proof.* Since the Jacobian of the expected moment  $m(x; \theta, h_0)$  has eigenvalues lower bounded by  $\sigma$  and each entry of the Jacobian of  $\psi$  is  $L$ -Lispchitz with respect to the nuisance, we have that for every vector  $v \in \mathbb{R}^p$  (with  $p$  the dimension of  $\theta(x)$ ):

$$\begin{aligned} \frac{v^T \nabla_{\theta} m(x; \theta, \hat{h}) v}{\|v\|^2} &\geq \frac{v^T \nabla_{\theta} m(x; \theta, h_0) v}{\|v\|^2} + \frac{v^T (\nabla_{\theta} m(x; \theta, \hat{h}) - m(x; \theta, h_0)) v}{\|v\|^2} \geq \sigma - L \cdot \mathbb{E} \left[ \|\hat{h}(W) - h_0(W)\| \mid x \right] \frac{\|v\|_1^2}{\|v\|_2^2} \\ &\geq \sigma - O_p(Lh_n p) = \sigma - o_p(1) \end{aligned}$$

Where in the last inequality we also used Holder's inequality to upper bound the  $L^1$  norm by the  $L^2$  norm of the first stage error. Thus the expected loss function  $L(\theta) = \mathbb{E}[\ell(Z; \theta, \hat{h}(W) \mid x)]$  is  $\hat{\sigma} = \sigma - o_p(1)$  strongly convex, since  $\nabla_{\theta} m(x; \theta, \hat{h})$  is the Hessian of  $L(\theta)$ . We then have:

$$L(\hat{\theta}) - L(\theta_0) \geq \nabla_{\theta} L(\theta_0)'(\hat{\theta} - \theta_0) + \frac{\hat{\sigma}}{2} \|\hat{\theta} - \theta_0\|_2^2 = m(x; \theta_0, \hat{h})'(\hat{\theta} - \theta_0) + \frac{\hat{\sigma}}{2} \|\hat{\theta} - \theta_0\|_2^2$$

Moreover, by convexity of  $L(\theta)$ , we have:

$$L(\theta_0) - L(\hat{\theta}) \geq \nabla_{\theta} L(\hat{\theta})'(\theta_0 - \hat{\theta}) = m(x; \hat{\theta}, \hat{h})'(\theta_0 - \hat{\theta})$$

Combining the above we get:

$$\frac{\hat{\sigma}}{2} \|\hat{\theta} - \theta_0\|_2^2 \leq (m(x; \hat{\theta}, \hat{h}) - m(x; \theta_0, \hat{h}))'(\hat{\theta} - \theta_0) \leq \|m(x; \hat{\theta}, \hat{h}) - m(x; \theta_0, \hat{h})\|_2 \|\hat{\theta} - \theta_0\|_2$$

Dividing over by  $\|\hat{\theta} - \theta_0\|$ , we get:

$$\|\hat{\theta} - \theta_0\|_2 \leq \frac{2}{\hat{\sigma}} \left( \|m(x; \hat{\theta}, \hat{h})\|_2 + \|m(x; \theta_0, \hat{h})\|_2 \right)$$

The term  $\|m(x; \hat{\theta}, \hat{h})\|_2$  is upper bounded by  $\|\Lambda_n(\hat{\theta})\|_2$ , which was shown in Lemma 3.8 to be of order:  $O\left(\sqrt{p} \left( s^{-\tau} + \psi_{\max} \sqrt{\frac{s \ln(n)}{n}} \right)\right) = o(1)$ . Subsequently, using a second order Taylor expansion around  $h_0$  and orthogonality argument almost identical to the proof of Lemma 3.6, we can show that the second term  $\|m(x; \theta_0, \hat{h})\|_2$  is it upper bounded by  $O_p(\sqrt{p} h_n^2) = o_p(1)$ . Hence,  $\|\hat{\theta} - \theta_0\|_2 = o_p(1)$ , which completes the proof of consistency.  $\square$

## 4 Nuisance Estimation with Kernel Lasso

We now study the error rate of Lasso as our nuisance estimation method. Recall that the nuisance estimate  $\hat{h}$  is the parameterized by two vectors  $\hat{\gamma}$  and  $\hat{q}$ , which are obtained by solving two Lasso regression problems in Equations (8) and (9). Then the error of the nuisance estimate  $\hat{h}$  can be written as

$$\|\hat{h}(W) - h_0(W)\|_2^2 = (\langle \hat{q} - q_0(x), W \rangle)^2 + (\langle \hat{\gamma} - \gamma_0, W \rangle)^2$$

where  $q_0(x) = \theta_0(x)\gamma_0 + \beta_0$  for any  $x$ . Thus, it suffices to bound the  $\ell_2$  error of the sparse vectors:  $\|\hat{q} - q_0(x)\|_1$  and  $\|\hat{\gamma} - \gamma_0\|_1$ . Recall that for any observation  $Z_i = (T_i, Y_i, W_i, x_i)$  in the input data set, we have the following:

$$Y_i = \langle W_i, q_0(x_i) \rangle + \eta_i \theta_0(x_i) + \varepsilon_i \tag{17}$$

$$T_i = \langle W_i, \gamma_0 \rangle + \eta_i \tag{18}$$

For each observation  $i$ , let  $w_i = \sum_{b=1}^B w_{ib}$ . To view our weighted Lasso problem as a standard Lasso problem, we will consider the following rescaled observation  $(\tilde{W}_i, \tilde{Y}_i)$  such that

$$\tilde{W}_i = \sqrt{w_i} W_i, \quad \tilde{Y}_i = \sqrt{w_i} Y_i, \quad \text{and,} \quad \tilde{T}_i = \sqrt{w_i} T_i$$

Then our Lasso estimates  $\hat{\gamma}$  and  $\hat{q}$  can be viewed as a solution to

$$\hat{\gamma} = \underset{\gamma}{\operatorname{argmin}} \frac{1}{2} \sum_i (\langle \tilde{W}_i, \gamma \rangle - \tilde{Y}_i)^2 + \lambda_\gamma \|\gamma\|_1 \quad (19)$$

$$\hat{q} = \underset{q}{\operatorname{argmin}} \frac{1}{2} \sum_i (\langle \tilde{W}_i, q \rangle - \tilde{Y}_i)^2 + \lambda_q \|q\|_1. \quad (20)$$

Furthermore, to relate each observation  $i$  to the target feature  $x$ , we have the following relationship:

$$\tilde{T}_i = \langle \tilde{W}_i, \gamma_0(x) \rangle + \underbrace{\sqrt{w_i} \eta_i}_{\tilde{\mathcal{E}}_i^T}, \quad \text{and,} \quad \tilde{Y}_i = \langle \tilde{W}_i, q_0(x) \rangle + \underbrace{\sqrt{w_i} (\Delta q(x, x_i, W_i) + \eta_i \theta_0(x_i) + \varepsilon_i)}_{\tilde{\mathcal{E}}_i^Y}$$

where  $\Delta q(x, x', X) = \langle X, (q_0(x') - q_0(x)) \rangle$ . Now we can view  $\tilde{Y}_i$  and  $\tilde{T}_i$  outcomes as generated from a linear model with weight vectors  $q_0(x)$  and  $\gamma_0$  and noise terms  $\tilde{\mathcal{E}}_i^Y$  and  $\tilde{\mathcal{E}}_i^T$ . Then we can bound the error of both  $\hat{q}$  and  $\hat{\gamma}$  by using the following result on Lasso.

**Theorem 4.1** (Follows from Theorem 11.1 of [Hastie et al. \[2015\]](#)). *Let  $r_0 \in \mathbb{R}^p$  be a  $k$ -sparse vector and let  $S$  be its support. Consider a set of  $n$  observations such that each observation  $(\tilde{W}_i, \tilde{Y}_i)$  satisfies*

$$\tilde{Y}_i = \langle \tilde{W}_i, r_0 \rangle + \tilde{\mathcal{E}}_i.$$

Let  $\mathbf{W} \in \mathbb{R}^{n \times p}$  denote the design matrix consisting the vectors  $\tilde{W}_i$  as rows. Suppose  $\mathbf{W}$  satisfies the restricted eigenvalue (RE) condition for  $r_0$  with parameters  $(3, \rho)$  that is

$$\frac{v \mathbf{W}^\top \mathbf{W} v}{\|v\|_2^2} \geq \rho \text{ for all non-zero } v \in C(S; 3)$$

where  $C(S; 3) = \{v \in \mathbb{R}^p \mid \|v_{S^c}\|_1 \leq 3\|v_S\|_1\}$ . Then any estimate  $\hat{r}$  obtained by solving

$$\hat{r} = \underset{r}{\operatorname{argmin}} \frac{1}{2} \sum_i (\langle \tilde{W}_i, r \rangle - \tilde{Y}_i)^2 + \lambda \|r\|_1$$

satisfies the following error bound

$$\|\hat{r} - r_0\|_1 \leq O\left(\frac{1}{\rho} k \|\mathbf{W}^\top \tilde{\mathcal{E}}\|_\infty\right)$$

as long as  $\lambda \geq 2\|\mathbf{W}^\top \tilde{\mathcal{E}}\|_\infty$ .

To invoke this result, we need two ingredients:

1. First, we will establish the restricted eigenvalue condition of  $\mathbf{W}$ , where  $\mathbf{W}$  is the design matrix such that each row of  $\mathbf{W}$  is the re-scaled vector  $\tilde{W}_i$ .
2. Then we will also provide bounds on  $\|\mathbf{W}^\top \tilde{\mathcal{E}}^Y\|_\infty$  and  $\|\mathbf{W}^\top \tilde{\mathcal{E}}^T\|_\infty$ . The analysis for bounding the  $\ell_2$  error of  $\hat{q}_b$  is more challenging since the noise terms  $\tilde{\mathcal{E}}_i^Y$  does not have mean 0.

## 4.1 Restricted Eigenvalue Condition for W

For any set of observations  $S \subset D_1$  of size  $s$ , let  $\text{Par}(J)$  denotes the set of all possible equal partitions  $(S^1, S^2)$  of  $S$  such that the cardinalities of the two subsets differ by at most 1. Then let  $\Sigma(S^1, S^2)$  denote the matrix  $\sum_{Z_i \in J} K(x_i, x, (S^1, S^2)) X_i X_i^\top$ , with weights  $K(x_i, x, (S^1, S^2))$  obtained by running the tree learner on  $S$  with partition  $(S^1, S^2)$ . Consider the following matrix

$$\hat{\Sigma}(D_1) = \frac{1}{\binom{n}{s}} \sum_{S \subset D_1: |S|=s} \frac{1}{|\text{Par}(S)|} \sum_{(S^1, S^2) \in \text{Par}(S)} \Sigma(S^1, S^2)$$

Observe that each entry of the matrix  $\hat{\Sigma}(D_1)$  is a U-statistic. Let  $\Sigma = \mathbb{E}[\hat{\Sigma}^U(D_1)]$ . The following lemma bounds the minimum eigenvalue of  $\Sigma$ .

**Lemma 4.2.** *Under Assumption 2.2, taking over the random draws of  $D_1$ , the expectation satisfies*

$$\Sigma \geq \lambda_0 I_p.$$

*Proof.* By linearity of expectation, it suffices to show that for any random subset  $S$  and any random equal partition  $(S^1, S^2)$ ,

$$\mathbb{E}[\Sigma(S^1, S^2)] \geq \lambda_0 I_p.$$

Since only observations in  $S^2$  have non-zero weights, we have

$$\Sigma(S^1, S^2) = \sum_{Z_i \in S} K(x_i, x, (S^1, S^2)) W_i W_i^\top = \sum_{Z_i \in S^2} K(x_i, x, (S^1, S^2)) W_i W_i^\top$$

Note that for each observation  $Z_i$  in  $S^2$ , the weight  $K(x_i, x, (S^1, S^2))$  is only a function of  $S^1$  and the feature  $x_i$ . By honesty, we have for each  $Z_i \in S^2$ ,

$$\begin{aligned} \mathbb{E}[K(x_i, x, (S^1, S^2)) W_i W_i^\top] &= \mathbb{E}_{x_i, S_1} \left[ \mathbb{E}[K(x_i, x, (S^1, S^2)) W_i W_i^\top \mid x_i, S_1] \right] \\ &= \mathbb{E}_{x_i, S_1} \left[ \mathbb{E}[K(x_i, x, (S^1, S^2)) \mid x_i, S_1] \mathbb{E}[W_i W_i^\top \mid x_i, S_1] \right] \\ &\geq \mathbb{E}[K(x_i, x, (S^1, S^2)) \lambda_0 I_p] \end{aligned}$$

Then the stated bound follows directly from the fact the weights are non-negative and sum to 1.  $\square$

We can also derive a concentration inequality for each entry of the matrix  $\hat{\Sigma}(D_1)$  by relying on the standard concentration result on U-statistic.

**Theorem 4.3.** *For any  $\varepsilon > 0$  and any pair  $(l, j) \in [p]^2$ ,*

$$\Pr_{Z_1, \dots, Z_n} \left[ \left| \hat{\Sigma}(D_1)_{lj} - \Sigma_{lj} \right| \geq \varepsilon \right] \leq 2 \exp\left(-\frac{(n/s)\varepsilon^2}{2}\right)$$

*Equivalently, for any  $\delta \in (0, 1)$ , with probability  $1 - \delta$ ,  $\left| \hat{\Sigma}(D_1)_{lj} - \Sigma_{lj} \right| \leq \sqrt{\frac{2}{n/s} \ln(2/\delta)}$ .*

By taking a union bound over all pairs  $(l, j) \in [p]^2$ , we can show that with probability at least  $1 - \delta$ ,

$$\|\hat{\Sigma}(D_1) - \Sigma\|_\infty \leq \sqrt{\frac{4s}{n} \ln(p/\delta)}.$$

Now we can rewrite the covariance matrix as

$$\mathbf{W}^\top \mathbf{W} = \sum_{Z_i \in D_1} \tilde{W}_i \tilde{W}_i^\top = \sum_{Z_i \in D_1} w_i W_i W_i^\top = \frac{1}{B} \sum_{Z_i \in D_1} \sum_{b=1}^B K(x_i, x, (S_b^1, S_b^2)) (W_i W_i^\top)$$

Since the subsets  $S_b$  and the partitions  $(S_b^1, S_b^2)$  are randomly selected, we can view  $\mathbf{W}^\top \mathbf{W}$  as a Monte Carlo approximation of  $\hat{\Sigma}(D_1)$ . Furthermore, by standard Chernoff bound, we know that as long as the number of trees is bigger than  $n/s$ , the error introduced by the Monte Carlo approximation will be subsumed by the U-statistic error.

**Corollary 4.4.** *As long as the number of trees  $B \geq (n/s)$ , the following inequality holds with probability at least  $1 - \delta$ ,*

$$\|\mathbf{W}^\top \mathbf{W} - \Sigma\|_\infty \leq O\left(\sqrt{\frac{s}{n} \ln(p/\delta)}\right).$$

**Lemma 4.5.** *Suppose that the number of trees  $B \geq n/s$ . Let  $r$  be a sparse vector in  $\mathbb{R}^p$  with a support size at most  $O(k)$ . With probability at least  $1 - \delta$ , the matrix  $\mathbf{W}$  satisfies the restricted eigenvalue condition for  $r$  with parameters  $(3, \rho)$ , where*

$$\rho \geq \lambda_0 - O\left(k \sqrt{\frac{s}{n} \ln(p/\delta)}\right)$$

*Proof.* Let  $r$  be a  $k$ -sparse vector in  $\mathbb{R}^p$  and let  $S(r)$  be the support of  $r$ . Let  $v \in C(S(r); 3)$ . To simplify notation, let  $M = \mathbf{W}^\top \mathbf{W} - \Sigma$ . Then we can write

$$\begin{aligned} \frac{v^\top M v}{\|v\|_2^2} &\leq \frac{\|v\|_1 \|M v\|_\infty}{\|v\|_2^2} && \text{(Cauchy-Swartz)} \\ &\leq \frac{\|v\|_1 \|M\|_\infty \|v\|_1}{\|v\|_2^2} && \text{(Cauchy-Swartz)} \\ &\leq \frac{\|v\|_1^2 \|M\|_\infty}{\|v\|_2^2} \end{aligned}$$

Let  $S^c$  denote the complement of  $S(r)$ , and let  $v_S$  and  $v_{S^c}$  denote the subvectors of  $v$  over the coordinates in  $S^c$ . By the definition of  $C(S(r), 3)$ , we know that

$$\|v\|_1 = \|v_S\|_1 + \|v_{S^c}\|_1 \leq 4\|v_S\|_1$$

It follows that

$$\frac{\|v\|_1^2}{\|v\|_2^2} \leq \frac{(4\|v_S\|_1)^2}{\|v\|_2^2} \leq 16 \frac{\|v_S\|_1^2}{\|v_S\|_2^2} = 16|S|$$

Note that  $|S| = O(k)$ . By Corollary 4.4, we have with probability at least  $1 - \delta$  that  $\|M\|_\infty \leq O\left(\sqrt{\frac{s}{n} \ln(p/\delta)}\right)$ , and so

$$\frac{v^\top M v}{\|v\|_2^2} \leq 16\|M\|_\infty |S| \leq O\left(k \sqrt{\frac{s}{n} \ln(p/\delta)}\right)$$

which completes the proof.  $\square$

## 4.2 Bounding the Noise Terms

Next, we show that both  $\|\mathbf{W}^\top \tilde{\mathcal{E}}^Y\|_\infty$  and  $\|\mathbf{W}^\top \tilde{\mathcal{E}}^T\|_\infty$  are bounded with high probability. First, note that for each  $j \in [p]$ ,

$$\begin{aligned}\langle \mathbf{W}^j, \tilde{\mathcal{E}}^Y \rangle &= \sum_i w_i W_{ij} (\langle W_i, q_0(x_i) - q_0(x) \rangle + \eta_i \theta_0(x_i) + \varepsilon_i) \\ \langle \mathbf{W}^j, \tilde{\mathcal{E}}^T \rangle &= \sum_i w_i W_{ij} \eta_i\end{aligned}$$

It suffices to bound  $\max_j \langle \mathbf{W}^j, \tilde{\mathcal{E}}^Y \rangle$  and  $\max_j \langle \mathbf{W}^j, \tilde{\mathcal{E}}^T \rangle$ . We will first define several useful functions. First, for any  $j \in [p]$ , any subset  $S$  of  $D_1$  of size  $s$ , along with any equal partition  $(S^1, S^2)$ , define

$$\begin{aligned}R_j^Y(S^1, S^2) &= \sum_{Z_i \in S} K(x_i, x, (S^1, S^2)) W_{ij} (\Delta q(x, x_i, W_i) + \eta_i \theta_0(x_i) + \varepsilon_i) \\ R_j^T(S^1, S^2) &= \sum_{Z_i \in S} K(x_i, x, (S^1, S^2)) W_{ij} \eta_i\end{aligned}$$

with weights  $K(x_i, x, (S^1, S^2))$  obtained by running the tree learner with the partition  $(S^1, S^2)$ . Now consider the following two U-statistics for each  $j \in [p]$ ,

$$\begin{aligned}\hat{R}_j^Y(D_1) &= \frac{1}{\binom{n}{s}} \sum_{S \subset D_1: |S|=s} \frac{1}{s!} \sum_{(S^1, S^2) \in \text{Par}(S)} R_j^Y(S^1, S^2) \\ \hat{R}_j^T(D_1) &= \frac{1}{\binom{n}{s}} \sum_{S \subset D_1: |S|=s} \frac{1}{s!} \sum_{(S^1, S^2) \in \text{Par}(S)} R_j^T(S^1, S^2)\end{aligned}$$

The following bound on  $\Delta q(x, x', X)$  will be a useful tool.

**Lemma 4.6.** *For any  $x, x', W$ ,  $\|\Delta q(x, x', W)\|_1 \leq \|x - x'\|_2 \|\gamma_0\|_1$ .*

*Proof.* We can write:

$$\begin{aligned}\|\Delta q(x, x', W)\|_1 &\leq (\|W\|_\infty \|q_0(x') - q_0(x)\|_1) && \text{(Cauchy-Swartz)} \\ &\leq \|q_0(x') - q_0(x)\|_1 && \text{(boundedness of } X) \\ &= \|\theta_0(x') \gamma_0 - \theta_0(x) \gamma_0\|_1 \\ &= \|\gamma_0\|_1 |\theta_0(x') - \theta_0(x)| \\ &\leq \|\gamma_0\|_1 \|x' - x\|_2 && \text{(Lipschitzness of } \theta_0)\end{aligned}$$

which completes the proof.  $\square$

The following lemma bounds the expected value of the U-statistic. In particular, we can bound the expectation of  $\hat{R}_j^Y(D_1)$  using the shrinkage of the leaf size in the tree.

**Lemma 4.7.** *Taking expectation over the random draws of  $D_1$ , the following holds for each  $j \in [p]$ ,*

$$\mathbb{E}[\hat{R}_j^T(D_1)] = 0, \quad \text{and,} \quad \mathbb{E}[\hat{R}_j^Y(D_1)] \leq O(k) \mathbb{E}_{D_1, S^1, S^2} \left[ \max_{i \in D_1} \|x - x_i\|_2 \mid K(x_i, x, (S^1, S^2)) > 0 \right].$$

*Proof.* By linearity of expectation, we have  $\mathbb{E}[\hat{R}_j^T(D_1)] = \mathbb{E}[R_j^T(S^1, S^2)]$  and  $\mathbb{E}[\hat{R}_j^Y(D_1)] = \mathbb{E}[R_j^Y(S^1, S^2)]$ , where the expectations of the right hand sides are taken over the random draws of  $D_1$ , random subset  $S$  and random equal partition  $(S^1, S^2)$ . The expectation of  $R_j^T(S^1, S^2)$  is

$$\mathbb{E}[R_j^T(S^1, S^2)] = \mathbb{E} \left[ \sum_{Z_i \in S} w_i W_{ij} \eta_i \right] = \mathbb{E} \left[ \sum_{Z_i \in S^2} K(x_i, x, (S^1, S^2)) W_{ij} \eta_i \right]$$

where the second equality follows since  $K(x_i, x, (S^1, S^2))$  is non-zero only for  $Z_i \in S^2$ . Similarly,

$$\begin{aligned}\mathbb{E}\left[\hat{R}_j^Y(S^1, S^2)\right] &= \mathbb{E}\left[\sum_{Z_i \in S^2} K(x_i, x, (S^1, S^2)) W_{ij} (\Delta q(x, x_i, W_i) + \eta_i \theta_0(x_i) + \varepsilon_i)\right] \\ &= \mathbb{E}\left[\sum_{Z_i \in S^2} K(x_i, x, (S^1, S^2)) W_{ij} (\Delta q(x, x_i, W_i))\right] + \mathbb{E}\left[\sum_{Z_i \in S^2} w_i W_{ij} (\eta_i \theta_0(x_i) + \varepsilon_i)\right]\end{aligned}$$

First, recall that by our assumption of the PLR model, we have

$$\mathbb{E}[\varepsilon_i | W_i, x_i, T_i] = 0, \quad \mathbb{E}[\eta_i | x_i, W_i] = 0 \quad (21)$$

Note that the learner assigns the weight  $w_i$  only depends on the subsample  $S^1$  and the feature  $x_i$ . Therefore, by honesty of the weights and the law of iterated expectations, for each  $Z_i \in S^2$ ,

$$\mathbb{E}\left[K(x_i, x, (S^1, S^2)) W_{ij} \eta_i\right] = \mathbb{E}_{x_i, W_i, S^1}\left[\mathbb{E}\left[K(x_i, x, (S^1, S^2)) W_{ij} \eta_i | x_i, W_i\right]\right] \quad (22)$$

$$= \mathbb{E}_{x_i, W_i, S^1}\left[\mathbb{E}\left[K(x_i, x, (S^1, S^2)) | x_i, W_i, S^1\right] \mathbb{E}\left[\eta_i W_{ij} | x_i, W_i, S^1\right]\right] = 0 \quad (23)$$

where the last equality follows from  $\mathbb{E}\left[\eta_i W_{ij} | x_i, W_i, S^1\right] = \mathbb{E}\left[\eta_i | x_i, W_i, S^1\right] \mathbb{E}\left[W_{ij} | x_i, W_i, S^1\right] = 0$ , which implies that  $\mathbb{E}\left[\hat{R}_j^T(D_1)\right] = 0$  by linearity of expectation. Similarly,

$$\begin{aligned}& \mathbb{E}\left[K(x_i, x, (S^1, S^2)) W_{ij} (\eta_i \theta_0(x_i) + \varepsilon_i)\right] \\ &= \mathbb{E}_{W_i, x_i, S^1}\left[\mathbb{E}\left[K(x_i, x, (S^1, S^2)) W_{ij} (\eta_i \theta_0(x_i) + \varepsilon_i) | W_i, x_i, S^1\right]\right] \\ &= \mathbb{E}_{W_i, x_i, S^1}\left[\mathbb{E}\left[K(x_i, x, (S^1, S^2)) \theta_0(x_i) W_{ij} \eta_i | W_i, x_i, S^1\right]\right] + \mathbb{E}_{W_i, x_i, S^1}\left[\mathbb{E}\left[K(x_i, x, (S^1, S^2)) W_{ij} \varepsilon_i | W_i, x_i, S^1\right]\right]\end{aligned}$$

By the same reasoning in Equation (23), the second term  $\mathbb{E}_{W_i, x_i, S^1}\left[\mathbb{E}\left[K(x_i, x, (S^1, S^2)) W_{ij} \varepsilon_i | W_i, x_i, S^1\right]\right] = 0$ . For the first term, we can write

$$\begin{aligned}& \mathbb{E}_{W_i, x_i, S^1}\left[\mathbb{E}\left[K(x_i, x, (S^1, S^2)) \theta_0(x_i) W_{ij} \eta_i | W_i, x_i, S^1\right]\right] \\ &= \mathbb{E}_{W_i, x_i, S^1}\left[\mathbb{E}\left[K(x_i, x, (S^1, S^2)) \theta_0(x_i) W_{ij} | W_i, x_i, S^1\right] \mathbb{E}\left[\eta_i | W_i, x_i, S^1\right]\right] = 0\end{aligned}$$

Moreover, by Lemma 4.6,

$$\mathbb{E}\left[\sum_{Z_i \in S} K(x_i, x, (S^1, S^2)) W_{ij} (\Delta q(x, x_i, W_i))\right] \leq \mathbb{E}\left[\sum_{Z_i \in S} K(x_i, x, (S^1, S^2)) (\|x_i - x\|_2 \|\gamma_0\|_1)\right]$$

Then our claim follows directly from the fact that the sum of the weights equals 1 and that  $\|\gamma_0\|_1 \leq O(k)$ .  $\square$

We can apply the standard concentration inequality for U-statistic again.

**Theorem 4.8.** *For any  $\varepsilon > 0$  and any  $j \in [p]$ ,*

$$\Pr\left[\max\left\{\left|\hat{R}_j^T(D_1) - \mathbb{E}\left[\hat{R}_j^T(D_1)\right]\right|, \left|\hat{R}_j^Y(D_1) - \mathbb{E}\left[\hat{R}_j^Y(D_1)\right]\right|\right\} \geq \varepsilon\right] \leq 4 \exp\left(-\frac{(n/s)\varepsilon^2}{18}\right)$$

Equivalently, for any  $\delta \in (0, 1)$ , with probability  $1 - \delta$ ,

$$\max\left\{\left|\hat{R}_j^T(D_1) - \mathbb{E}\left[\hat{R}_j^T(D_1)\right]\right|, \left|\hat{R}_j^Y(D_1) - \mathbb{E}\left[\hat{R}_j^Y(D_1)\right]\right|\right\} \leq \sqrt{\frac{18s}{n} \ln(4/\delta)}.$$

Now we can view  $\langle \mathbf{W}^j, \tilde{\mathcal{E}}^Y \rangle = \frac{1}{B} \sum_{b=1}^B \sum_{i=1}^n w_{ib} W_{ij} (\Delta q(x, x_i, W_i) + \eta_i \theta_0(x_i) + \varepsilon_i)$  as a Monte Carlo approximation to the U-statistic  $\hat{R}_j^Y(D_1)$ , and view  $\langle \mathbf{W}^j, \tilde{\mathcal{E}}^T \rangle = \frac{1}{B} \sum_{b=1}^B \sum_{i=1}^n w_{ib} W_{ij} \eta_i$  as a Monte Carlo approximation to the U-statistic  $\hat{R}_j^T(D_1)$ . By Chernoff bound, we know that as long as  $B \geq n/s$  is sufficiently large, we know that Monte Carlo approximation error will be subsumed by the U-statistic deviation error.

**Corollary 4.9.** *As long as the number of trees  $B \geq (n/s)$ , with probability at least  $1 - \delta$ , the following inequality holds*

$$\begin{aligned} \max_j |\langle \mathbf{W}^j, \mathcal{E}^T \rangle| &\leq O\left(\sqrt{\frac{s}{n} \ln(p/\delta)}\right) \\ \max_j |\langle \mathbf{W}^j, \mathcal{E}^Y \rangle| &\leq O\left(\sqrt{\frac{s}{n} \ln(p/\delta)} + k \mathbb{E}_{D_1, S^1, S^2} \left[ \max_{i \in D_1} \|x - x_i\|_2 \mid K(x_i, x, (S^1, S^2)) > 0 \right]\right) \end{aligned}$$

Taking the kernel shrinkage result we establish in Corollary 5.2, we obtain the following bound on  $\|\mathbf{W}^\tau \mathcal{E}^Y\|_\infty$ .

**Wrapping up.** We now have all the ingredients to apply Theorem 4.1.

**Theorem 4.10.** *Suppose that the tree learner satisfies the following shrinkage condition*

$$\mathbb{E}_{D_1, S^1, S^2} \left[ \max_{i \in D_1} \|x - x_i\|_2 \mid K(x_i, x, (S^1, S^2)) > 0 \right] \leq O(s^{-\tau})$$

Then with probability at least  $1 - \delta$ , the Lasso solutions  $\hat{q}$  and  $\hat{\gamma}$  satisfy

$$\begin{aligned} \|\hat{q} - q_0(x)\|_1 &\leq O\left(\frac{k}{\lambda_0} \left(\sqrt{\frac{s}{n} \ln(p/\delta)} + ks^{-\tau}\right)\right) \\ \|\hat{\gamma} - \gamma_0\|_1 &\leq O\left(\frac{k}{\lambda_0} \sqrt{\frac{s}{n} \ln(p/\delta)}\right) \end{aligned}$$

as long as the regularization parameter satisfies  $\lambda_q \geq \Omega\left(\sqrt{\frac{s}{n} \ln(p/\delta)} + ks^{-\tau}\right)$ ,  $\lambda_\gamma \geq \Omega\left(\sqrt{\frac{s}{n} \ln(p/\delta)}\right)$ , and the sample size satisfies

$$n \geq \Omega(k^2 s \ln(p/\delta)).$$

## 5 Analysis of Orthogonal Random Forest

Finally, we will use the tools we develop in the previous sections to provide a full analysis for the ORF algorithm. We need to combine two main technical ingredients to invoke our general convergence result of Theorem 3.4. First, we need to show the tree learner satisfy the kernel shrinkage assumption. Second, we rely on the kernel Lasso analysis in Section 4 to bound the nuisance estimation error.

### 5.1 Kernel Shrinkage for Tree Learners

The analysis on kernel shrinkage rate essentially follows from the result of [Wager and Athey \[2015\]](#) on the localization of the kernel weights.

**Lemma 5.1** (Follows from Lemma 2 of [Wager and Athey \[2015\]](#)). *Consider the tree learner as the base kernel learner  $\mathcal{L}_k$  under Assumption 2.1. Then given a set of observations  $S = (Z_1, \dots, Z_s)$  such that the associated feature vectors  $x_1, \dots, x_s$  are drawn independently from uniform distribution  $U([0, 1]^d)$ . Let  $L(x)$  be the leaf containing the target feature vector  $x$ . Then for sufficiently large enough  $s$ ,*

$$\Pr \left[ \text{diam}(L(x)) \geq \sqrt{d} \left( \frac{s}{2r-1} \right)^{\frac{-0.51}{ad}} \right] \leq d \left( \frac{s}{2r-1} \right)^{\frac{-1}{2ad}}$$

where  $r$  is the minimum number of points from  $S^2$  that fall in each leaf,  $\text{diam}(L(x))$  denotes the diameter inside the leaf  $L(x)$  and  $\alpha = \frac{\log(\omega^{-1})}{\pi \log((1-\omega)^{-1})}$ .

**Corollary 5.2** (Kernel shrinkage of a tree learner). *Suppose for any input data set of size  $s$ , the minimum leaf size parameter of the tree learner is set to be  $r = O(1)$ . Then under Assumption 2.1 and assume that the dimension  $d = O(1)$ . Then the kernel weighting function output by the tree learner satisfies  $\mathbb{E}[\sup\{\|x - x_i\|: K(x, x_i, S) > 0\}] = O(s^{-\frac{1}{2\alpha d}})$ , with  $\alpha = \frac{\log(\omega^{-1})}{\pi \log((1-\omega)^{-1})}$ .*

## 5.2 Wrapping up: proof of Theorem 2.3.

By the kernel shrinkage result in Corollary 5.2, we have

$$\mathbb{E}_{D_1, S^1, S^2} \left[ \max_{i \in D_1} \|x - x_i\|_2 \mid K(x_i, x, (S^1, S^2)) > 0 \right] \leq O(s^{-\tau})$$

with  $\tau = \frac{1}{2\alpha d}$  and  $\alpha = \frac{\log(\omega^{-1})}{\pi \log((1-\omega)^{-1})}$ . By Theorem 4.1, we can bound the  $\ell_1$  Lasso error: with probability at least  $1 - \delta$ ,

$$\|\hat{q} - q_0(x)\|_1 \leq O\left(\frac{k}{\lambda_0} \left(\sqrt{\frac{s}{n} \ln(p/\delta)} + ks^{-\tau}\right)\right), \quad \|\hat{\gamma} - \gamma_0\|_1 \leq O\left(\frac{k}{\lambda_0} \sqrt{\frac{s}{n} \ln(p/\delta)}\right)$$

Recall that the error of the nuisance estimate  $\hat{h}$  can be written as

$$\|\hat{h}(W) - h_0(W)\|_2^2 = (\langle \hat{q} - q_0(x), W \rangle)^2 + (\langle \hat{\gamma} - \gamma_0, W \rangle)^2 \quad (24)$$

In the remainder of the proof, we set  $\delta = 1/n$  and define the Lasso condition in Equation (24) as event  $E$ . By Hölder inequality, we can also bound,

$$\mathbb{E}[\|\hat{h}(W) - h_0(W)\|_2^2 \mid x, E] \leq O\left(\frac{k}{\lambda_0} \left(\sqrt{\frac{s}{n} \ln(p)} + ks^{-\tau}\right)\right)$$

By Lemma A.2, we know that under the event  $E$  that  $\psi_{\max} \leq O(k)$  as long as  $\|\hat{q} - q_0(x)\|, \|\hat{\gamma} - \gamma_0\| \leq O(1)$ . Then by Theorem 3.4, we know

$$\text{if } \mathbb{E}[\|\hat{h}(W) - h_0(W)\|_2^2 \mid x, E] \leq O\left(s^{-\tau} + k\sqrt{\frac{s \ln(n)}{n}}\right) \text{ then } \mathbb{E}[|\hat{\theta} - \theta_0(x)| \mid E] \leq O\left(s^{-\tau} + k\sqrt{\frac{s \ln(n)}{n}}\right)$$

Note that if we set  $s = \left(\frac{n}{k^2 \ln(p)}\right)^{\frac{1}{1+2\tau}}$ , then  $s^{-\tau} = k\sqrt{\frac{s \ln(p)}{n}}$  and

$$s^{-\tau} + k\sqrt{\frac{s \ln(n)}{n}} = \Theta\left(\left(\frac{n}{k^2 \ln(p)}\right)^{\frac{-\tau}{1+2\tau}}\right)$$

Furthermore, if the support size satisfies  $k \leq \left(\frac{n}{\ln(p)}\right)^{\frac{\tau}{10\tau+4}}$ , then

$$\mathbb{E}[\|\hat{h}(W) - h_0(W)\|_2^2 \mid x, E] \leq O\left(\left(\frac{n}{k^2 \ln(p)}\right)^{\frac{-\tau}{1+2\tau}}\right)$$

This implies that

$$\mathbb{E}[|\hat{\theta} - \theta_0(x)| \mid E] \leq O\left(\left(\frac{n}{k^2 \ln(p)}\right)^{\frac{-\tau}{1+2\tau}}\right)$$

Finally, since the range of  $\hat{\theta}$  is bounded, we know that  $\mathbb{E}[|\hat{\theta} - \theta_0(x)| - E] = O(1/n)$ , which has lower order than  $\mathbb{E}[|\hat{\theta} - \theta_0(x)| \mid E]$ . This recovers our final stated bound.

## 6 Monte Carlo Experiments

We perform a comprehensive empirical evaluation of ORF by comparing its performance with other methods in the literature (and their variants). The source code for running these experiments is available at [github.com/Microsoft/EconML/tree/master/prototypes/orthogonal\\_forests](https://github.com/Microsoft/EconML/tree/master/prototypes/orthogonal_forests).

**Data Generating Process (DGP).** The observations  $Z_i = (T_i, Y_i, W_i, x_i)$  are generated according to the partial linear model in Equations (1) and (2), where  $x_i$  is drawn from the uniform distribution  $U[0, 1]$ ,  $W_i$  is drawn from  $\mathcal{N}(0, I_p)$ , and the noise terms  $\varepsilon_i \sim U[-1, 1]$ ,  $\eta_i \sim U[-1, 1]$ . The  $k$ -sparse vectors  $\beta_0, \gamma_0 \in \mathbb{R}^p$  have coefficients drawn independently from  $U[0, 1]$ . The dimension  $p = 500$  and we vary the support size  $k$  over the range of  $\{1, 5, 10, 15, 20, 25, 30\}$ . We consider three treatment effect functions:

1. A continuous, piecewise linear function

$$\theta_0(x) = (a_1 + b_1x)\mathbb{I}\{x \leq c_1\} + (a_2 + b_2x)\mathbb{I}\{x > c_1 \text{ and } x \leq c_2\} + (a_3 + b_3x)\mathbb{I}\{x > c_2\}$$

where  $a_i, b_i$  are random generated constants chosen so that the overall function is continuous.

2. A discontinuous, piecewise constant function

$$\theta_0(x) = a_1\mathbb{I}\{x \leq c_1\} + a_2\mathbb{I}\{x > c_1 \text{ and } x \leq c_2\} + a_3\mathbb{I}\{x > c_2\}$$

3. A discontinuous, piecewise polynomial function

$$\theta_0(x) = 3x^2\mathbb{I}\{x < .2\} + (3x^2 + 1)\mathbb{I}\{x \geq .2 \text{ and } x \leq .6\} + (6x + 2)\mathbb{I}\{x \geq .6\}$$

Similarly, we generate data for a two-dimensional feature vector  $x = (x_1, x_2)$ ,  $x_{1i} \sim U[0, 1]$ ,  $x_{2i} \sim \text{Bern}(0.5)$ , and the corresponding treatment effect function given by:

$$\theta_0(x_1, x_2) = \theta_{\text{piecewise linear}}(x_1)\mathbb{I}_{x_2=0} + \theta_{\text{piecewise constant}}(x_1)\mathbb{I}_{x_2=1}$$

**Experiments setup.** For each fixed treatment function, we repeat 100 experiments, each of which consists of generating 5000 or 10000 observations from the DGP, drawing the vectors  $\beta_0$  and  $\gamma_0$ , and estimating  $\hat{\theta}(x)$  at 100 test points  $x$  over a grid in  $[0, 1]$ . We then calculate the bias, variance and root mean squared error (RMSE) of each estimate  $\hat{\theta}(x)$ . Here we report summary statistics of the median and 5 – 95 percentiles of these three quantities across test points, so as to evaluate the average performance of each method. We compare two variants of ORF with three variants of GRF [Athey et al., 2017] and two extensions of double ML methods for heterogeneous treatment estimation [Chernozhukov et al., 2017]. Let us describe the methods in more details:

*ORF variants.* (1) ORF: We implement ORF as described in Section 2, setting parameters under the guidance of our theoretical result (Theorem 2.3 and 4.1): subsample size  $s \approx (n/\log(p))^{1/(2\tau+1)}$ , Lasso regularization  $\lambda_\gamma, \lambda_q \approx \sqrt{\log(p)s/n/20}$  (for both tree learner and kernel estimation), number of trees  $B = 100 \geq n/s$ , a max tree depth of 20, and a minimum leaf size of  $r = 5$ . (2) ORF with LassoCV (ORF-CV): we replaced the Lasso algorithm in ORF’s kernel estimation, with a cross-validated Lasso for the selection of the regularization parameter  $\lambda_\gamma$  and  $\lambda_q$ . ORF-CV provides a more systematic optimization over the parameters.

*GRF variants.* (1) GRF-xW: We run GRF R package by [Tibshirani et al., 2018] directly on the observations, using features and controls  $(x, W)$  jointly as the covariates. (2) GRF-x: We also run GRF R package on the observations, but only using the features  $x$  as covariates, ignoring the controls  $W$ . (3) GRF-Res: We perform a naive combination of double ML and GRF by first residualizing the treatments and outcomes on the both the features  $x$  and controls  $W$ , then running GRF R package on the residualized treatments  $\hat{T}$ , residualized outcomes  $\hat{Y}$ , and features  $x$ .

*Double ML with Polynomial Heterogeneity (DML-Poly).* An extension of the classic Double ML procedure for heterogeneous treatment effects introduced in Chernozhukov et al. [2017]. This method accounts for

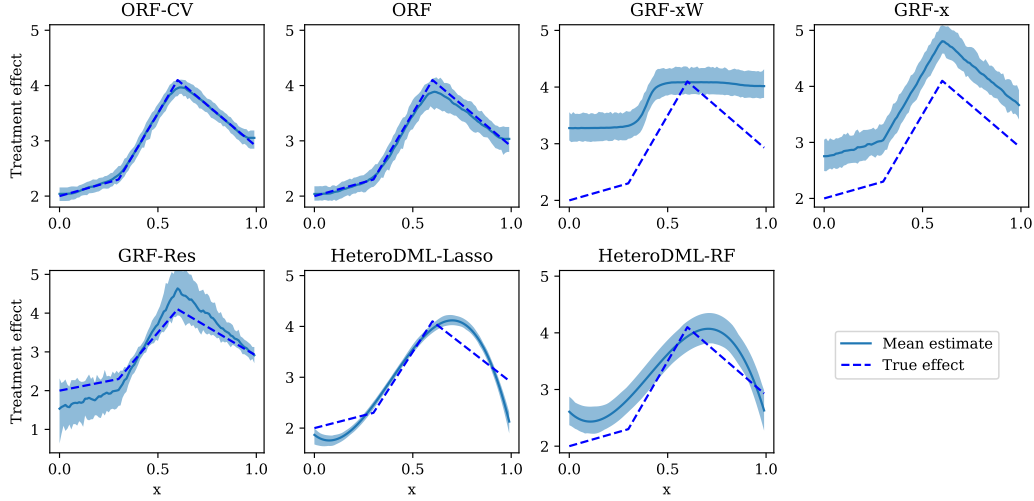


Figure 1: Treatment effect estimations for 100 Monte Carlo experiments with parameters  $n = 5000$ ,  $p = 500$ ,  $d = 1$ ,  $k = 15$ , and  $\theta(x) = (x + 2)\mathbb{I}_{x \leq 0.3} + (6x + 0.5)\mathbb{I}_{x > 0.3 \text{ and } x \leq 0.6} + (-3x + 5.9)\mathbb{I}_{x > 0.6}$ . The shaded regions depict the mean and the 5%-95% interval of the 100 experiments.

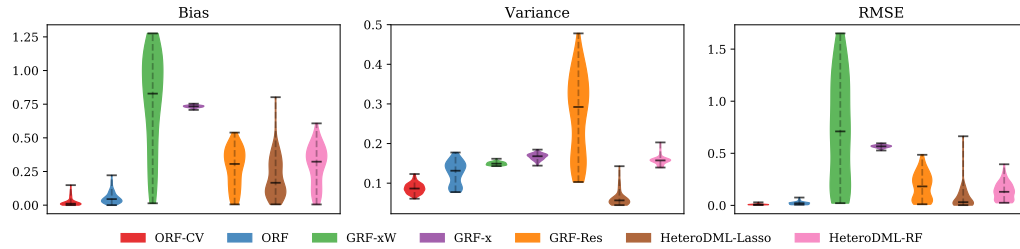


Figure 2: Distributions of bias, variance and RMSE across test points, averaged over Monte Carlo experiments, for the examined estimators. The filled regions represent the probability density function of the metrics. The top, middle and bottom horizontal bars represent the minimum, maximum and median for that measurement, respectively.

heterogeneity by creating an expanded linear base of composite treatments (cross products between treatments and features). (1) Heterogeneous Double ML using LassoCV for first-stage estimation (HeteroDML-Lasso): In this version, we use Lasso with cross-validation for calculating residuals on  $x \cup W$  in the first stage. (2) Heterogeneous Double ML using random forest for first-stage estimation (HeteroDML-RF): A more flexible version that uses random forests to perform residualization on treatments and outcomes. The latter performs better when treatments and outcomes have a non-linear relationship with the joint features of  $(x, W)$ .

**Experimental results.** For the comparison, we report the results with  $n = 5000$ ,  $k = 15$  and a fixed treatment function. The remainder of the results are qualitatively similar and can be found in Appendix D. In Figure 1, we inspect the goodness of fit for the chosen estimation methods across 100 Monte Carlo experiments. We note the limitations of two version of the GRF, GRF-x and GRF-xW, in capturing the treatment effect function well. The GRF-x estimations have a consistent bias as the algorithm cannot capture the dependency of the treatment effect on the controls  $W$ . The GRF-xW could potentially capture this dependency, but fails to do so due to the high-dimensionality of the controls. The HeteroDML methods are not flexible enough to capture the complexity of the treatment effect function. The best performers are the ORF-CV, ORF and GRF-Res, with the latter estimator having a larger bias and variance.

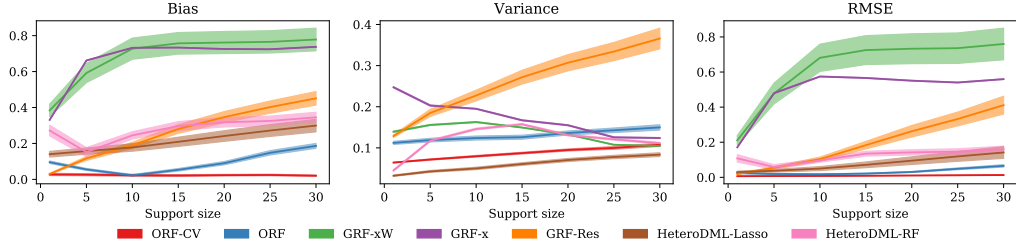


Figure 3: Bias, variance and RMSE as a function of support size for  $n = 5000$ ,  $p = 500$ ,  $d = 1$  and a piecewise linear treatment response function. The solid lines represent the mean of the metrics across test points, averaged over the Monte Carlo experiments, and the filled regions depict the standard deviation, scaled down by a factor of 3 for clarity.

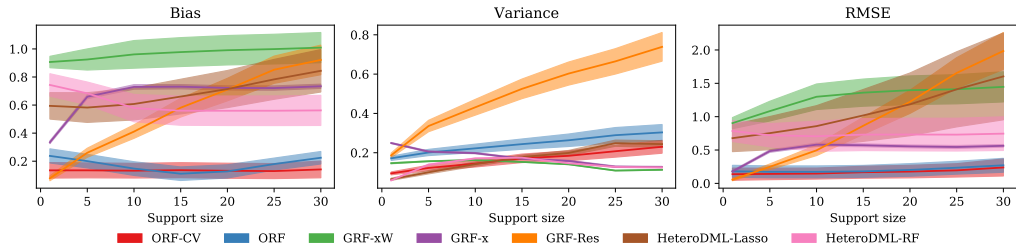


Figure 4: Bias, variance and RMSE as a function of support size for  $n = 5000$ ,  $p = 500$ ,  $d = 1$  a piecewise constant treatment response function. The solid lines represent the mean of the metrics across test points, averaged over the Monte Carlo experiments, and the filled regions depict the standard deviation, scaled down by a factor of 3 for clarity.

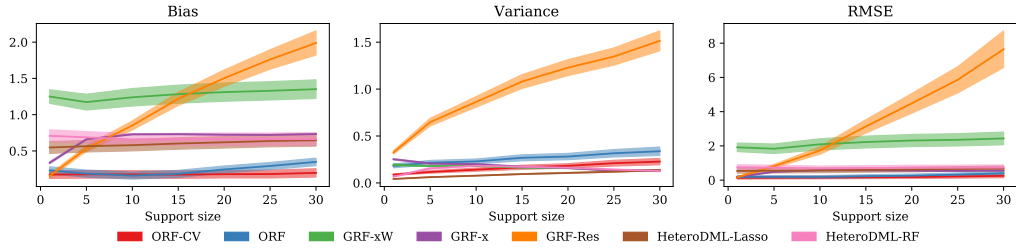


Figure 5: Bias, variance and RMSE as a function of support size for  $n = 5000$ ,  $p = 500$ ,  $d = 1$  a piecewise polynomial treatment response function. The solid lines represent the mean of the metrics across test points, averaged over the Monte Carlo experiments, and the filled regions depict the standard deviation, scaled down by a factor of 3 for clarity.

In Figure 2, we show the distribution of these evaluation metrics across test points, averaged over the Monte Carlo experiments. The ORF-CV and ORF algorithms perform better than the GRF-Res on all metrics: 0.01 and 0.05 vs 0.30 bias, 0.08 and 0.13 vs 0.29 variance and 0.008, 0.02 vs 0.18 RMSE for this example. We observe this pattern for the other choices of support size, sample size and treatment effect function: our algorithms consistently outperform the other methods we considered (see Appendix D).

We analyze the behavior of these estimators as we increase the support size of  $W$ . Figures 3-5 illustrate the variability in the evaluation metrics across different support sizes for the three treatment effect functions described above. The ORF-CV performs very well, with consistent bias and RMSE across support sizes and treatment functions. The bias, variance and RMSE of the ORF grow with support size, but this growth is at a lower rate compared to the alternative estimators.

**Two-forest ORF v.s. One-forest ORF.** A natural question about ORF is whether it is necessary to have two separate forests for the two-stage estimation. We investigate this question by implementing a vari-

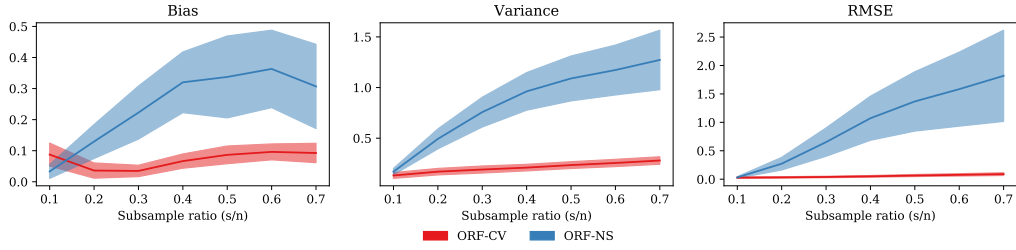


Figure 6: Bias, variance and RMSE versus subsample ratio used for training individual trees. The solid lines represent the means and the filled regions depict the standard deviation for the different metrics across test points, averaged over 100 Monte Carlo experiments.

ant of ORF without sample splitting (ORF-NS)—it builds only one random forest over the entire dataset, and perform the two-stage estimation using the same set of importance weights. We empirically compare ORF-CV with ORF-NS. In Figure 6, we note that the bias, variance and RMSE of the ORF-NS increase drastically with the subsample ratio ( $s/n$ ), whereas the same metrics are almost constant for the ORF-CV. This phenomenon is consistent with the theory, since larger subsamples induce a higher probability of collision between independently drawn samples, and the “spill-over” can incur large bias and error.

## References

- Miguel A. Arcones. A Bernstein-type inequality for  $u$ -statistics and  $u$ -processes. *Statistics & Probability Letters*, 22(3):239 – 247, 1995. ISSN 0167-7152. doi: [https://doi.org/10.1016/0167-7152\(94\)00072-G](https://doi.org/10.1016/0167-7152(94)00072-G). URL <http://www.sciencedirect.com/science/article/pii/016771529400072G>.
- S. Athey, J. Tibshirani, and S. Wager. Generalized Random Forests. *ArXiv e-prints*, October 2017.
- V. Chernozhukov, M. Goldman, V. Semenova, and M. Taddy. Orthogonal Machine Learning for Demand Estimation: High Dimensional Causal Inference in Dynamic Panels. *ArXiv e-prints*, December 2017.
- Victor Chernozhukov, Denis Chetverikov, Mert Demirer, Esther Duflo, Christian Hansen, and Whitney Newey. Double/debiased/neyman machine learning of treatment effects. *American Economic Review*, 107(5):261–65, May 2017. doi: 10.1257/aer.p20171038. URL <http://www.aeaweb.org/articles?id=10.1257/aer.p20171038>.
- J. Hartford, G. Lewis, K. Leyton-Brown, and M. Taddy. Counterfactual Prediction with Deep Instrumental Variables Networks. *ArXiv e-prints*, December 2016.
- Trevor Hastie, Robert Tibshirani, and Martin Wainwright. *Statistical Learning with Sparsity: The Lasso and Generalizations*. Chapman & Hall/CRC, 2015. ISBN 1498712169, 9781498712163.
- Wassily Hoeffding. Probability inequalities for sums of bounded random variables. *Journal of the American Statistical Association*, 58(301):13–30, 1963. ISSN 01621459. URL <http://www.jstor.org/stable/2282952>.
- Guido W. Imbens and Donald B. Rubin. *Causal Inference for Statistics, Social, and Biomedical Sciences: An Introduction*. Cambridge University Press, 2015. doi: 10.1017/CBO9781139025751.
- X. Nie and S. Wager. Learning Objectives for Treatment Effect Estimation. *ArXiv e-prints*, December 2017.
- S. Powers, J. Qian, K. Jung, A. Schuler, N. H. Shah, T. Hastie, and R. Tibshirani. Some methods for heterogeneous treatment effect estimation in high-dimensions. *ArXiv e-prints*, July 2017.
- P. M. Robinson. Root- $n$ -consistent semiparametric regression. *Econometrica*, 56(4):931–954, 1988. ISSN 00129682, 14680262. URL <http://www.jstor.org/stable/1912705>.
- Adith Swaminathan and Thorsten Joachims. Counterfactual risk minimization: Learning from logged bandit feedback. *CoRR*, abs/1502.02362, 2015. URL <http://arxiv.org/abs/1502.02362>.
- Adith Swaminathan, Akshay Krishnamurthy, Alekh Agarwal, Miroslav Dudík, John Langford, Damien Jose, and Imed Zitouni. Off-policy evaluation for slate recommendation. *CoRR*, abs/1605.04812, 2016. URL <http://arxiv.org/abs/1605.04812>.
- Julie Tibshirani, Susan Athey, Stefan Wager, Rina Friedberg, Luke Miner, and Marvin Wright. *grf: Generalized Random Forests (Beta)*, 2018. URL <https://CRAN.R-project.org/package=grf>. R package version 0.9.6.
- S. Wager and S. Athey. Estimation and Inference of Heterogeneous Treatment Effects using Random Forests. *ArXiv e-prints*, October 2015.
- Yu-Xiang Wang, Alekh Agarwal, and Miroslav Dudík. Optimal and adaptive off-policy evaluation in contextual bandits. In Doina Precup and Yee Whye Teh, editors, *Proceedings of the 34th International Conference on Machine Learning*, volume 70 of *Proceedings of Machine Learning Research*, pages 3589–3597, International Convention Centre, Sydney, Australia, 06–11 Aug 2017. PMLR. URL <http://proceedings.mlr.press/v70/wang17a.html>.

## A Moment Conditions for PLR

Recall that for any observation  $Z = (T, Y, W, x)$ , any parameters  $\theta \in \mathbb{R}^d$ , nuisance estimate  $\hat{h}$  parameterized by vectors  $\hat{q}, \hat{\gamma} \in \mathbb{R}^p$ , the score function for PLR is defined as:

$$\psi(Z; \theta, \hat{h}(W, x)) = \{Y - \langle W, \hat{q} \rangle - \theta(T - \langle W, \hat{\gamma} \rangle)\}(T - \langle W, \hat{\gamma} \rangle), \quad (25)$$

with  $\hat{h}(W, x) = (\langle W, \hat{q} \rangle, \langle W, \hat{\gamma} \rangle)$ .

**Lemma A.1.** *The moment condition with respect to the score function  $\psi$  defined in (14) satisfies conditional orthogonality.*

*Proof of Lemma A.1.* In the following, we will write  $\nabla_h \psi$  to denote the gradient of  $\psi$  with respect to the nuisance argument of the input. For any  $W, x$ , we can write

$$\mathbb{E}[\nabla_h \psi(Z; \theta(x), (\langle W, q_0 \rangle, \langle W, \gamma_0 \rangle)) \mid W, x] = \mathbb{E}[(T - \langle W, \gamma_0 \rangle, -Y + \langle W, q_0 \rangle + 2\theta(x)(T - \langle W, \gamma_0 \rangle)) \mid W, x]$$

Furthermore, we have  $\mathbb{E}[T - \langle \gamma_0, W \rangle \mid W, x] = \mathbb{E}[\eta \mid W, x] = 0$  and

$$\mathbb{E}[-Y + \langle W, q_0 \rangle + 2\theta(x)(T - \langle W, \gamma_0 \rangle) \mid W, x] = \mathbb{E}[\langle W, q_0 \rangle - Y + 2\theta(x)\eta \mid W, x] = 0$$

where the last equality follows from that  $\mathbb{E}[\eta \mid W, x] = 0$  and  $\mathbb{E}[\langle W, q_0 \rangle - Y \mid W, x] = 0$ .  $\square$

The next lemma allows us to bound the maximum scale of the PLR score function.

**Lemma A.2.** *Suppose that the nuisance parameters satisfy  $\max\{\|\hat{q} - q_0(x)\|_1 \leq L_q, \|\hat{\gamma} - \gamma_0\|_1 \leq L_\gamma\}$ . Then for any  $\theta \in [-1, 1]$  any observation  $Z_i = (T_i, Y_i, W_i, x_i)$ ,  $\psi(Z_i; \theta, \hat{h}) \leq O((k + L_q + L_\gamma)L_\gamma)$ .*

*Proof.* By Hölder inequality and the boundedness assumption that  $\|q_0(x)\|_1 \leq O(k)$ ,  $|Y_i|, |T_i| \leq O(k)$  for any observation  $i$ , we have:

$$|Y_i - \langle \hat{q}, W_i \rangle| \leq O(k + L_q), \quad |T_i - \langle \hat{\gamma}, W_i \rangle| \leq O(L_\gamma).$$

It follows that for any  $\theta \in [-1, 1]$ ,

$$\psi(Z_i; \theta, \hat{h}) \leq \{O(k + L_q) + T_i - \langle \hat{\gamma}, W_i \rangle\}(T_i - \langle \hat{\gamma}, W_i \rangle) \leq O((k + L_q + L_\gamma)L_\gamma),$$

which recovers the stated bound.  $\square$

## B Proof of Lemma 3.9

In this section, we derive a high-probability bound for the sampling error term  $\Delta(\theta)$  in the decomposition of  $\Lambda_n$ . First, consider the following base function  $f_0$  defined in Algorithm 3 that is parameterized by a base kernel learner  $\mathcal{L}_k$ , a target point  $x$  and estimate  $\theta$ .

Given this definition of base function, we will also define the following function  $f_\theta$  that takes as input  $s$  number of examples:

$$f_\theta(z_1, \dots, z_s) = \frac{1}{s!} \sum_p f_0(z'_1, \dots, z'_s)$$

where  $\sum_p$  denotes the summation over all of the  $s!$  number of permutations  $(z'_1, \dots, z'_s)$  of the input examples  $(z_1, \dots, z_s)$ . Finally, given a dataset  $D$  of  $n$  observations and any fixed integer  $s$ , we consider the following U-statistic:

$$U_\theta(D) = \frac{1}{\binom{n}{s}} \sum_c f_\theta(z_{i_1}, \dots, z_{i_s})$$

---

**Algorithm 3** Base function  $f_0$ , parameterized by a target point  $x$ , an estimate  $\theta$ , and a base kernel learner  $\mathcal{L}_k$

---

**Input:** data set  $S$  of size  $s$

**Initialize:** For each  $z_i \in S$ , set weight  $a_{ib} = 0$  for all  $b \in [B]$

Let  $S^1, S^2$ , and  $S^3$  denote the first, second, and third  $s/3$  parts of the input data set  $S$

Let  $K$  be the kernel function computed by  $\mathcal{L}_k$  using data set  $S^1$

Let  $H = \{z \in S^2 \mid K(x, x_i, S^2) > 0\}$  be the set of points with non-zero weight

Compute nuisance estimator  $\hat{h}$  using the data set  $H$

**Output:**  $\sum_{z_i \in S^3} K(x, x_i, S^3) \psi(z_i; \theta, \hat{h})$

---

where  $\sum_c$  denotes the summation over all of the  $\binom{n}{s}$  combinations of  $s$  distinct choices in  $D$ .

Observe that we can view  $U_\theta(D)$  as a random variable with randomness taken over the random draws of  $D$ . Then its expectation satisfies

$$\mathbb{E}_D[U_\theta(D)] = \mu(\theta).$$

The following first-order tail inequality for U-Statistics is useful for our analysis.

**Theorem B.1** (Hoeffding [1963]). For any  $\varepsilon > 0$ ,

$$\Pr_D[|U_\theta(D) - \mu(\theta)| \geq \varepsilon] \leq 2 \exp\left(-\frac{n}{s} \varepsilon^2\right)$$

Equivalently, for any  $\delta \in (0, 1)$ , with probability  $1 - \delta$ ,  $|U_\theta(D) - \mu(\theta)| \leq \sqrt{\frac{1}{n/s} \ln(2/\delta)}$ .

Recall that

$$\Psi(\theta, \hat{h}) = \frac{1}{B} \sum_{b=1}^B \sum_{i=1}^n a_{ib} \psi(z_i; \theta, \hat{h}_b)$$

We can obtain a high-probability bound for the deviation between  $\Psi(\theta, \hat{h})$  and  $U_\theta(D)$  for any fixed data set  $D$ .

**Lemma B.2.** Fix any  $\theta \in \Theta$ , data set  $D$  and number of iterations  $B$ . Then with probability at least  $1 - \delta$  over the randomness of the algorithm,

$$|\Psi(\theta, \hat{h}) - U_\theta(D)| \leq \sqrt{\frac{\ln(2/\delta)}{2B}}$$

*Proof.* Note that in each iteration  $b$  of the algorithm, the quantity  $\sum_{i=1}^n a_{ib} \psi(z_i; \theta, \hat{h}_b)$  satisfies

$$\mathbb{E} \left[ \sum_{i=1}^n a_{ib} \psi(z_i; \theta, \hat{h}_b) \right] = U_\theta(D)$$

Then we can view  $\Psi(\theta, \hat{h})$  as the average of  $B$  i.i.d. random variables with mean  $U_\theta(D)$ . By applying the standard Chernoff bound, we have for any  $\varepsilon > 0$ ,

$$\Pr \left[ |\Psi(\theta, \hat{h}) - U_\theta(D)| > \varepsilon \right] \leq 2 \exp(-2B\varepsilon^2)$$

Then setting the deviation  $\varepsilon = \sqrt{\ln(2/\delta)/(2B)}$  recovers our stated bound.  $\square$

**Proof of Lemma 3.9** By combining the results from Theorem B.1 and Lemma B.2, we can also bound the difference between  $\Psi(\theta, \hat{h})$  and  $\mu(\theta)$ . The final bound follows from the fact that  $\sqrt{s/n} \geq \sqrt{1/B}$  as long as  $B \geq n/s$ .

## C Setting Minimum Leaf Size $r$

Recall that our main convergence analysis uses the general convergence result of GMM estimation (Theorem 3.4), so it does not optimize the dependence on the minimum leaf size  $r$ . We now give a heuristic on how one can optimize the dependence on  $r$ , which is useful for choosing this parameter in the experiments when the features  $x$  are higher-dimensional.

Recall that in the final bound of Theorem 3.4, there are two terms. The first term comes from the kernel error, which is upper bounded the kernel shrinkage  $O(s^{-\tau})$ . We can replace  $s^{-\tau}$  by a more refined bound  $d\left(\frac{s}{2r-1}\right)^{\frac{-1}{2\alpha d}}$  as given in Lemma 5.1. The second term comes from the sampling error  $|\Psi(\theta, \hat{h}) - \mu(\theta)|$ , which can be bounded by  $O(k\sqrt{s\ln(1/\delta)/n})$  using the first-order tail bound for  $U$ -statistic. We can in fact obtain a second-order error bound by using the Bernstein inequality [Arcones, 1995]:

$$|\Psi(\theta, \hat{h}) - \mu(\theta)| \leq O\left(\sqrt{\frac{V^2}{(n/s)} \ln(1/\delta)} + \frac{k}{(n/s)} \ln(1/\delta)\right)$$

where  $V$  denotes the variance of the following random variable

$$\Psi' = \sum_{i=1}^s a_{ib} \psi(Z_i; \theta, \hat{h}(W_i))$$

where  $\{Z_i\}_{i=1}^s$  is a set of i.i.d. observations, and each  $a_{ib}$  is the tree weight assigned by the tree learner that partitions the input data as  $S_b^1 = \{Z_1, \dots, Z_{\lfloor s/2 \rfloor}\}$  and  $S_b^2 = \{Z_{\lfloor s/2 \rfloor + 1}, \dots, Z_s\}$ . We can further rewrite the expression

$$\Psi' = \sum_{Z_i \in L_b^2(x)} \frac{1}{|L_b^2(x)|} \psi(Z_i; \theta, \hat{h}(W_i))$$

where  $L_b^2(x)$  denotes the subset of observations in  $S_b^2$  that fall into the same leaf as  $x$ . Note that for any observation in  $S_b^2$ , the terms  $\psi(Z_i; \theta, \hat{h}(W_i))$  are independent conditioned on the realization of  $x_i$ 's and  $S_b^1$ . Thus, the random variable  $\Psi'$  conditioned on the realization of  $x_i$ 's and  $S_b^1$  can be viewed as a sum of  $|L_b^2(x)|$  independent random variables. By law of total variance we can write

$$\begin{aligned} V &= \mathbb{E}\left[\text{Var}(\Psi' \mid x_1, \dots, x_s, S_b^1)\right] + \text{Var}\left(\mathbb{E}[\Psi' \mid x_1, \dots, x_s, S_b^1]\right) \\ &\leq O(k^2/r) + \text{Var}\left(\mathbb{E}[\Psi' \mid x_1, \dots, x_s, S_b^1]\right) \end{aligned}$$

where the last inequality follows from the fact that  $r \leq |L_b^2(x)| \leq 2r$ . Note that as  $\theta$  converges to the target value  $\theta_0$ , and the  $\hat{h}$  converges the target nuisance parameter  $h_0$ , the conditional expectation  $\mathbb{E}[\Psi' \mid x_1, \dots, x_s, S_b^1]$  is tending to 0, so its variance has lower order than  $k^2/r$ . Therefore, it suffices to choose  $r$  to optimize the sum of the dominating terms from the kernel error and the sampling error:

$$\frac{k^2}{r} \sqrt{\frac{s \ln(1/\delta)}{n}} + d\left(\frac{s}{2r-1}\right)^{\frac{-1}{2\alpha d}}$$

If subsample size  $s = \left(\frac{n}{k^2 \ln(p)}\right)^{\frac{1}{2\tau+1}}$ , then we can set  $r = \frac{k}{d}^{2/2+2\tau}$  to balance the two sources of error.

## D All Experimental Results

We present all experimental results for the parameter choices described in Section 6. We vary the number of samples  $n \in \{5000, 10000\}$ , the support size  $k \in \{1, 5, 10, 15, 20, 25, 30\}$ , the dimension  $d \in \{1, 2\}$  of the feature vector  $x$  and the treatment response function  $\theta \in \{\text{piecewise linear, piecewise constant and piecewise polynomial}\}$ . We measure the bias, variance and root mean square error (RMSE) as evaluation metrics for the different estimators we consider. For the parameter space we consider, the ORF-CV and the ORF algorithms outperform the other estimators on all regimes.

### D.1 Experimental results for one-dimensional, piecewise linear $\theta_0$

We highlight the results for a piecewise linear function given by:

$$\theta_0(x) = (x + 2)\mathbb{I}_{x \leq 0.3} + (6x + 0.5)\mathbb{I}_{x > 0.3 \text{ and } x \leq 0.6} + (-3x + 5.9)\mathbb{I}_{x > 0.6}$$

- $n = 5000, k \in \{1, 5, 10, 15, 20, 25, 30\}$

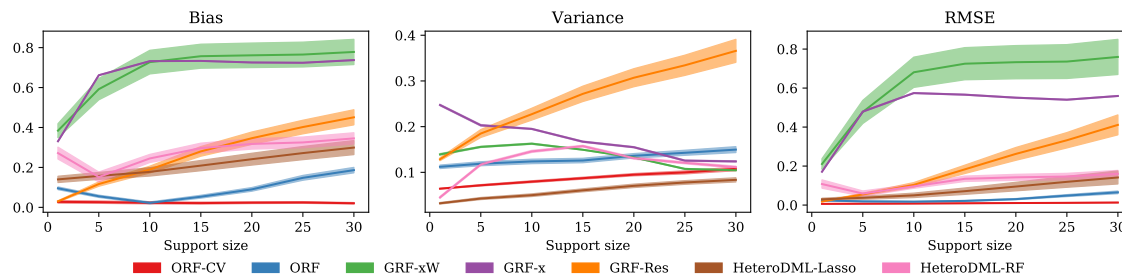


Figure 7: Bias, variance and RMSE as a function of support size for  $n = 5000, p = 500, d = 1$  and a piecewise linear treatment function. The solid lines represent the mean of the metrics across test points, averaged over the Monte Carlo experiments, and the filled regions depict the standard deviation, scaled down by a factor of 3 for clarity.

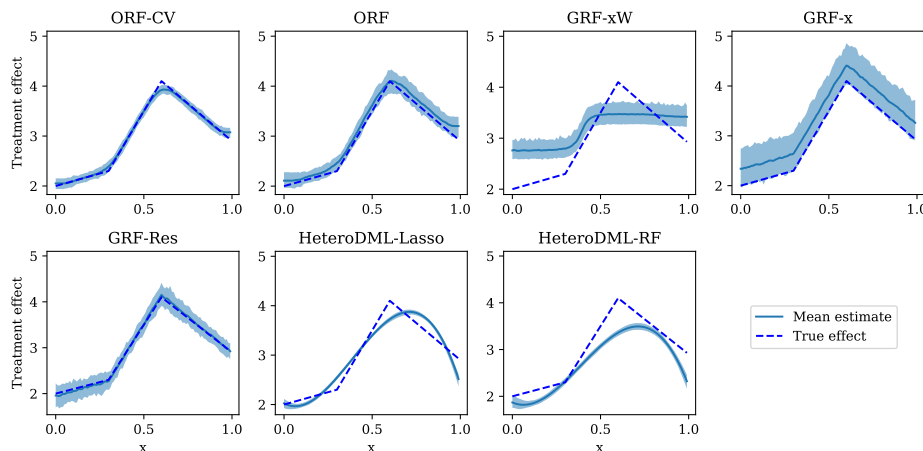


Figure 8: Treatment effect estimations for 100 Monte Carlo experiments with parameters  $n = 5000, p = 500, d = 1, k = 1$ , and a piecewise linear treatment response. The shaded regions depict the mean and the 5%-95% interval of the 100 experiments.

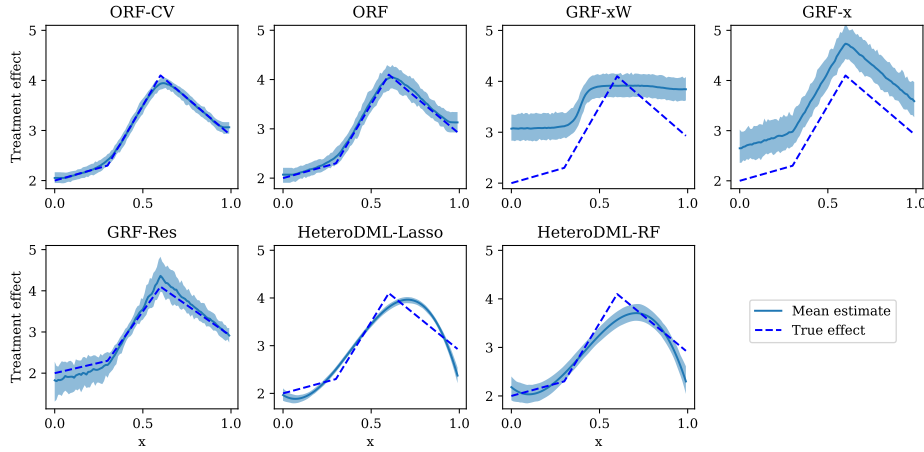


Figure 9: Treatment effect estimations for 100 Monte Carlo experiments with parameters  $n = 5000$ ,  $p = 500$ ,  $d = 1$ ,  $k = 5$ , and a piecewise linear treatment response. The shaded regions depict the mean and the 5%-95% interval of the 100 experiments.

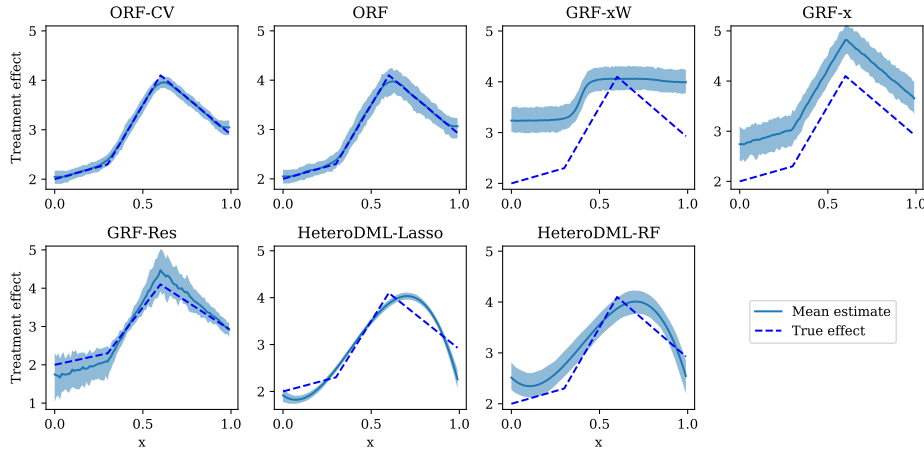


Figure 10: Treatment effect estimations for 100 Monte Carlo experiments with parameters  $n = 5000$ ,  $p = 500$ ,  $d = 1$ ,  $k = 10$ , and a piecewise linear treatment response. The shaded regions depict the mean and the 5%-95% interval of the 100 experiments.

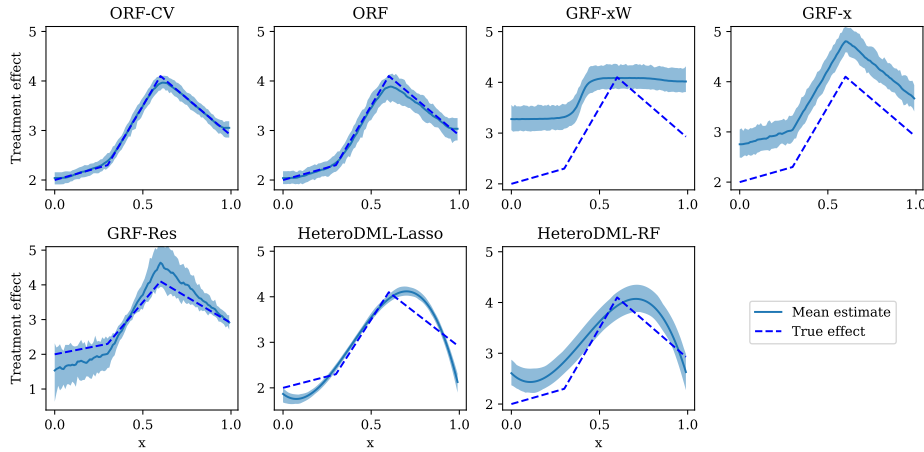


Figure 11: Treatment effect estimations for 100 Monte Carlo experiments with parameters  $n = 5000$ ,  $p = 500$ ,  $d = 1$ ,  $k = 15$ , and a piecewise linear treatment response. The shaded regions depict the mean and the 5%-95% interval of the 100 experiments.

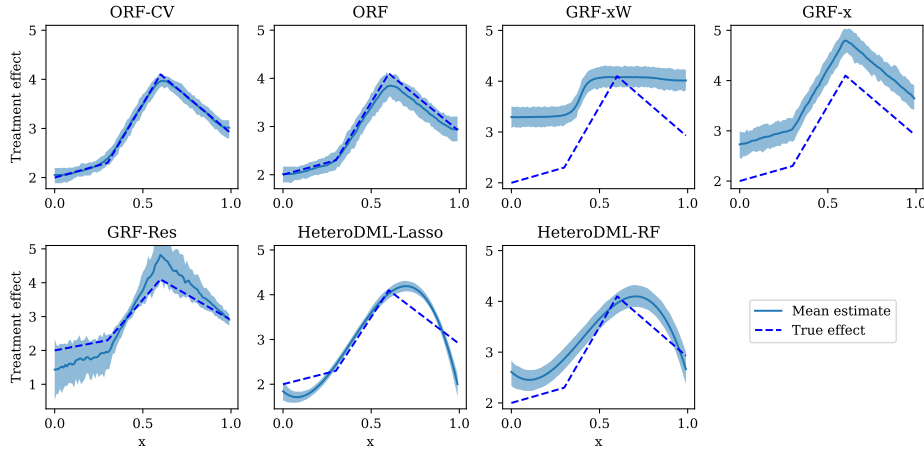


Figure 12: Treatment effect estimations for 100 Monte Carlo experiments with parameters  $n = 5000$ ,  $p = 500$ ,  $d = 1$ ,  $k = 20$ , and a piecewise linear treatment response. The shaded regions depict the mean and the 5%-95% interval of the 100 experiments.

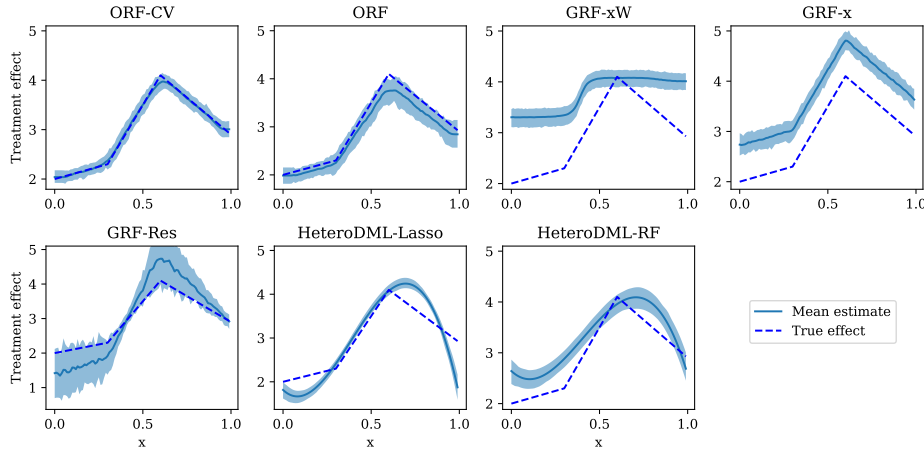


Figure 13: Treatment effect estimations for 100 Monte Carlo experiments with parameters  $n = 5000$ ,  $p = 500$ ,  $d = 1$ ,  $k = 25$ , and a piecewise linear treatment response. The shaded regions depict the mean and the 5%-95% interval of the 100 experiments.

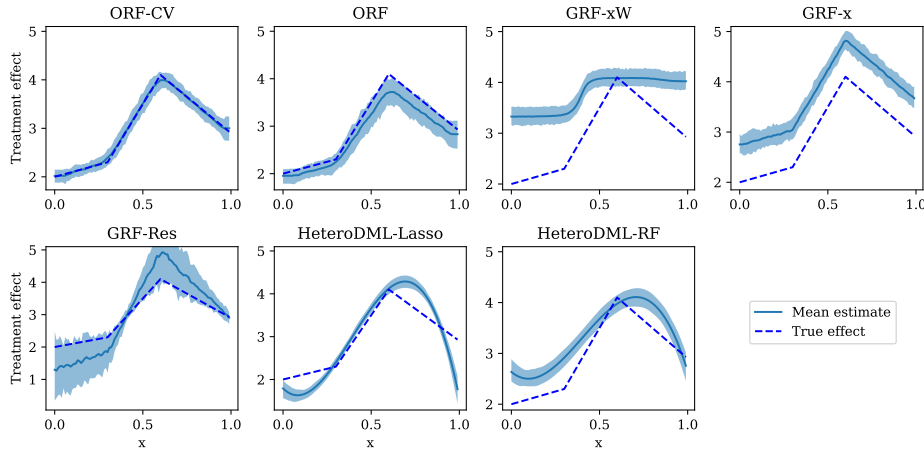


Figure 14: Treatment effect estimations for 100 Monte Carlo experiments with parameters  $n = 5000$ ,  $p = 500$ ,  $d = 1$ ,  $k = 30$ , and a piecewise linear treatment response. The shaded regions depict the mean and the 5%-95% interval of the 100 experiments.

- $n = 10000, k \in \{1, 5, 10, 15, 20, 25, 30\}$

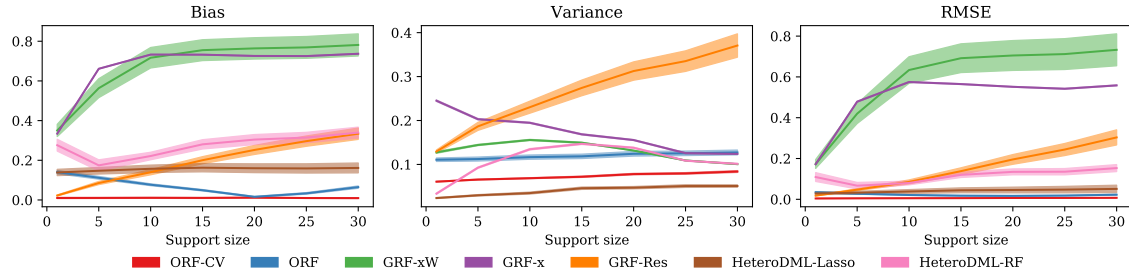


Figure 15: Bias, variance and RMSE as a function of support size for  $n = 10000, p = 500, d = 1$  and a piecewise linear treatment function. The solid lines represent the mean of the metrics across test points, averaged over the Monte Carlo experiments, and the filled regions depict the standard deviation, scaled down by a factor of 3 for clarity.

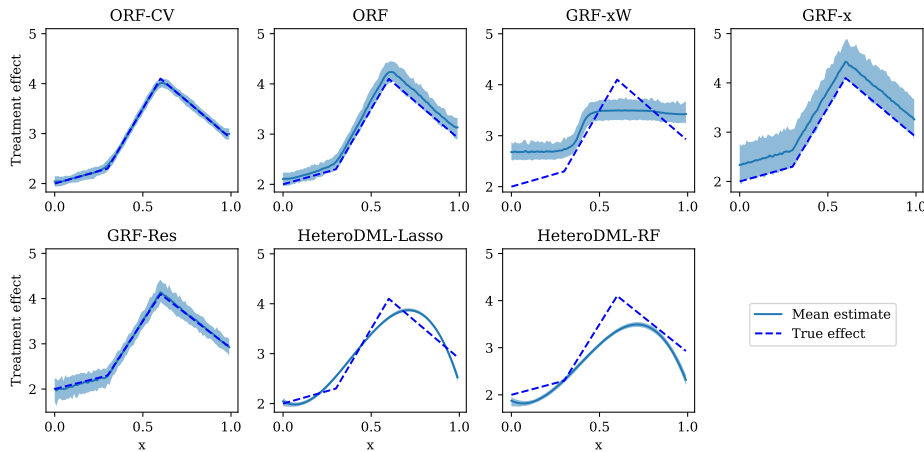


Figure 16: Treatment effect estimations for 100 Monte Carlo experiments with parameters  $n = 10000, p = 500, d = 1, k = 1$ , and a piecewise linear treatment response. The shaded regions depict the mean and the 5%-95% interval of the 100 experiments.

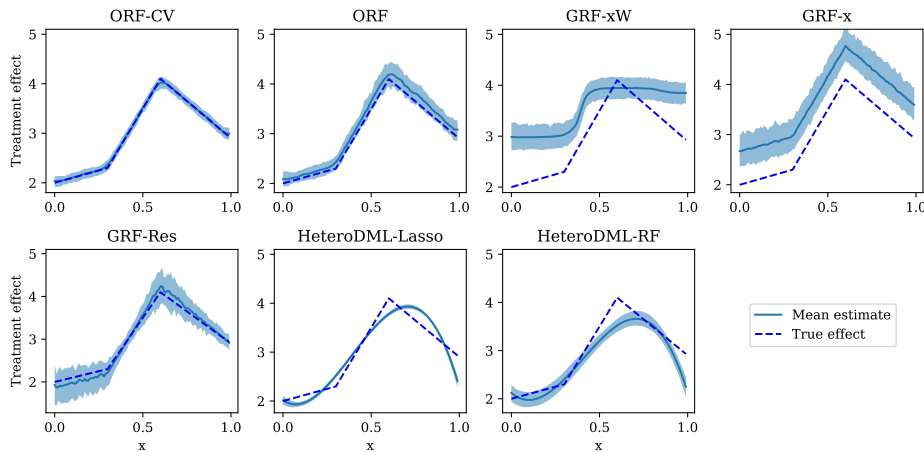


Figure 17: Treatment effect estimations for 100 Monte Carlo experiments with parameters  $n = 10000, p = 500, d = 1, k = 5$ , and a piecewise linear treatment response. The shaded regions depict the mean and the 5%-95% interval of the 100 experiments.

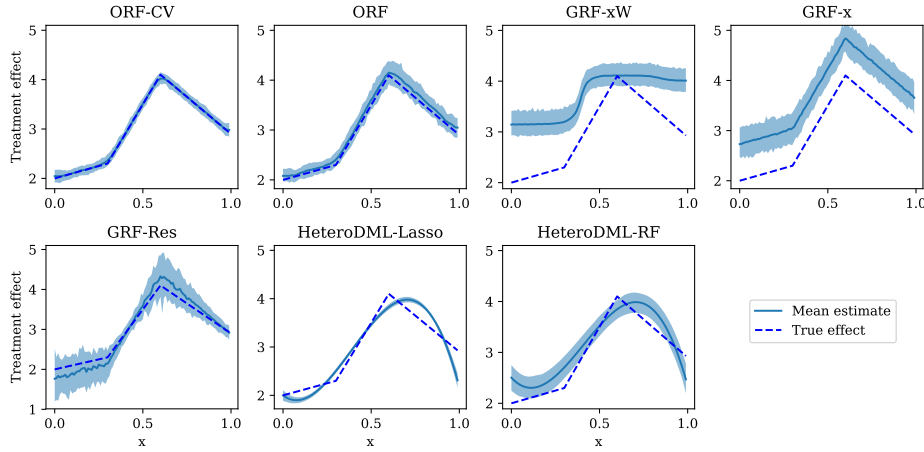


Figure 18: Treatment effect estimations for 100 Monte Carlo experiments with parameters  $n = 10000$ ,  $p = 500$ ,  $d = 1$ ,  $k = 10$ , and a piecewise linear treatment response. The shaded regions depict the mean and the 5%-95% interval of the 100 experiments.

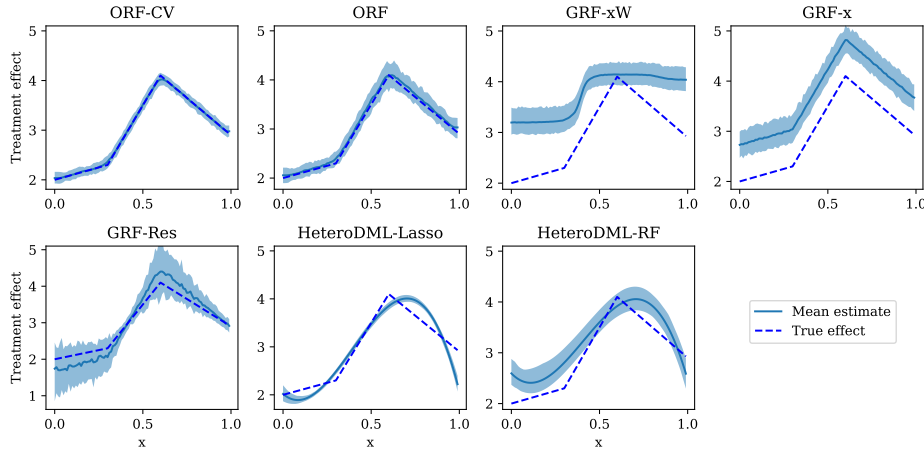


Figure 19: Treatment effect estimations for 100 Monte Carlo experiments with parameters  $n = 10000$ ,  $p = 500$ ,  $d = 1$ ,  $k = 15$ , and a piecewise linear treatment response. The shaded regions depict the mean and the 5%-95% interval of the 100 experiments.

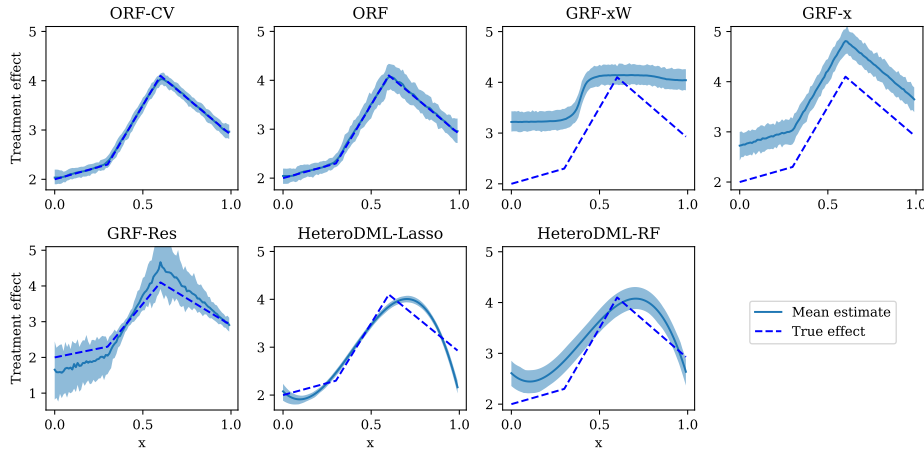


Figure 20: Treatment effect estimations for 100 Monte Carlo experiments with parameters  $n = 10000$ ,  $p = 500$ ,  $d = 1$ ,  $k = 20$ , and a piecewise linear treatment response. The shaded regions depict the mean and the 5%-95% interval of the 100 experiments.

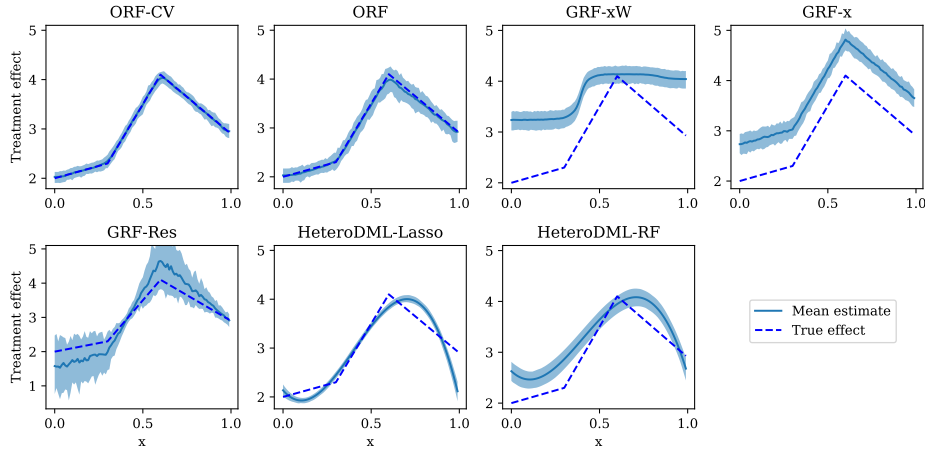


Figure 21: Treatment effect estimations for 100 Monte Carlo experiments with parameters  $n = 10000$ ,  $p = 500$ ,  $d = 1$ ,  $k = 25$ , and a piecewise linear treatment response. The shaded regions depict the mean and the 5%-95% interval of the 100 experiments.

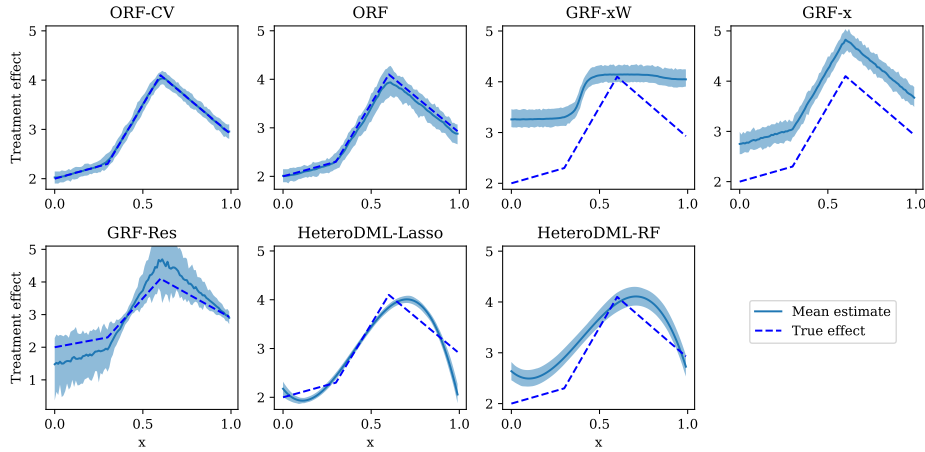


Figure 22: Treatment effect estimations for 100 Monte Carlo experiments with parameters  $n = 10000$ ,  $p = 500$ ,  $d = 1$ ,  $k = 30$ , and a piecewise linear treatment response. The shaded regions depict the mean and the 5%-95% interval of the 100 experiments.

## D.2 Experimental results for one-dimensional, piecewise constant $\theta_0$

We introduce the results for a piecewise constant function given by:

$$\theta_0(x) = \mathbb{I}_{x \leq 0.2} + 5\mathbb{I}_{x > 0.2 \text{ and } x \leq 0.6} + 3\mathbb{I}_{x > 0.6}$$

- $n = 5000, k \in \{1, 5, 10, 15, 20, 25, 30\}$

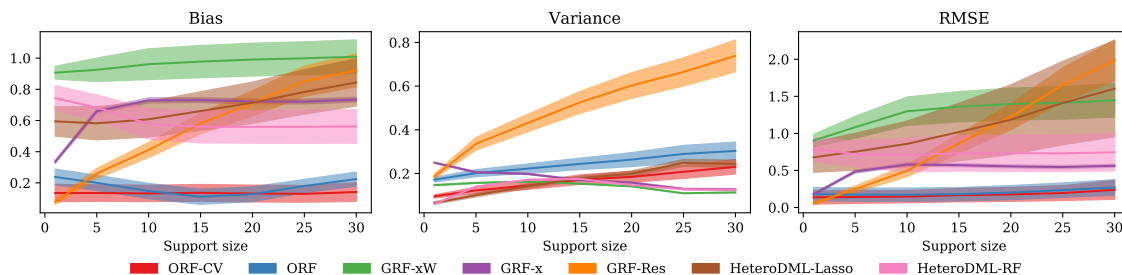


Figure 23: Bias, variance and RMSE as a function of support size for  $n = 5000, p = 500, d = 1$  and a piecewise constant treatment function. The solid lines represent the mean of the metrics across test points, averaged over the Monte Carlo experiments, and the filled regions depict the standard deviation, scaled down by a factor of 3 for clarity.

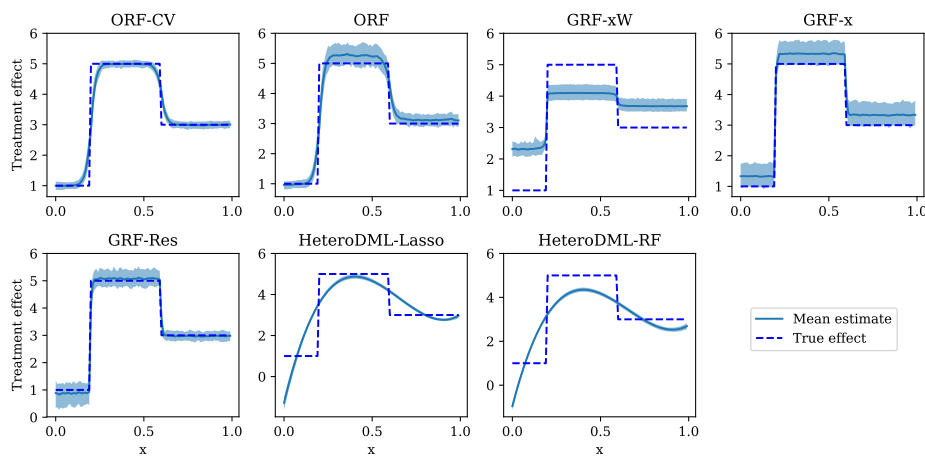


Figure 24: Treatment effect estimations for 100 Monte Carlo experiments with parameters  $n = 5000, p = 500, d = 1, k = 1$ , and a piecewise constant treatment response. The shaded regions depict the mean and the 5%-95% interval of the 100 experiments.

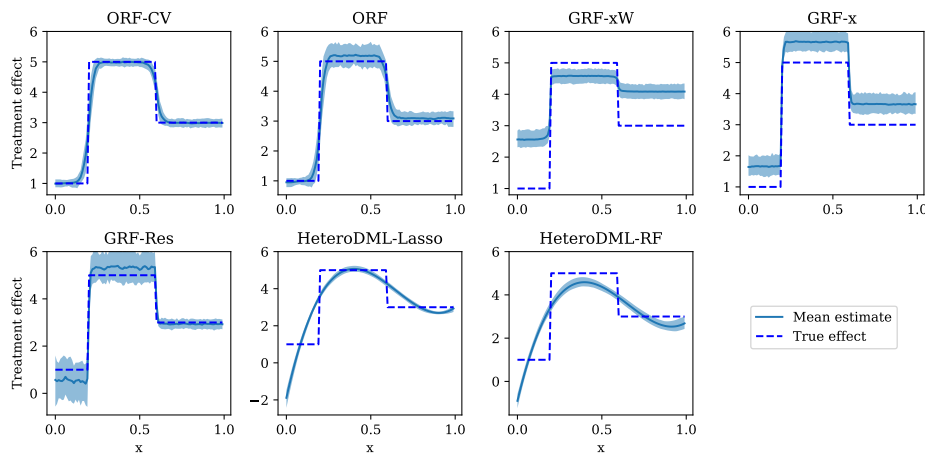


Figure 25: Treatment effect estimations for 100 Monte Carlo experiments with parameters  $n = 5000, p = 500, d = 1, k = 5$ , and a piecewise constant treatment response. The shaded regions depict the mean and the 5%-95% interval of the 100 experiments.

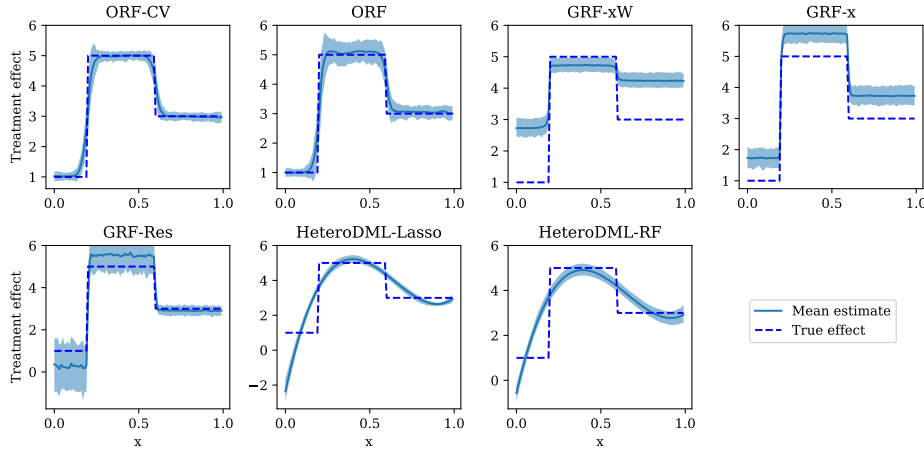


Figure 26: Treatment effect estimations for 100 Monte Carlo experiments with parameters  $n = 5000$ ,  $p = 500$ ,  $d = 1$ ,  $k = 10$ , and a piecewise constant treatment response. The shaded regions depict the mean and the 5%-95% interval of the 100 experiments.

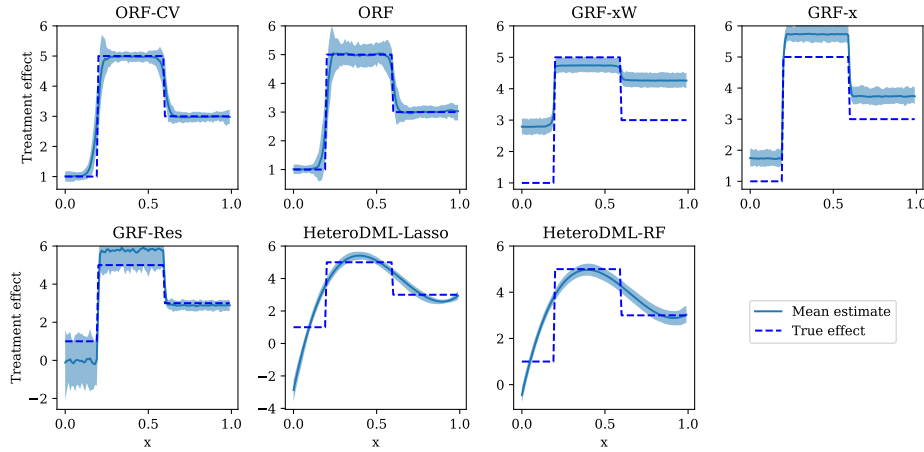


Figure 27: Treatment effect estimations for 100 Monte Carlo experiments with parameters  $n = 5000$ ,  $p = 500$ ,  $d = 1$ ,  $k = 15$ , and a piecewise constant treatment response. The shaded regions depict the mean and the 5%-95% interval of the 100 experiments.

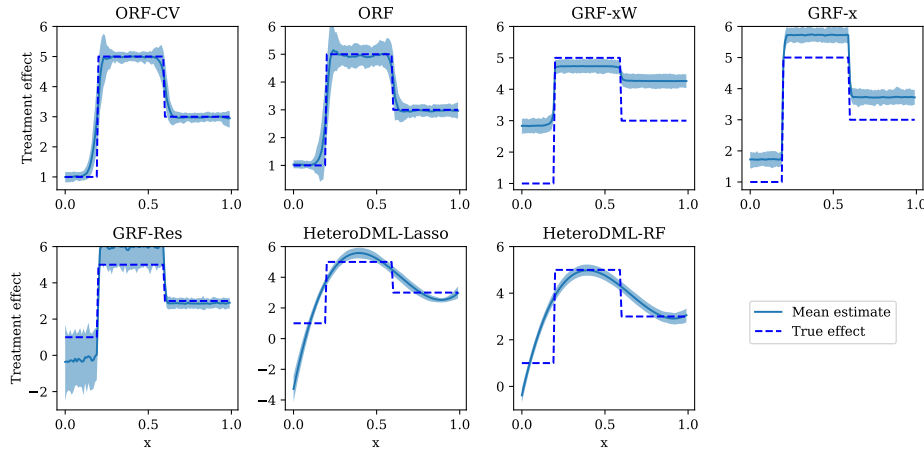


Figure 28: Treatment effect estimations for 100 Monte Carlo experiments with parameters  $n = 5000$ ,  $p = 500$ ,  $d = 1$ ,  $k = 20$ , and a piecewise constant treatment response. The shaded regions depict the mean and the 5%-95% interval of the 100 experiments.

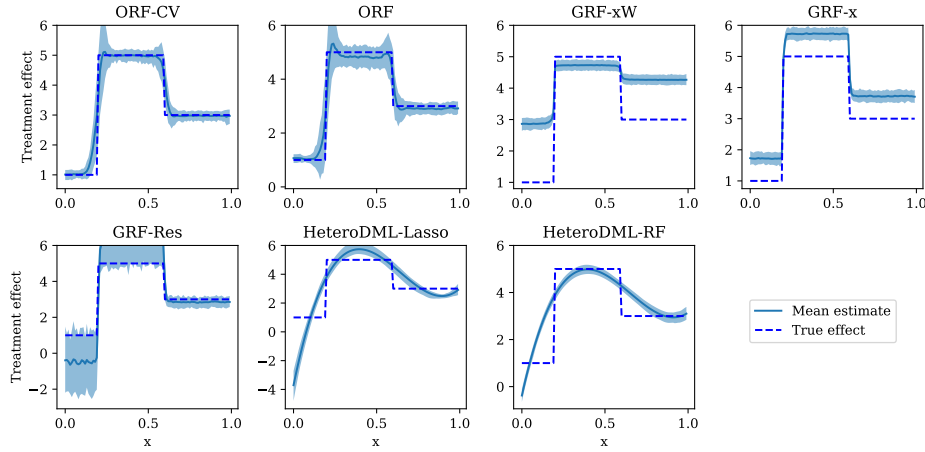


Figure 29: Treatment effect estimations for 100 Monte Carlo experiments with parameters  $n = 5000$ ,  $p = 500$ ,  $d = 1$ ,  $k = 25$ , and a piecewise constant treatment response. The shaded regions depict the mean and the 5%-95% interval of the 100 experiments.

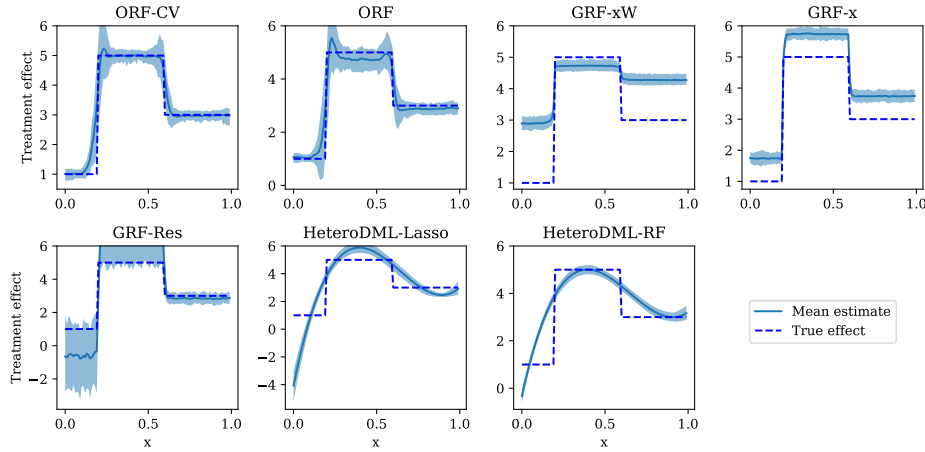


Figure 30: Treatment effect estimations for 100 Monte Carlo experiments with parameters  $n = 5000$ ,  $p = 500$ ,  $d = 1$ ,  $k = 30$ , and a piecewise constant treatment response. The shaded regions depict the mean and the 5%-95% interval of the 100 experiments.

- $n = 10000, k \in \{1, 5, 10, 15, 20, 25, 30\}$

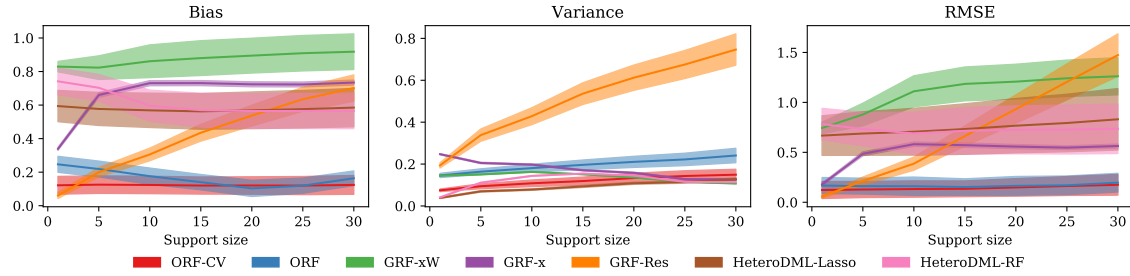


Figure 31: Bias, variance and RMSE as a function of support size for  $n = 10000, p = 500, d = 1$  and a piecewise constant treatment function. The solid lines represent the mean of the metrics across test points, averaged over the Monte Carlo experiments, and the filled regions depict the standard deviation, scaled down by a factor of 3 for clarity.

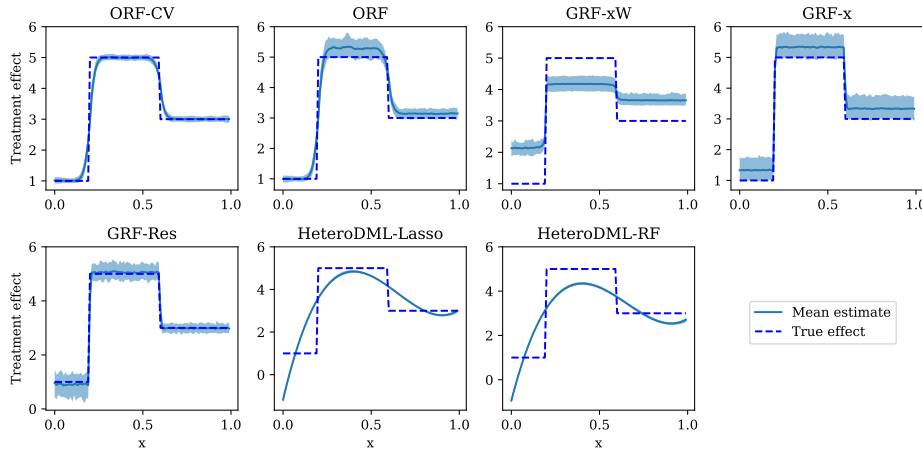


Figure 32: Treatment effect estimations for 100 Monte Carlo experiments with parameters  $n = 5000, p = 500, d = 1, k = 1$ , and a piecewise constant treatment response. The shaded regions depict the mean and the 5%-95% interval of the 100 experiments.

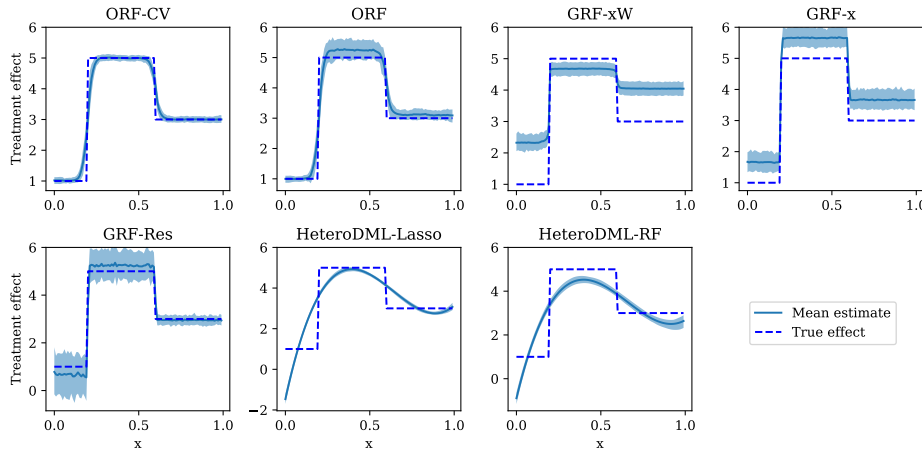


Figure 33: Treatment effect estimations for 100 Monte Carlo experiments with parameters  $n = 5000, p = 500, d = 1, k = 5$ , and a piecewise constant treatment response. The shaded regions depict the mean and the 5%-95% interval of the 100 experiments.

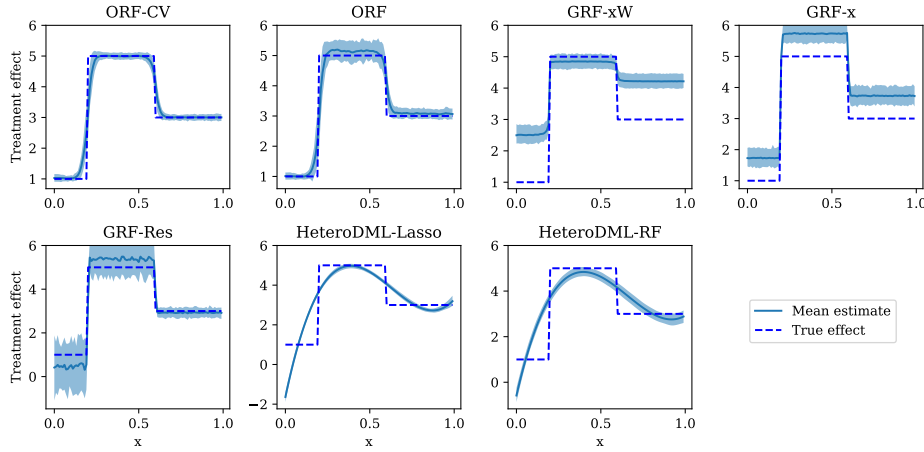


Figure 34: Treatment effect estimations for 100 Monte Carlo experiments with parameters  $n = 5000$ ,  $p = 500$ ,  $d = 1$ ,  $k = 10$ , and a piecewise constant treatment response. The shaded regions depict the mean and the 5%-95% interval of the 100 experiments.

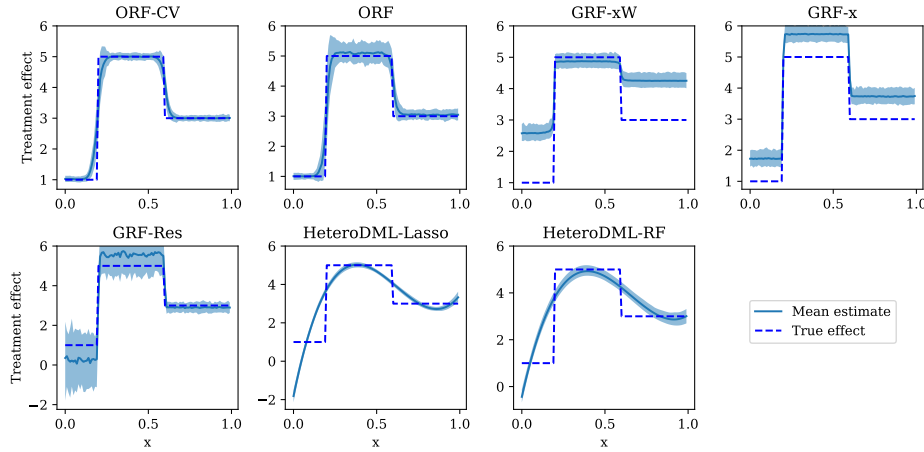


Figure 35: Treatment effect estimations for 100 Monte Carlo experiments with parameters  $n = 5000$ ,  $p = 500$ ,  $d = 1$ ,  $k = 15$ , and a piecewise constant treatment response. The shaded regions depict the mean and the 5%-95% interval of the 100 experiments.

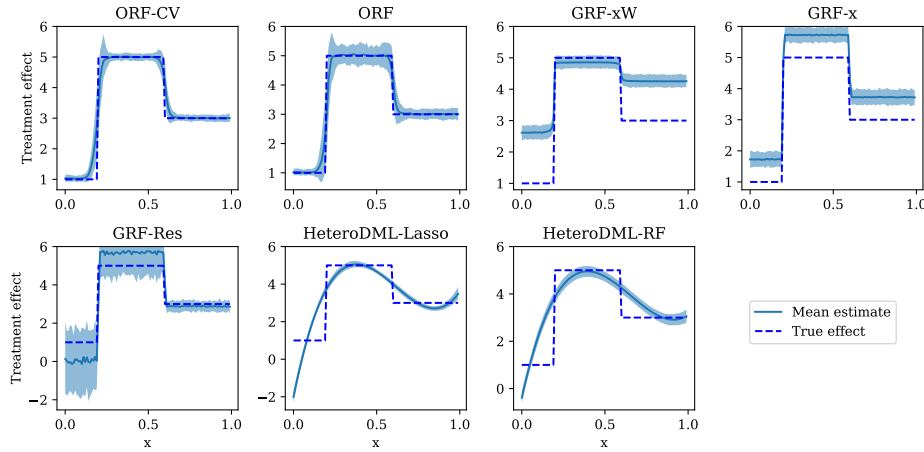


Figure 36: Treatment effect estimations for 100 Monte Carlo experiments with parameters  $n = 5000$ ,  $p = 500$ ,  $d = 1$ ,  $k = 20$ , and a piecewise constant treatment response. The shaded regions depict the mean and the 5%-95% interval of the 100 experiments.

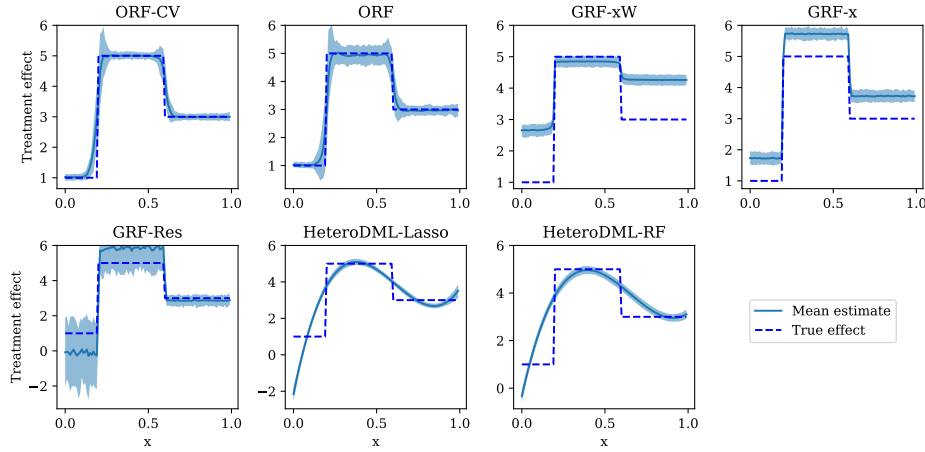


Figure 37: Treatment effect estimations for 100 Monte Carlo experiments with parameters  $n = 5000$ ,  $p = 500$ ,  $d = 1$ ,  $k = 25$ , and a piecewise constant treatment response. The shaded regions depict the mean and the 5%-95% interval of the 100 experiments.

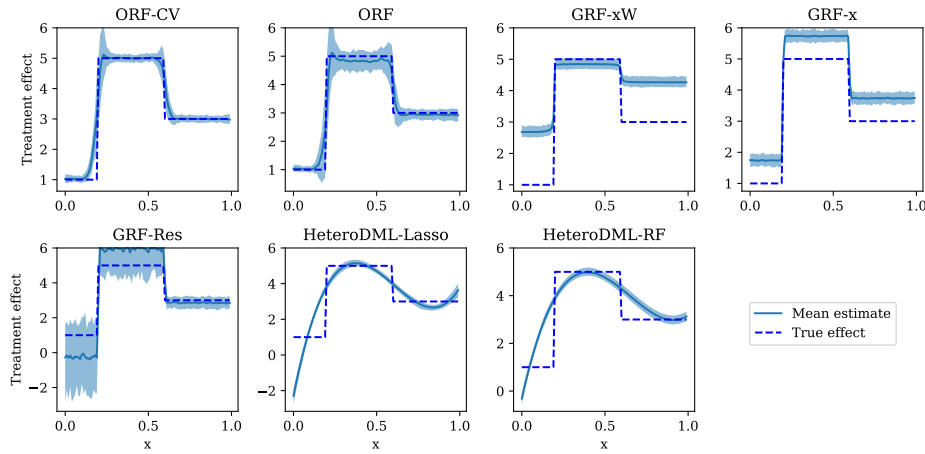


Figure 38: Treatment effect estimations for 100 Monte Carlo experiments with parameters  $n = 5000$ ,  $p = 500$ ,  $d = 1$ ,  $k = 30$ , and a piecewise constant treatment response. The shaded regions depict the mean and the 5%-95% interval of the 100 experiments.

### D.3 Experimental results for one-dimensional, piecewise polynomial $\theta_0$

We present the results for a piecewise polynomial function given by:

$$\theta_0(x) = 3x^2\mathbb{I}_{x \leq 0.2} + (3x^2 + 1)\mathbb{I}_{x > 0.2 \text{ and } x \leq 0.6} + (6x + 2)\mathbb{I}_{x > 0.6}$$

- $n = 5000, k \in \{1, 5, 10, 15, 20, 25, 30\}$

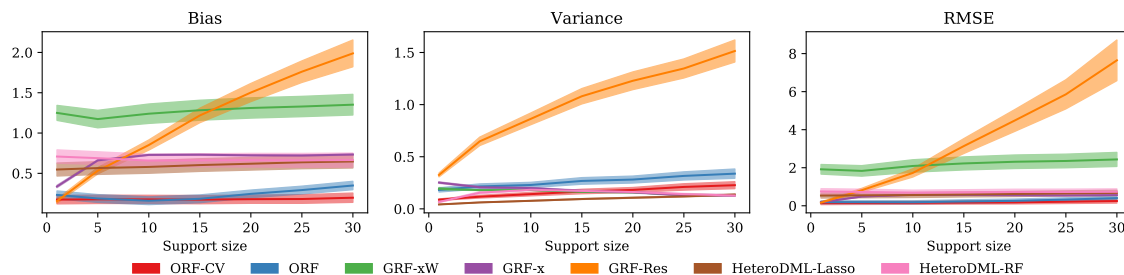


Figure 39: Bias, variance and RMSE as a function of support size for  $n = 5000, p = 500, d = 1$  and a piecewise polynomial treatment function. The solid lines represent the mean of the metrics across test points, averaged over the Monte Carlo experiments, and the filled regions depict the standard deviation, scaled down by a factor of 3 for clarity.

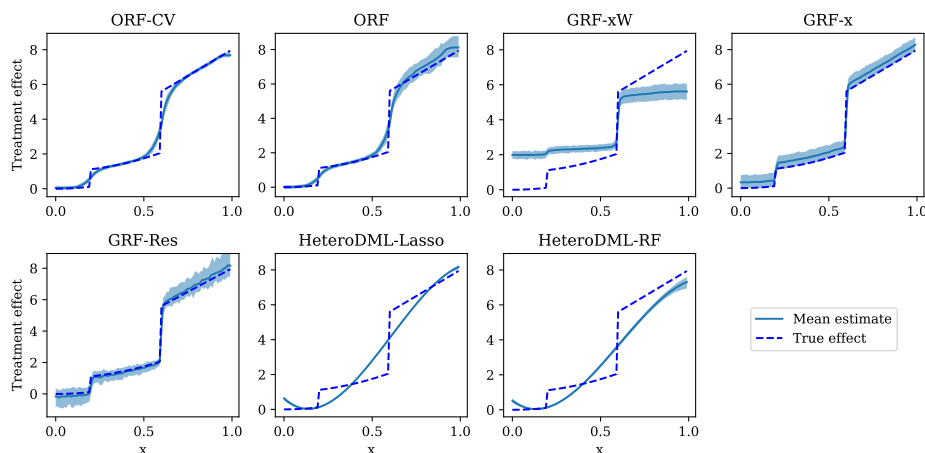


Figure 40: Treatment effect estimations for 100 Monte Carlo experiments with parameters  $n = 5000, p = 500, d = 1, k = 1$ , and a piecewise polynomial treatment response. The shaded regions depict the mean and the 5%-95% interval of the 100 experiments.

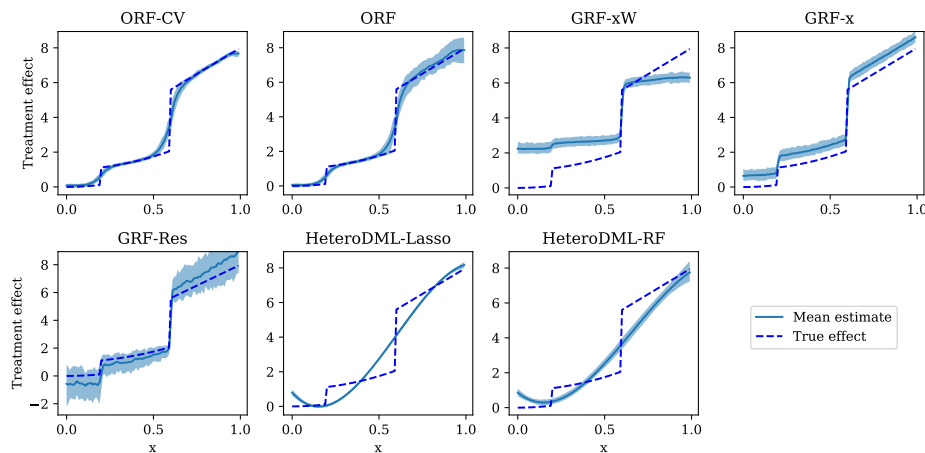


Figure 41: Treatment effect estimations for 100 Monte Carlo experiments with parameters  $n = 5000, p = 500, d = 1, k = 5$ , and a piecewise polynomial treatment response. The shaded regions depict the mean and the 5%-95% interval of the 100 experiments.

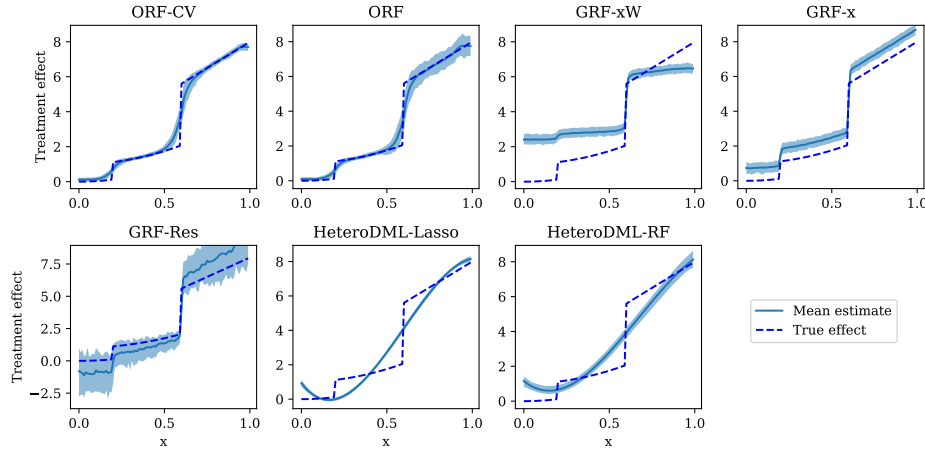


Figure 42: Treatment effect estimations for 100 Monte Carlo experiments with parameters  $n = 5000$ ,  $p = 500$ ,  $d = 1$ ,  $k = 10$ , and a piecewise polynomial treatment response. The shaded regions depict the mean and the 5%-95% interval of the 100 experiments.

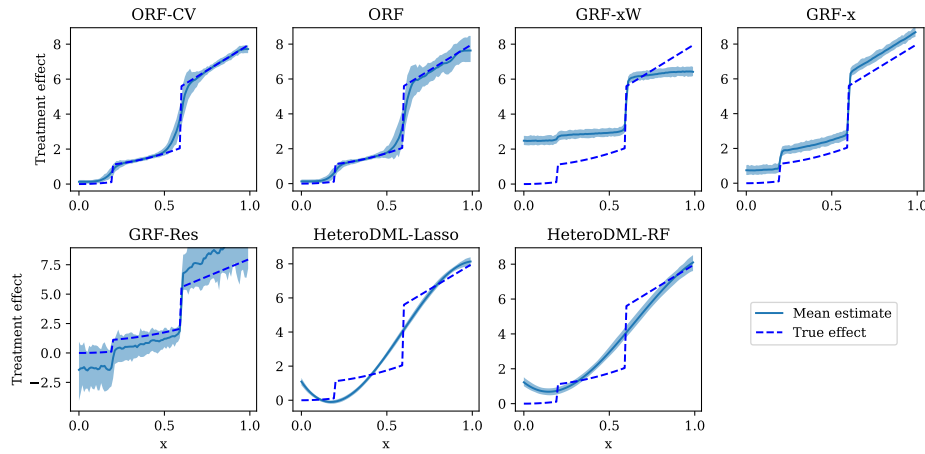


Figure 43: Treatment effect estimations for 100 Monte Carlo experiments with parameters  $n = 5000$ ,  $p = 500$ ,  $d = 1$ ,  $k = 15$ , and a piecewise polynomial treatment response. The shaded regions depict the mean and the 5%-95% interval of the 100 experiments.

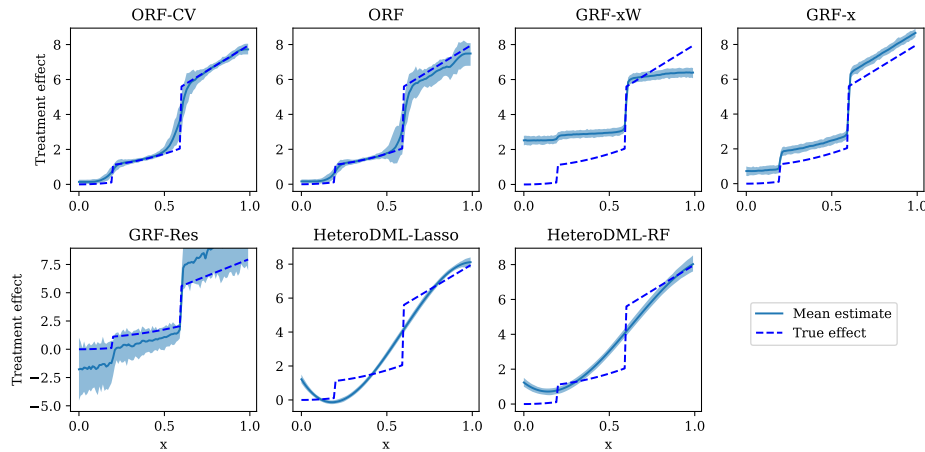


Figure 44: Treatment effect estimations for 100 Monte Carlo experiments with parameters  $n = 5000$ ,  $p = 500$ ,  $d = 1$ ,  $k = 20$ , and a piecewise polynomial treatment response. The shaded regions depict the mean and the 5%-95% interval of the 100 experiments.

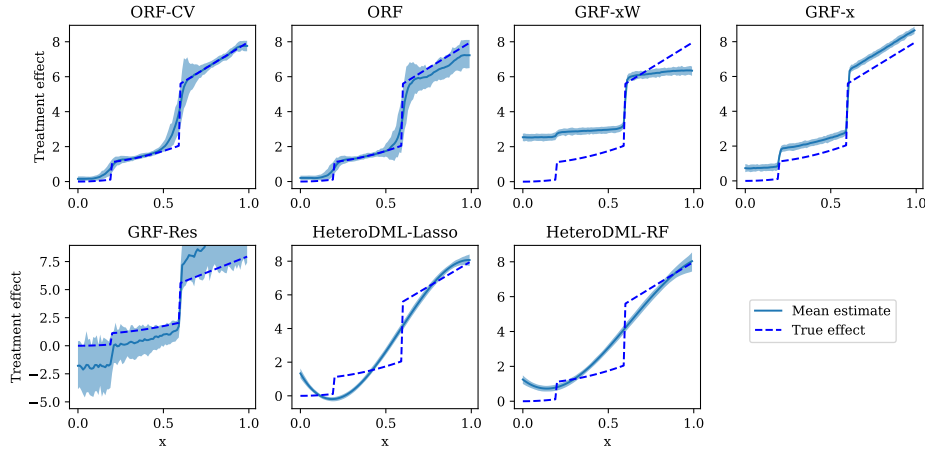


Figure 45: Treatment effect estimations for 100 Monte Carlo experiments with parameters  $n = 5000$ ,  $p = 500$ ,  $d = 1$ ,  $k = 25$ , and a piecewise polynomial treatment response. The shaded regions depict the mean and the 5%-95% interval of the 100 experiments.

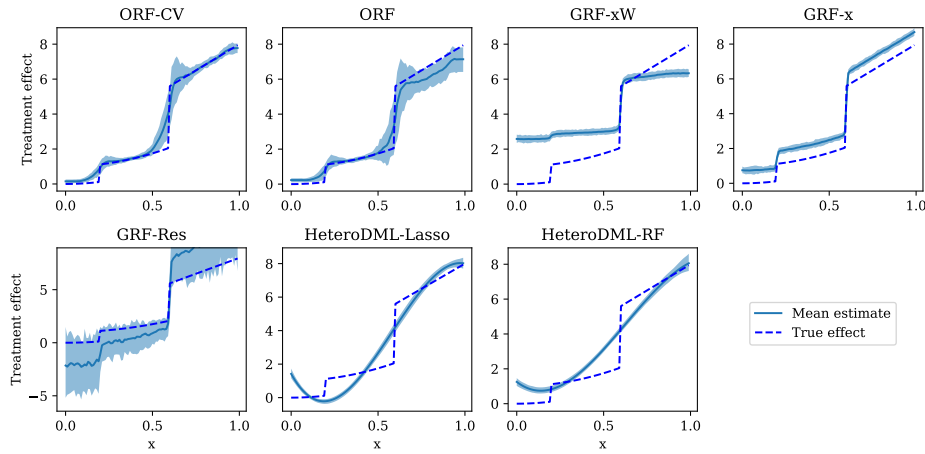


Figure 46: Treatment effect estimations for 100 Monte Carlo experiments with parameters  $n = 5000$ ,  $p = 500$ ,  $d = 1$ ,  $k = 30$ , and a piecewise polynomial treatment response. The shaded regions depict the mean and the 5%-95% interval of the 100 experiments.

- $n = 10000, k \in \{1, 5, 10, 15, 20, 25, 30\}$

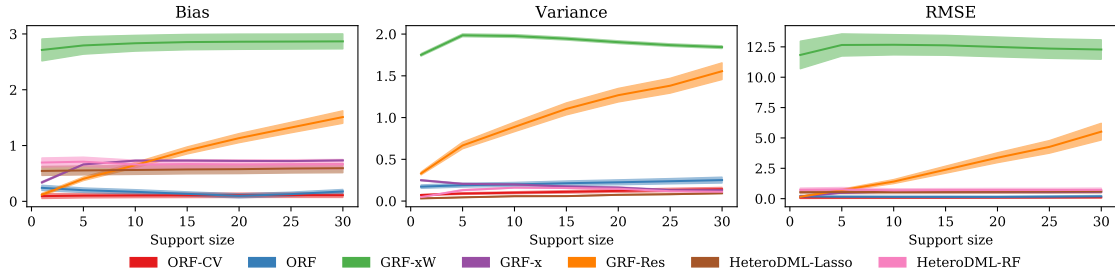


Figure 47: Bias, variance and RMSE as a function of support size for  $n = 10000, p = 500, d = 1$  and a piecewise polynomial treatment function. The solid lines represent the mean of the metrics across test points, averaged over the Monte Carlo experiments, and the filled regions depict the standard deviation, scaled down by a factor of 3 for clarity.

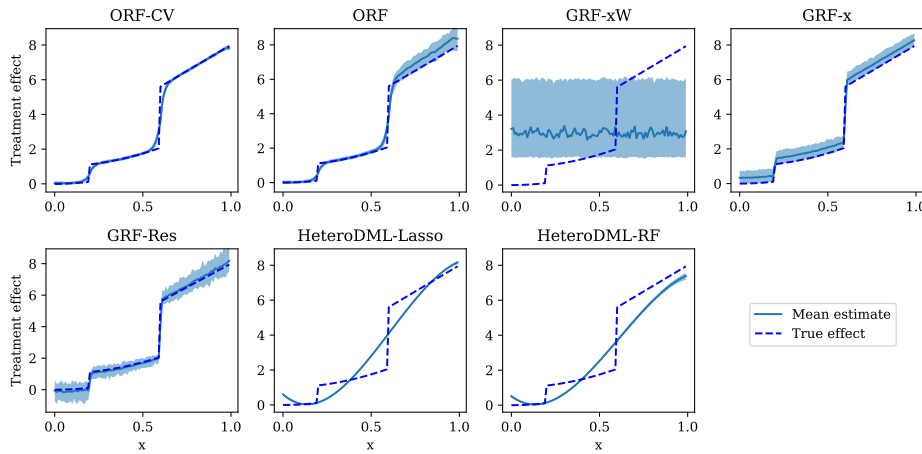


Figure 48: Treatment effect estimations for 100 Monte Carlo experiments with parameters  $n = 10000, p = 500, d = 1, k = 1$ , and a piecewise polynomial treatment response. The shaded regions depict the mean and the 5%-95% interval of the 100 experiments.

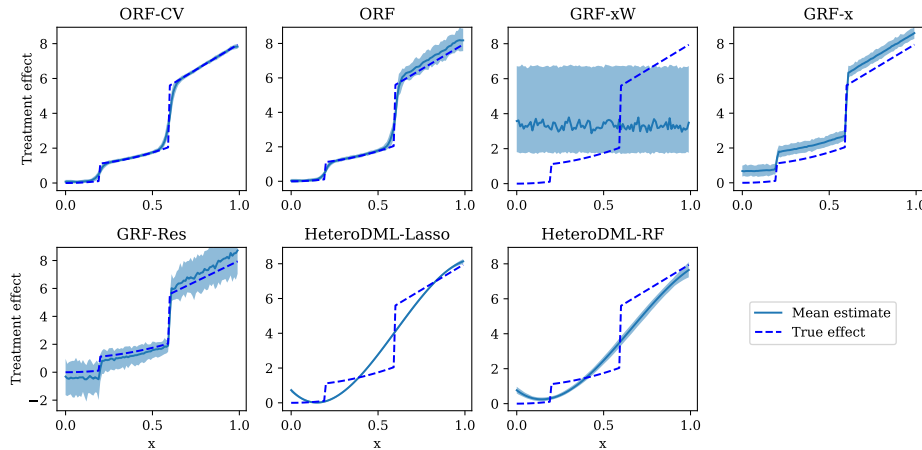


Figure 49: Treatment effect estimations for 100 Monte Carlo experiments with parameters  $n = 10000, p = 500, d = 1, k = 5$ , and a piecewise polynomial treatment response. The shaded regions depict the mean and the 5%-95% interval of the 100 experiments.

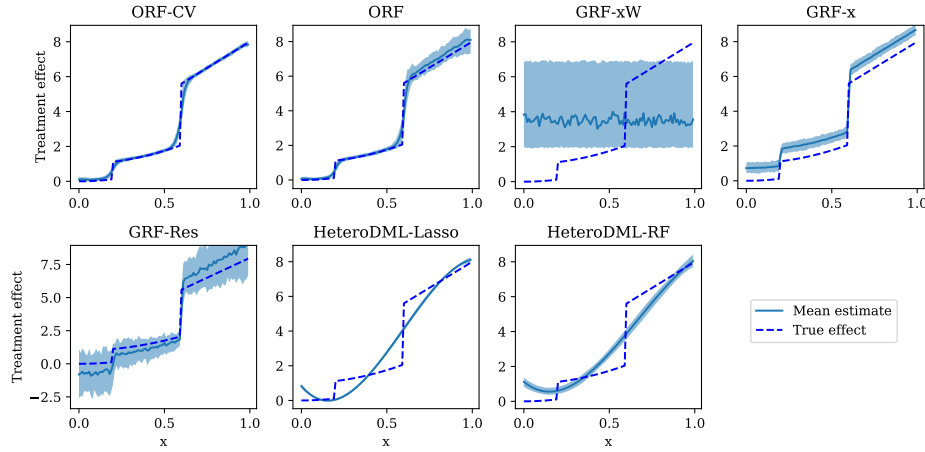


Figure 50: Treatment effect estimations for 100 Monte Carlo experiments with parameters  $n = 10000$ ,  $p = 500$ ,  $d = 1$ ,  $k = 10$ , and a piecewise polynomial treatment response. The shaded regions depict the mean and the 5%-95% interval of the 100 experiments.

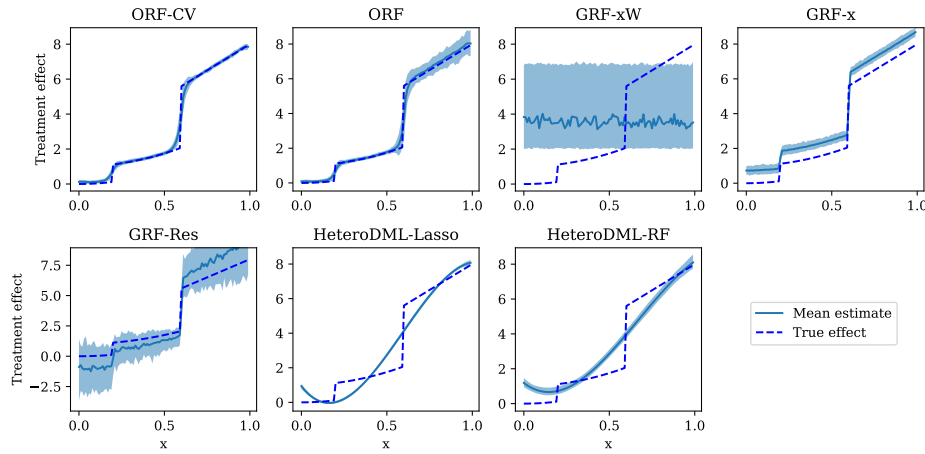


Figure 51: Treatment effect estimations for 100 Monte Carlo experiments with parameters  $n = 10000$ ,  $p = 500$ ,  $d = 1$ ,  $k = 15$ , and a piecewise polynomial treatment response. The shaded regions depict the mean and the 5%-95% interval of the 100 experiments.

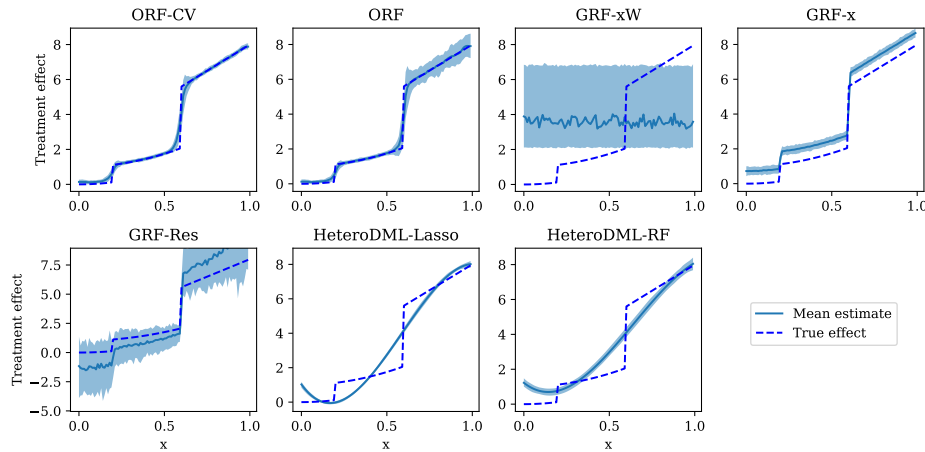


Figure 52: Treatment effect estimations for 100 Monte Carlo experiments with parameters  $n = 10000$ ,  $p = 500$ ,  $d = 1$ ,  $k = 20$ , and a piecewise polynomial treatment response. The shaded regions depict the mean and the 5%-95% interval of the 100 experiments.

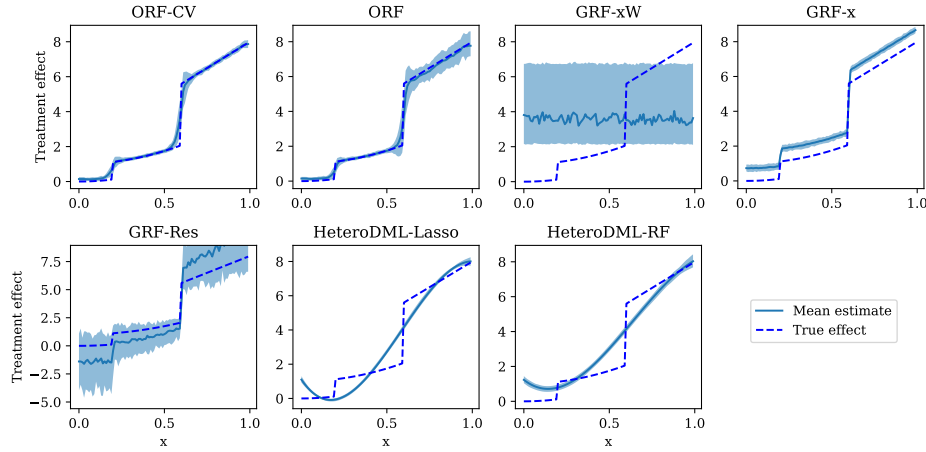


Figure 53: Treatment effect estimations for 100 Monte Carlo experiments with parameters  $n = 10000$ ,  $p = 500$ ,  $d = 1$ ,  $k = 25$ , and a piecewise polynomial treatment response. The shaded regions depict the mean and the 5%-95% interval of the 100 experiments.

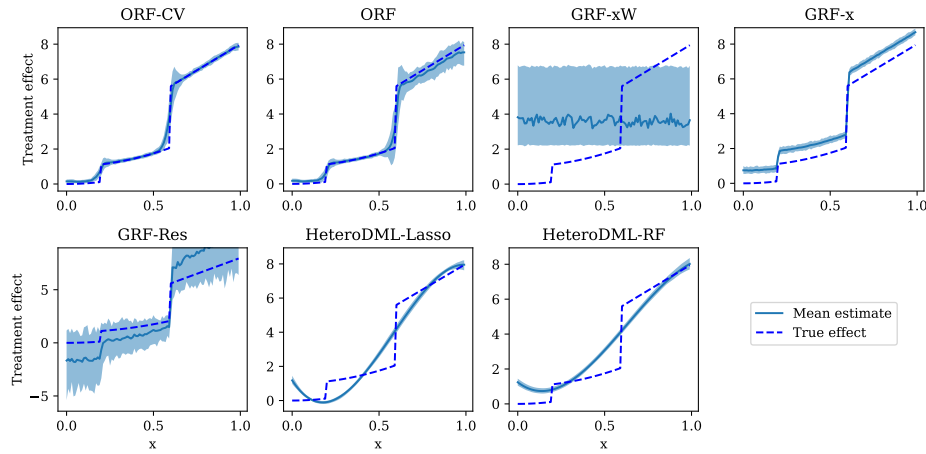


Figure 54: Treatment effect estimations for 100 Monte Carlo experiments with parameters  $n = 10000$ ,  $p = 500$ ,  $d = 1$ ,  $k = 30$ , and a piecewise polynomial treatment response. The shaded regions depict the mean and the 5%-95% interval of the 100 experiments.

## D.4 Experimental results for larger control support

We present experimental results for a piecewise linear treatment response  $\theta_0$ , with  $n = 5000$  samples and large support  $k \in \{50, 75, 100, 150, 200\}$ . Figures 55-60 illustrate that the behavior of the ORF-CV algorithm, with parameters set in accordance our theoretical results, is consistent up until fairly large support sizes. Our method performs well with respect to the chosen evaluation metrics and outperform other estimators for larger support sizes.

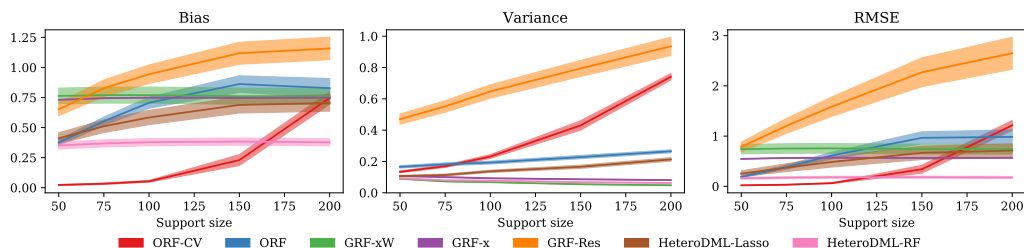


Figure 55: Bias, variance and RMSE as a function of support size. The solid lines represent the mean of the metrics across test points, averaged over the Monte Carlo experiments, and the filled regions depict the standard deviation, scaled down by a factor of 3 for clarity.

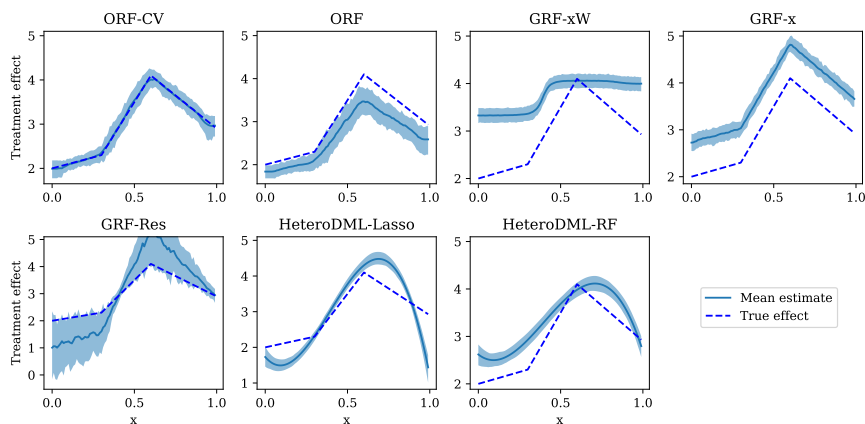


Figure 56: Treatment effect estimations for 100 Monte Carlo experiments with parameters  $n = 5000$ ,  $p = 500$ ,  $d = 1$ ,  $k = 50$ , and a piecewise linear treatment response. The shaded regions depict the mean and the 5%-95% interval of the 100 experiments.

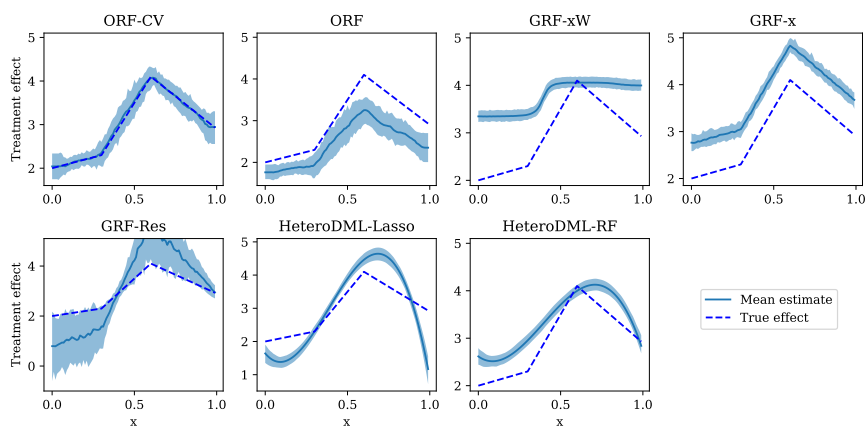


Figure 57: Treatment effect estimations for 100 Monte Carlo experiments with parameters  $n = 5000$ ,  $p = 500$ ,  $d = 1$ ,  $k = 75$ , and a piecewise linear treatment response. The shaded regions depict the mean and the 5%-95% interval of the 100 experiments.

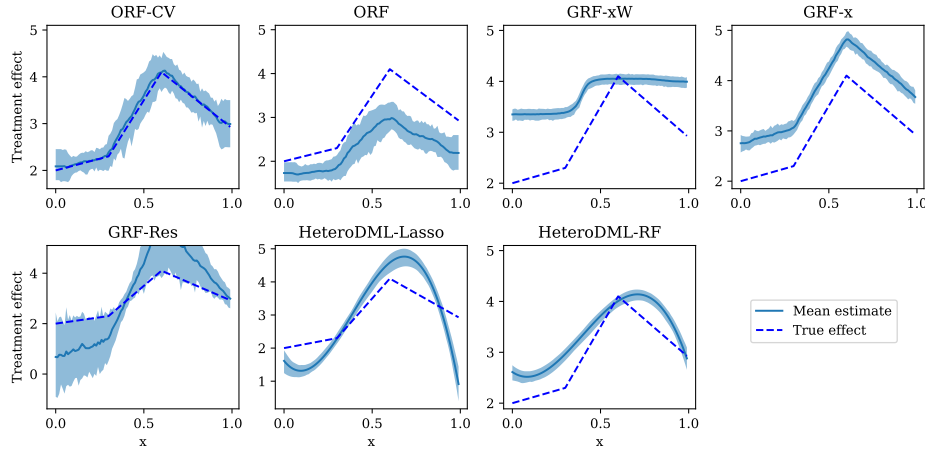


Figure 58: Treatment effect estimations for 100 Monte Carlo experiments with parameters  $n = 5000$ ,  $p = 500$ ,  $d = 1$ ,  $k = 100$ , and a piecewise linear treatment response. The shaded regions depict the mean and the 5%-95% interval of the 100 experiments.

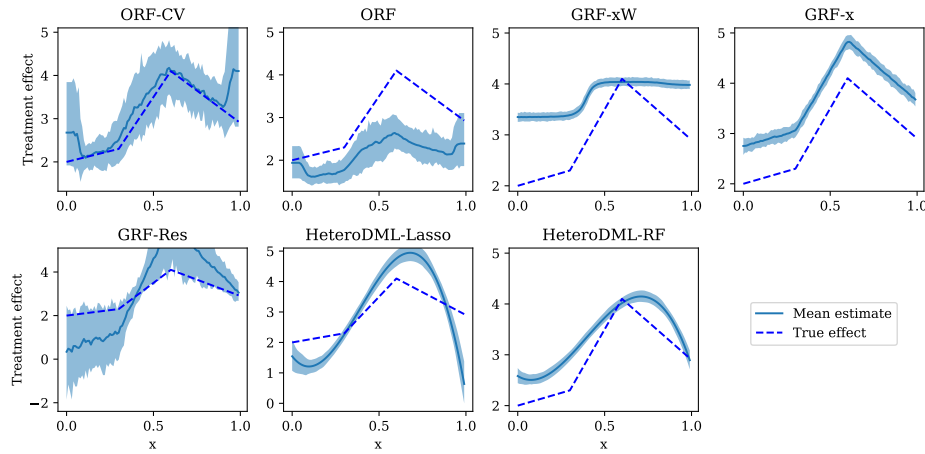


Figure 59: Treatment effect estimations for 100 Monte Carlo experiments with parameters  $n = 5000$ ,  $p = 500$ ,  $d = 1$ ,  $k = 150$ , and a piecewise linear treatment response. The shaded regions depict the mean and the 5%-95% interval of the 100 experiments.

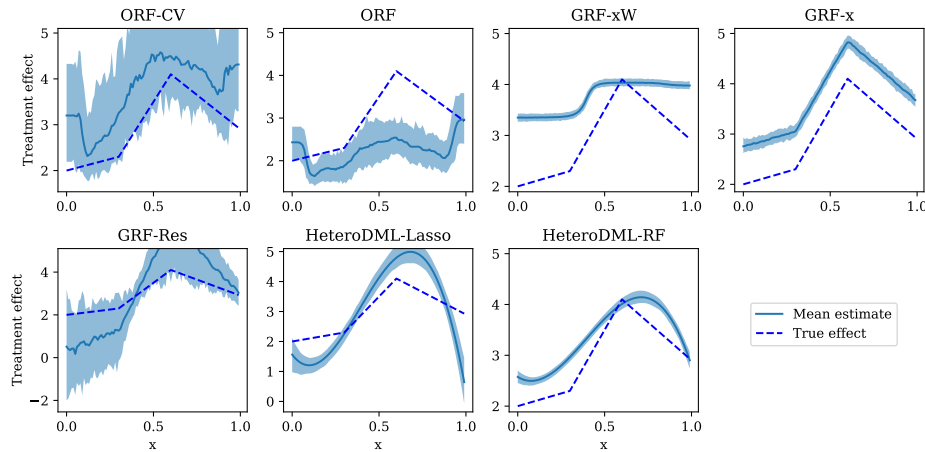


Figure 60: Treatment effect estimations for 100 Monte Carlo experiments with parameters  $n = 5000$ ,  $p = 500$ ,  $d = 1$ ,  $k = 200$ , and a piecewise linear treatment response. The shaded regions depict the mean and the 5%-95% interval of the 100 experiments.

## D.5 Experimental results for two-dimensional heterogeneity

We introduce experimental results for a two-dimensional  $x$  and corresponding  $\theta_0$  given by:

$$\theta_0(x_1, x_2) = \theta_{\text{piecewise linear}}(x_1)\mathbb{I}_{x_2=0} + \theta_{\text{piecewise constant}}(x_1)\mathbb{I}_{x_2=1}$$

where  $x_1 \sim U[0,1]$  and  $x_2 \sim \text{Bern}(0.5)$ . In Figures 61-69, we examine the overall behavior of the ORF-CV and ORF estimators, as well as the behavior across the slices  $x_2 = 0$  and  $x_2 = 1$ . We compare the performance of the ORF-CV and ORF estimators with alternative methods for  $n = 5000$  and  $k \in \{1, 5, 10, 15, 20, 25, 30\}$ . We conclude that the ORF-CV algorithm yields a better performance for all support sizes and evaluation metrics.

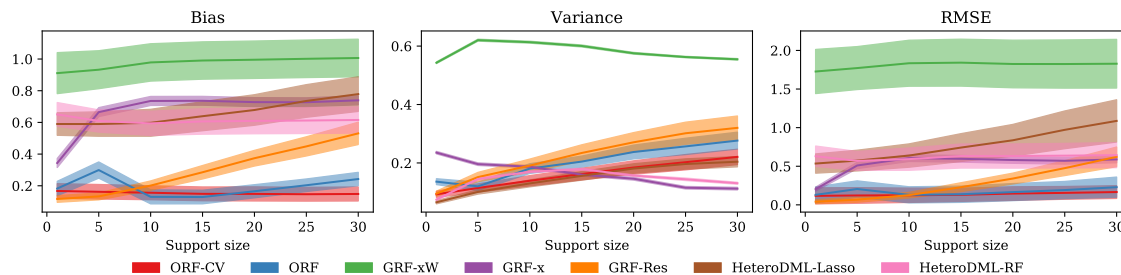


Figure 61: Overall bias, variance and RMSE as a function of support size for  $n = 5000$ ,  $p = 500$ ,  $d = 2$ . The solid lines represent the mean of the metrics across test points, averaged over the Monte Carlo experiments, and the filled regions depict the standard deviation, scaled down by a factor of 3 for clarity.

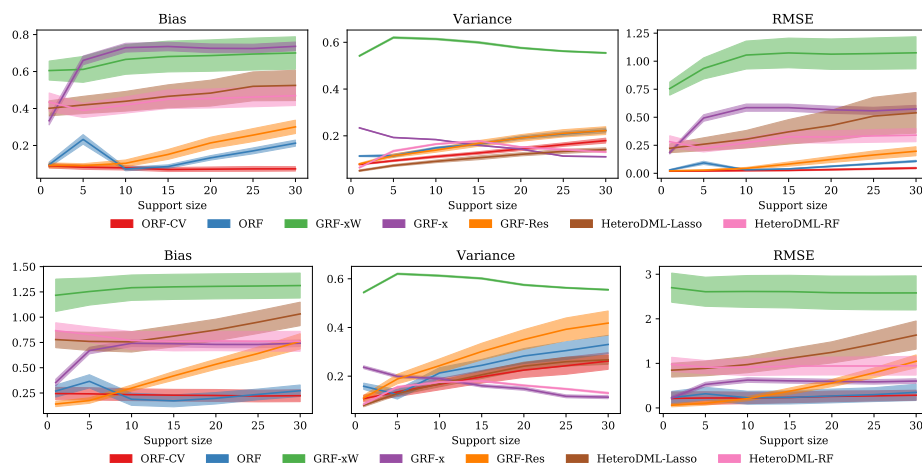


Figure 62: Bias, variance and RMSE as a function of support for  $n = 5000$ ,  $p = 500$ ,  $d = 2$  and slices  $x_2 = 0$  and  $x_2 = 1$ , respectively. The solid lines represent the mean of the metrics across test points, averaged over the Monte Carlo experiments, and the filled regions depict the standard deviation, scaled down by a factor of 3 for clarity.

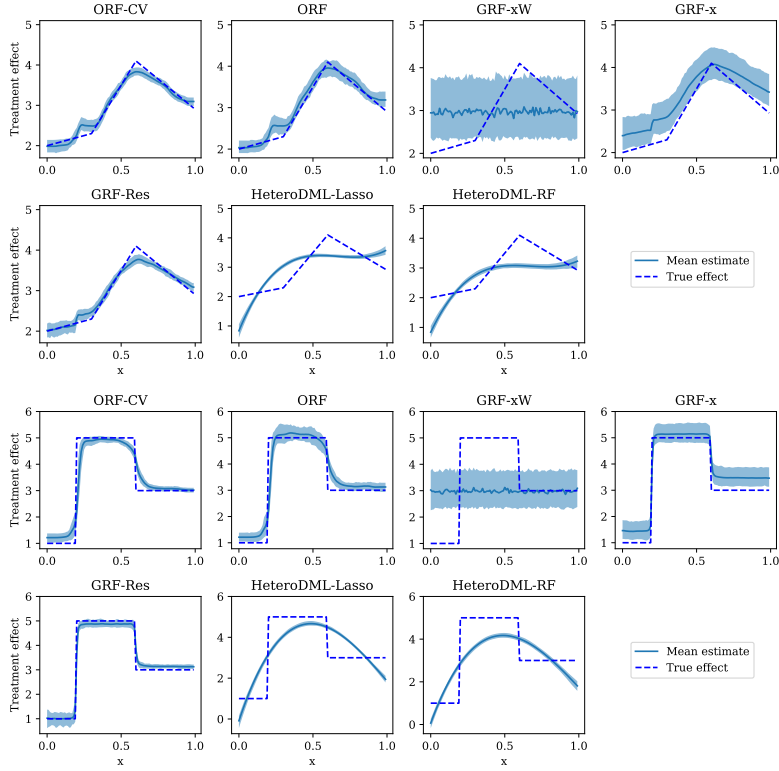


Figure 63: Treatment effect estimations for 100 Monte Carlo experiments with parameters  $n = 5000$ ,  $p = 500$ ,  $d = 2$ ,  $\mathbf{k} = \mathbf{1}$ , and slices  $\mathbf{x}_2 = \mathbf{0}$  and  $\mathbf{x}_2 = \mathbf{1}$ , respectively. The shaded regions depict the mean and the 5%-95% interval of the 100 experiments.

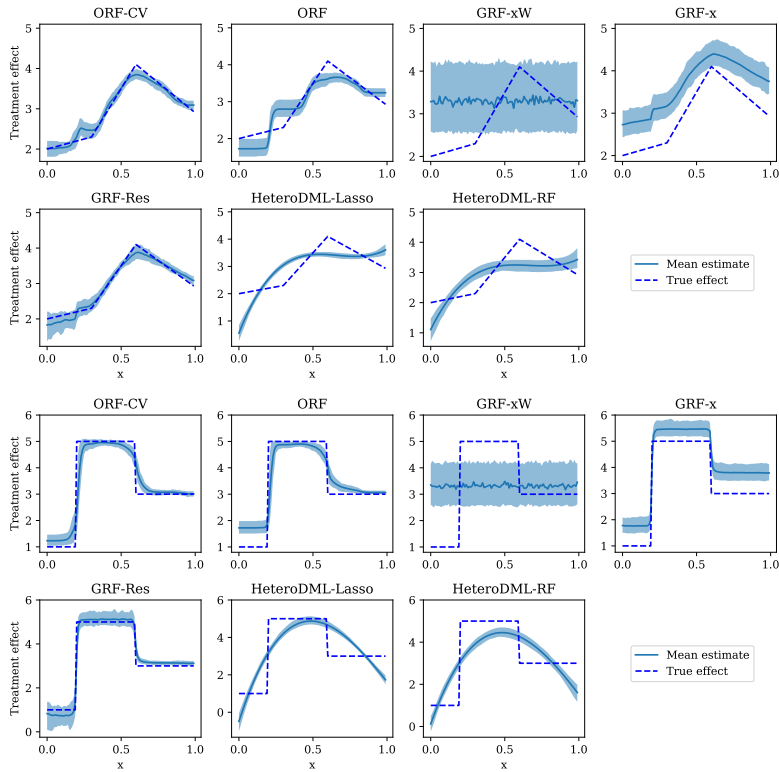


Figure 64: Treatment effect estimations for 100 Monte Carlo experiments with parameters  $n = 5000$ ,  $p = 500$ ,  $d = 2$ ,  $\mathbf{k} = \mathbf{5}$ , and slices  $\mathbf{x}_2 = \mathbf{0}$  and  $\mathbf{x}_2 = \mathbf{1}$ , respectively. The shaded regions depict the mean and the 5%-95% interval of the 100 experiments.

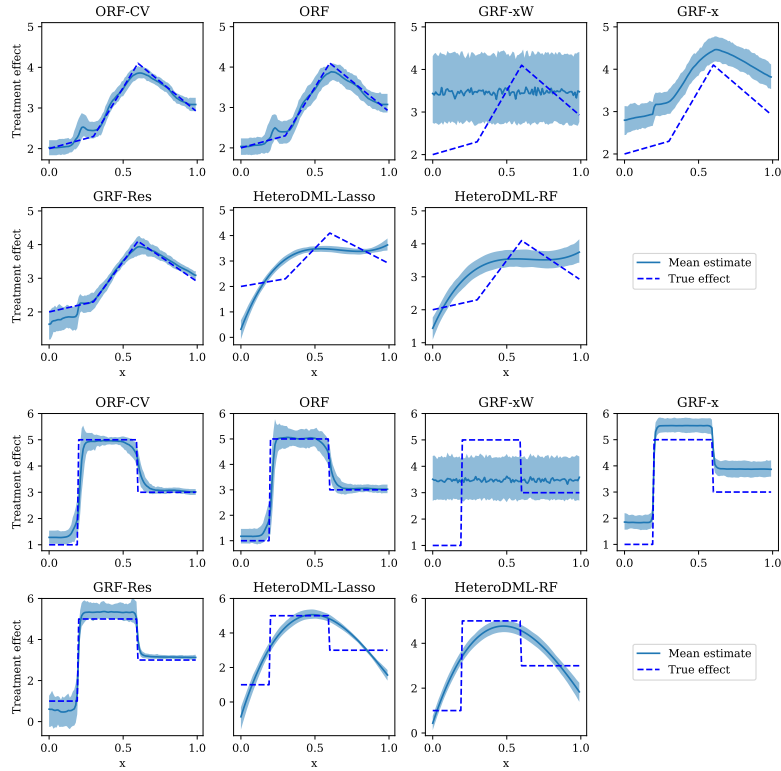


Figure 65: Treatment effect estimations for 100 Monte Carlo experiments with parameters  $n = 5000$ ,  $p = 500$ ,  $d = 2$ ,  $\mathbf{k} = \mathbf{10}$ , and slices  $\mathbf{x}_2 = \mathbf{0}$  and  $\mathbf{x}_2 = \mathbf{1}$ , respectively. The shaded regions depict the mean and the 5%-95% interval of the 100 experiments.

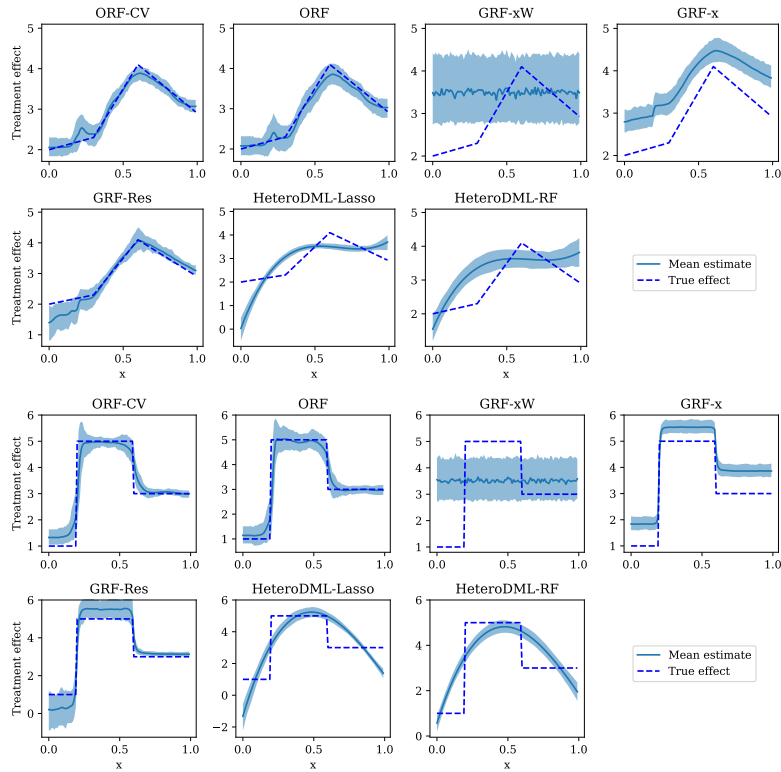


Figure 66: Treatment effect estimations for 100 Monte Carlo experiments with parameters  $n = 5000$ ,  $p = 500$ ,  $d = 2$ ,  $\mathbf{k} = \mathbf{15}$ , and slices  $\mathbf{x}_2 = \mathbf{0}$  and  $\mathbf{x}_2 = \mathbf{1}$ , respectively. The shaded regions depict the mean and the 5%-95% interval of the 100 experiments.

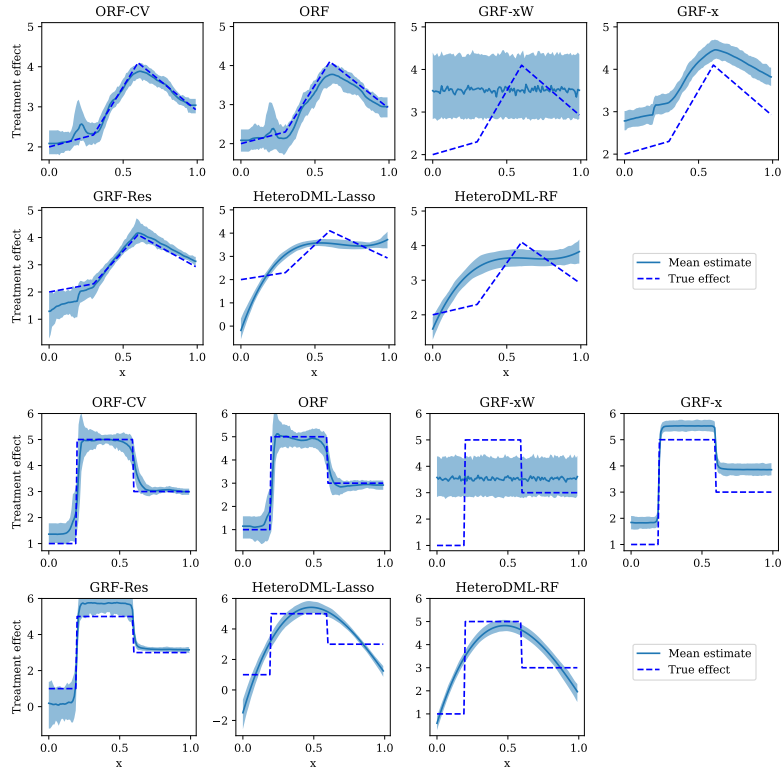


Figure 67: Treatment effect estimations for 100 Monte Carlo experiments with parameters  $n = 5000$ ,  $p = 500$ ,  $d = 2$ ,  $k = 20$ , and slices  $x_2 = 0$  and  $x_2 = 1$ , respectively. The shaded regions depict the mean and the 5%-95% interval of the 100 experiments.

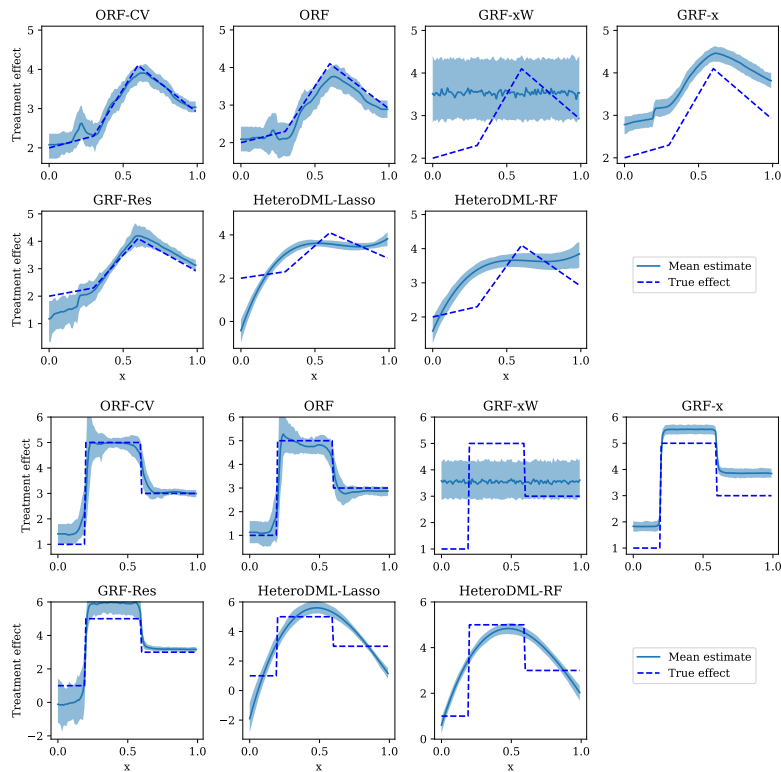


Figure 68: Treatment effect estimations for 100 Monte Carlo experiments with parameters  $n = 5000$ ,  $p = 500$ ,  $d = 2$ ,  $k = 25$ , and slices  $x_2 = 0$  and  $x_2 = 1$ , respectively. The shaded regions depict the mean and the 5%-95% interval of the 100 experiments.

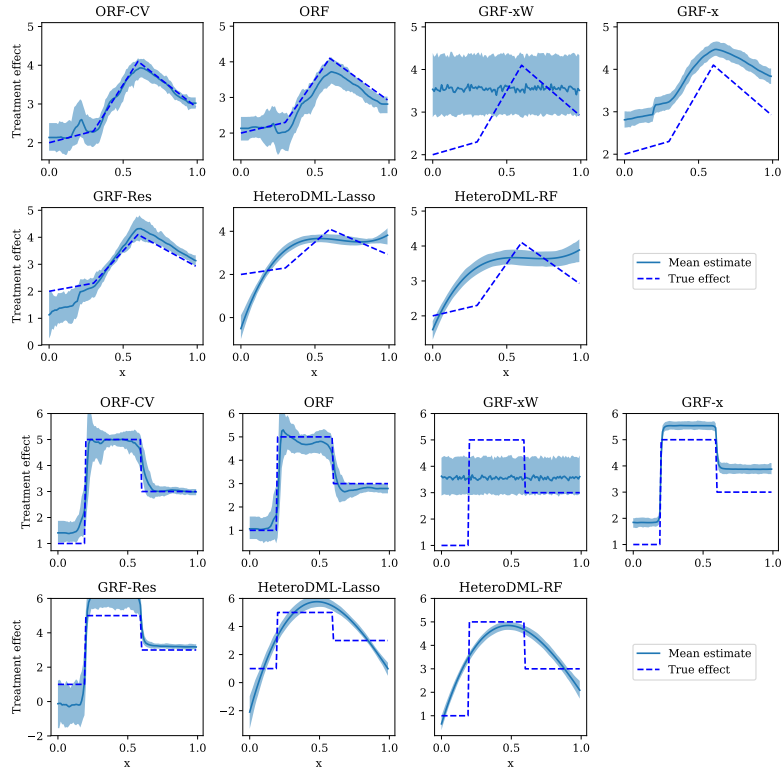


Figure 69: Treatment effect estimations for 100 Monte Carlo experiments with parameters  $n = 5000$ ,  $p = 500$ ,  $d = 2$ ,  $\mathbf{k} = 30$ , and slices  $\mathbf{x}_2 = \mathbf{0}$  and  $\mathbf{x}_2 = \mathbf{1}$ , respectively. The shaded regions depict the mean and the 5%-95% interval of the 100 experiments.